01/20/23

Title:
"Gut OncoMicrobiome Signatures as next generation biomarkers for cancer immunotherapy"

Authors:
Andrew Maltez Thomas[1-2*], Marine Fidelle[3-6*], Bertrand Routy[7-8*], Guido Kroemer[9-11], Jennifer A. Wargo[12-14], Nicola Segata[1,2], Laurence Zitvogel [3, 4, 6, 15£]

Affiliations:
[1] Department CIBIO, University of Trento, Trento, Italy.
[2] IEO, European Institute of Oncology IRCCS, Milan, Italy.
[3] Gustave Roussy Cancer Campus, Villejuif, France.
[4] Institut National de la Santé Et de la Recherche Médicale (INSERM) U1015, ClinicObiome, Equipe Labellisée - Ligue Nationale contre le Cancer, Villejuif, France.
[5] Pharmacology Department, Gustave Roussy, Villejuif, France.
[6] Center of Clinical Investigations in Biotherapies of Cancer (BIOTHERIS) 1428, Villejuif, France.
[7] Centre de Recherche du Centre Hospitalier de l'Université de Montréal (CRCHUM), Montréal, QC, Canada.
[8] Hematology-Oncology Division, Department of Medicine, Centre Hospitalier de l'Université de Montréal (CHUM), Montréal, QC, Canada.
[9] Centre de Recherche des Cordeliers, INSERM U1138, Equipe labellisée—Ligue Nationale contre le cancer, Université de Paris, Institut Universitaire de France, Paris, France.
[10] Metabolomics and Cell Biology Platforms, Gustave Roussy, Villejuif, France.
[11] Institut du Cancer Paris CARPEM, Department of Biology, Hôpital Européen Georges Pompidou, Assistance Publique-Hôpitaux de Paris, Paris, France.
[12] Department of Genomic Medicine, The University of Texas MD Anderson Cancer Center, Houston, TX, USA.
[13] Platform for Innovative Microbiome and Translational Research (PRIME-TR), MD Anderson Cancer Center, Houston, TX, USA.
[14] Department of Surgical Oncology, The University of Texas MD Anderson Cancer Center, Houston, TX 77030, USA.
[15] Université Paris-Saclay, Ile-de-France, France.

*Equal contribution

[£]Corresponding author: Laurence ZITVOGEL, Gustave Roussy cancer center, 114 rue Édouard Vaillant, 94805 VILLEJUIF Cedex, France, e-mail: laurence.zitvogel@gustaveroussy.fr, Phone: +33-1-42-11-50-41

Total number of words without references: 7300

Abstract

Since the advent of successful cancer immunotherapy, biomarkers for predicting their efficacy before starting the treatment have been unmet medical need. Intestinal dysbiosis is a satellite syndrome of oncogenesis and stool metagenomics represents a non-invasive and increasingly cost-effective approach with the potential to early diagnosis of cancer in different cancer types. The prognostic impact of antibiotic uptake and gut microbiota composition urged investigators to develop tools for the detection of gut dysbiosis for patient stratification and microbiota-centered

clinical interventions. This review will outline that cancer patients share several Gut OncoMicrobiome Signatures (GOMS) with individuals suffering from seemingly unrelated chronic inflammatory disorders across various histotypes that instead tend to be different from the microbiome profiles of healthy individuals. This review presents the largest integrative meta-analysis of GOMS patterns associated with clinical benefit or resistance to immune checkpoint inhibitors (ICI) across 808 patients with cancer. We will discuss metabolic and immunological surrogate markers of gut dysbiosis and practical guidelines to incorporate GOMS in decision making for prospective clinical trials in immuno-oncology.

Key points

- **Intestinal dysbiosis is a satellite manifestation of oncogenesis**
- **Cancer patients share gut microbiome signatures with individuals suffering from seemingly unrelated diseases**
- **Gut OncoMicrobiome signatures (GOMS) share profile commonalities across cancer histotypes**
- **GOMS represent a non-invasive cost-effective promising approach to early diagnosis of cancer in different cancer types**
- **Links between gut dysbiosis and microbial tissue colonization or infection offer new prospects of etiology, prevention and therapeutic intervention in distinct cancers such as PDAC or urothelial cancers**
- **GOMS are candidate predictors of resistance to immune checkpoint inhibitors**

Introduction

Adulthood carcinogenesis is a complex cell-autonomous disease caused by (epi-)genetically unstable cells that have the potential to acquire (at least) fourteen phenotypic capacities corrupting local tissue barriers and culminating in a chronic inflammatory process[1]. A more "ecological" view of malignant disease encompasses its malicious modulation of distant systems including the autophagic machinery[2], senescence[3], metabolism, immunity, clonal hematopoiesis, endocrine and neurological networks and the local and intestinal microbiota community[1,4,5]. In fact, many pathophysiological disorders associated with cancer, so called "comorbidities" (**GLOSSARY)**, namely, systemic inflammation[6–8], obesity, lung and liver dysfunctions, aging-related abnormalities[9,10], cachexia[11,12], heart or circulatory failures, as well as specific antitumor therapies and their comedications (**GLOSSARY),** can directly or indirectly converge towards altering the gut barrier integrity and the taxonomic composition of the local microbial ecosystem with a feed-forward loop[13] (**Table 1**). It is well established that cancer incidence increases with aging. Studies focusing on microbiome characteristics of aging unveiled that the lifetime-induced gut microbiota drift may influence survival span[10,14]. Hence, unhealthy aging is

characterized by high relative abundance of certain taxa such as those from the *Bacteroides* genus, low gut microbiome uniqueness and the presence of gut xenobiotic metabolites such as those with toxic phenylalanine/tyrosine microbial fermentation products (p-cresol sulfate, phenylacetylglutamine, p-cresol glucuronide)[9,10]. In contrast, healthy aging exhibits a series of gut microbial features including increased presence of indoles (3-indoxyl sulfate, 6-hydroxyindole sulfate, indoleacetate and indolepropionate), which are gut bacterial degradation products of tryptophan mediating immune homeostasis through binding to aryl hydrocarbon and IL-10 receptors[15–17]. A sizeable subset of advanced cancer patients present frailty, sarcopenia, and fat loss corollary of gut permeability and systemic inflammation[18]. *Enterobacteriaceae* family members including typically proinflammatory *Gammaproteobacteria* and *Veillonella* typically become more abundant among cachectic cancer patients. Fecal levels of short-chain fatty acids (SCFA), more specifically acetate, are associated with health-related regulatory pathways, but tend to be reduced in cancer patients presenting with cachexia[12]. Specific secondary bile acids (including isoallo-lithocholic acid) resulting from the prevalence of distinct gut species (including *Alistipes putredinis* and *Odoribacter splanchnicus*) are preferentially found in centenarians and reportedly contribute to intestinal homeostasis[19]. An unhealthy gut microbiome signature reflects both the diseased state and the associated medication. Strong effects on the taxonomic composition of the intestinal microbial ecosystem were observed for comedications often prescribed in cancer patients, such as proton pump inhibitors (PPI), antibiotics (ATB), anti-inflammatory agents, osmotic laxatives and biguanide antidiabetics[20]. For instance, both PPI and ATB significantly induced lower microbial diversities, overrepresentation of supraglottic commensals (such as *Streptococcaceae* family members for PPI[21]) and increased relative abundances of "immunosuppressive" gut commensals (such as the *Hungatella* and *Enterocloster* genera for ATB[22,23]). Lastly, polychemotherapy and hormonotherapy (such as androgen deprivation) can modulate the alpha and beta-diversities of the microbiota, influencing treatment side effects[24,25] or drug metabolism and efficacy[26,27]. Altogether, this pathological or iatrogenic conjecture converges to deviate the healthy repertoire of the intestinal ecosystem, referred to as "gut dysbiosis" henceforth **(GLOSSARY)**, observed in patients diagnosed with localized or advanced intestinal and extra-intestinal malignancies.

Likewise, carcinogenesis can drive compositional shifts of the microbiome to its own benefit **(Figure 1)**. Indeed, as shown in the early 1960s, certain malignancies can cause jejunal and ileal mucosa atrophy[22,28,29]. Mouse models of transplantable tumors highlighted that this ileal mucosa atrophy (monitored by the villous/crypt height ratio) was characterized by crypt apoptosis, defects in proliferation, in ER stress response and autophagy induction by villus enterocytes[11,22]. Transplantable

tumorigenesis also disturbed the secretory components of ileal crypts, inducing Paneth cell degranulation, release of the antimicrobial peptide (AMP) REG3γ by ileal cells, and an ectopic accumulation of enteroendocrine cells expressing the tyrosine hydroxylase (TH^+EEC) (leading to L-dopa synthesis and catecholamine end products). This ileal atrophy correlated with villous microvascular constriction and reduced accumulation of $CD8^+$ T lymphocytes, eosinophils and granulocytes in the lamina propria (LP). Moreover, neurological imbalances between catecholamine and cholinergic signaling were observed in the ileal mucosa of tumor bearers[22] **(Figure 1)**. Choline acetyltransferase (ChAT) expression was decreased in the ileal stroma shortly after tumor inoculation in preclinical models. Nerve fibers extending into each villus of the lamina propria and expressing vesicular acetylcholine transporter (VAChT) were clearly reduced by tumor injection. Incubation of mouse and human 3D-crypt stem cell derived-ileal enteroids with physiological concentrations of biogenic amines (epinephrine and to some extent norepinephrine) blunted enterocyte proliferation and increased REG3γ secretion, suggesting a potential link between TH^+enteroendocrine cells and antimicrobial peptide release. This ileal atrophy led to a transient intestinal permeability paving the way to an overt and protracted dysbiosis. A prototypic "dysbiosis" accompanied tumor growth, that was dominated by Gram-positive *Clostridium* species (belonging to the *Enterocloster* genus such as *E. bolteae, E. clostridioformis, E. asparagiformis, E. citroniae…*), *Flavonifractor plautii* and the relative underrepresentation of *Eubacterium* and *Lactobacilli* spp.[22]. A cause-effect relationship between this stress ileopathy and carcinogenesis was unveiled in cohousing experiments. Pharmacological blockade of β-adrenergic receptors or *Adrb2* gene deficiency, vancomycin or co-housing of tumor bearers with tumor free littermates all prevented cancer-induced ileopathy, eventually slowing tumor growth kinetics. Cancer patients also exhibit hallmarks of this stress ileopathy. A correlation between crypt apoptosis and ectopic enteroendocrine cells was observed in patients diagnosed with gastrointestinal (including colon adenocarcinoma and neuroendocrine intestinal tumors) or genitourinary malignancies[22]. In addition, the fecal composition of cancer patients significantly differed from that of healthy controls with a relative overrepresentation of the *Enterocloster* genus and loss of *Lachnospiraceae* or *Oscillospiraceae* family members (including *Eubacterium, Dorea, Faecalibacterium* spp.). Hence, stress ileopathy is a corollary disease of extra-intestinal malignancies culminating in a protracted gut dysbiosis. Of note, this stress ileopathy is not cancer-specific. Thus, Stanley *et al.* showed that ischemic brain injuries caused gut barrier dysfunction with increased permeability allowing the translocation of ileal bacteria to peripheral organs[30]. The authors unveiled a biologically significant imbalance between adrenergic and cholinergic signaling within the submucosal plexus in the ileum post-stroke. Indeed, reduction in cholinergic signaling stimulated the pro-inflammatory

immune response, while its activation prevented the brain injury-induced increase in both intestinal and cerebral vascular permeability[31].

Therefore, cancer patients have many reasons to present an intestinal dysbiosis that may be harnessed to stratify patient cohorts, given its clinical relevance as discussed henceforth.

Gut OncoMicrobiome Signatures (GOMS) and prognostic impact

The intestinal microbiota is modulated during the course of many different diseases, most specifically inflammatory bowel diseases, metabolic syndrome, autoimmune disorders and cancer[13,32]. However, universal healthy or unhealthy gut microbiome signatures are difficult to be identified, because of intrinsic variability and subject specificity of the microbiome, technical issues, geographical variance and many confounding factors such as genetics, exposome, lifestyle and diet. The Dutch Microbiome Project (DMP) within Lifelines, a three-generational population cohort comprising >8,000 individuals with >25,000 fecal samples from the northern Netherlands analyzed associations between the stool taxonomic composition and function and well-defined phenotypes[20]. The DMP identified nine core species (*Subdoligranulum* sp., *Alistipes onderdonkii*, *Alistipes putredinis*, *Alistipes shahii*, *Bacteroides uniformis*, *Bacteroides vulgatus*, *Eubacterium rectale*, *Faecalibacterium prausnitzii* and *Oscillibacter* spp.) that form central nodes in microbial co-abundance networks in more than 95% of individuals[20]. The DMP gut microbiome signature of health replicated most of the signals identified in the other broad study, the Gut Microbiome Health Index (GMHI)[33], at genus or species levels. In addition, the DMP identified other health-related microbiome patterns comprising *Butyrivibrio*, *Akkermansia* and *Prevotella* genera. Surprisingly, seemingly unrelated diseases (such as cancer, cardiovascular diseases, metabolic disorders, gastrointestinal syndromes, and mental disorders) share a common gut microbiome signature that is independent of comorbidities. The shared gut microbiome signature is detailed in **Table S1**, and in brief, mainly consisted of relative increases in *Enterocloster, Flavonifractor Eggerthella, Streptococcus, Hungatella* and *Veillonella* genera and relative decreases of members of several families *(Prevotellaceae*, *Lachnospiraceae*, *Oscillospiraceae*) and immunogenic representatives of the *Bacteroidales* order (*Barnesiella intestinihominis*, *Alistipes shahii*, *A. senegalensis*). Gut microbiome-associated functional pathways shared across unrelated diseases consisted mainly of increases in biosynthesis of l-ornithine, ubiquinol and menaquinol, enterobacterial common antigen, Kdo-2-lipid-A and molybdenum cofactor, as well as decreases in biosynthesis of amino acids, deoxyribonucleosides and nucleotides, anaerobic energy metabolism and fermentation to SCFA

(mainly butanoate)[20]. These findings are in line with another independent study showing that gut dysbiosis is a corollary syndrome of cancer[22]. Indeed, the pan-cancer metagenome from a prospective cohort of 1,426 patients diagnosed with 8 different malignancies (including colon, kidney, breast, lung, ovarian, prostate cancers, melanoma and chronic leukemia) at various stages were admixed with 705 colon cancers from publicly available databases and compared with >5,570 healthy metagenomes. Confirming other studies[20,33], significant differences separated the normal from the cancerous taxonomic profile. Selected bacteria taxa (*Prevotellaceae* and *Lachnospiraceae* family members, *Bifidobacterium* spp.) were overrepresented in healthy individuals while Gram-positive *Enterocloster and Clostridium* spp., *Eisenbergiella* spp. and gamma/ delta-proteobacteria were relatively dominant across 6 of 8 cancer types[22] (**Table S1**).

To refine the definition of the pan-cancer-associated gut dysbiosis ("GOMS") discussed above, we propose herein the following meta-analysis **(GLOSSARY)**. We performed microbiome taxonomic profiling with MetaPhlAn 4[34] on stool samples collected from adult individuals from a first collection of 1,879 patients spanning 8 different cancers comprising 30 cohorts from 23 published studies[22–26,35–52] and 5,341 control individuals comprising 17 cohorts of healthy adult subjects from 14 published studies across diverse geographic locations[45,53–65] **(Table S2, refer to supplemental materials for meta-analysis methodology)**. With the exception of colorectal cancer, the cancer datasets typically contained only cancer patients as they are focused on studying response to treatment and matched controls individuals are difficult to be collected in oncological settings. This integrative analysis was conducted by considering all pairs of cohorts composed by a cohort of cancer patients and a cohort of controls and applying a random-effect meta-analysis on all the detected species-level genome bins (SGBs). By computing the ranking of the significant associations of each SGB with the cancer or control conditions, we highlighted several species consistently associated with cancer individuals across distinct cohorts for the same cancer and across different cancers **(Figure 2, Table S1, Table S2)**. Specifically, cancer stools across the 8 cancer types harbor a consistent relative increase in *Enterocloster* genus, *Hungatella and Clostridium* spp., *Pseudoflavonifractor*, and species from the genus *Eisenbergiella* and a relative decrease of members of several families including *Lachnospiraceae*, and *Oscillospiraceae* (including *Faecalibacterium* spp.) **(Table S1, Figure 2, Table S3)**. Notably, many such biomarkers belong to yet-to-be-characterized species represented by SGBs solely defined based on metagenome-assembled genomes, lacking any cultivated representative, and assignable only at high taxonomic levels (e.g., families), highlighting once again the need for further microbiological cultivation-based studies.

Histotype specificities for GOMS and impact on prognosis (Table S4)

While pan-cancer GOMS may indirectly reflect the systemic chronic inflammatory process, certain deviations of the gut microbiota repertoire may be more specifically attributable to distinct tumor types. We will only focus on large cohorts that unveiled important and robust specific features as described henceforth and discuss their potential clinical relevance.

Breast cancer (BC)

A French study analyzed the fecal compositional differences between BC and healthy volunteers (HV)[24]. The BC GOMS comprised families from the *Bacteroidales* order, *Tannerellaceae*, *Rikenellaceae*, *Prevotellaceae, Odoribacteraceae* families as well as viruses (*C2 like virus unclass., Lactococcus phage 936, Enterobacteria phage JL1, E. coli phage phAPEC8, Sodalis phage SO1*)[24] (**Table S4**). Here again, the *Enterocloster* genus reported to be associated with pathophysiological disorders[20,22] was also overrepresented in BC GOMS. Importantly, there was a prognostic significance of the BC GOMS, in thus far that microbes of this list tended to be associated with stage II/III BC at diagnosis while women with a stage I rather harbored a normal-like stool MG profiling (**Table S1**). Reinforcing this notion, microbes within the BC GOMS were also associated with resistance to neoadjuvant chemotherapy[24]. Hence, *Bacteroides uniformis*, *Parabacteroides merdae, Enterocloster* spp. were overrepresented in stools from women presenting with stage II/III at baseline while *B. thetaiotaomicron*, *E. bolteae*, *E. clostridioformis* were associated with resistance to cytotoxic agents. In fact, chemotherapy significantly affected the alpha and beta-diversity of the stool composition of BC females towards an anti-inflammatory pattern[24], entailing the relative underrepresentation of distinct species commonly found across several pathological disorders (*V. parvula*, *V. atypica*, *E. lenta*, *E. asparagiformis*)[20]. Finally, many BC GOMS spp. (*B. uniformis*, *B. thetaiotaomicron,* and many members of the *Enterocloster* genus) were also culprits associated with BC adjuvant therapy-induced neurotoxicity[24]. Interestingly, many of these BC GOMS culprits (*V. parvula*, *B. uniformis*, *E. clostridioformis* …) were also identified in the BC microbiome comprising >9,000 species after filtering for artefactual contaminants[66]. Future work is awaited to identify links between gut and tumor microbiome patterns, their relevance with BC oncogene or tumor suppressor gene profiles (HER2, p53, PI3K/PTEN signaling…), and the resistance to endocrine therapies.

Pancreatic ductal carcinoma (PDAC)

Here again, across various studies taking into account all possible cofounding factors relevant in this devastating disease, the fecal microbiome composition of PDAC differed from that of controls[42,51]. Shotgun metagenomics profiling of three PDAC cohorts across Asia and Europe identified a shared PDAC GOMS consisting in significant enrichments of the pro-inflammatory *Streptococcus* and *Veillonella* spp.[67] and 58 of their bacteriophages as well as the depletion of SCFA producers (e.g., *Faecalibacterium prausnitzii, E. rectale, and R. bicirculans*)[42](**Table S4**). These PDAC GOMS match gut microbiome signatures observed with PPI uptake. Given the epidemiological association between PPI use and risk of PDAC[68], it is tempting to hypothesize that PPIs might accelerate the development or progression of PDAC. Prospective follow-up revealed correlations between GOMS and PDAC-related mortality. The gut relative abundances of SCFA producers (such as *F. prausnitzii* and *Clostridiales* spp.) over that of *R. torques*, *H. parainfluenzae* and *Neisseria bacilliformis* were associated with prolonged overall survival (OS). Functional analysis of GOMS in these three PDAC cohorts across Asia and Europe revealed the significant enrichments of biosynthesis of C5 isoprenoid from the mevalonate pathway, and ADP-L-glycero-D-manno-heptose in PDAC[42]. The former generates isoprenoids mandatory for the activity of GTPases, putatively the mutated Ras gene product involved in the initiation and maintenance of PDAC. The latter pathway leads to a precursor of the proinflammatory lipopolysaccharide (LPS), culminating in procarcinogenic NF-kB activation.

Two Spanish and German case-control studies reported a microbiota-based classification model with an accuracy of up to 0.84 area under the receiver operating characteristic curve based on a set of 27 microbial species confined to PDAC-GOMS. It was highly disease-specific when validated against 25 publicly available metagenomes from various health conditions (encompassing >5,000 individuals)[51]. Albeit similar to the previous report, this study unveiled complementary observations. First, unexpected taxa, such as *Romboutsia timonensis* or the *Methanobrevibacter smithii* archaea stood out in the PDAC specific-GOMS classifier. Secondly, molecular traits of specific gut microbes (belonging to *Akkermansia* spp., *Lactobacillus* spp., *Bifidobacterium* spp., *Veillonella* spp., *Bacteroides* spp. *and Streptococcus* spp.) were detectable in pancreatic tissues using 16S rRNA sequencing and/or FISH assays with genus-specific primers. Third, distinct strains of fecal PDAC-associated microbes could be sourced from the oral cavity.

Altogether, these studies demonstrated the feasibility of constructing a global, specific, and reproducible predictive model based on non-invasive gut microbiome profiling to screen for early PDAC.

Colorectal cancer (CRC)

The gut microbiome has been extensively studied in the context of colorectal cancer and is arguably the main showcase of the gut microbiome's role in cancer. Initial studies elucidated the gut microbiomes' potential as a diagnostic tool to detect CRC in single cohorts[43,49,69], and has been validated in multiple geographically distinct cohorts, identifying reproducible gut microbiome signatures[46,47,70]. This signature, identified through both supervised machine learning and meta-analysis **(GLOSSARY)**, included bacterial species *Solobacterium moorei*, *Fusobacterium nucleatum*, *Parvimonas micra*, *Peptostreptococcus stomatis, Peptostreptococcus anaerobius* and *Gemella morbillorum* (**Table S4**). Members of this signature, such as *F. nucleatum* and *P. anaerobius* have been shown to promote colorectal carcinogenesis and modulate tumor immunity[71,72] and, along with *P. stomatis* and *P. micra,* are commonly found in the oral cavity. The enrichment of bacterial species from the oral cavity is characteristic of CRC GOMS[47,73–76], along with an enrichment of invasive polymicrobial bacterial biofilms in right-sided tumors[73,77,78]. Most studies thus far have focused on studying CRC GOMS in patients who were diagnosed at a later age (median 68 and 72 years in men and women), however, incidence rates of CRC in patients <50 years old, termed early-onset (EO), are on the rise [79]. EO-CRC patients usually present a more advanced disease, different pathological features and differences in CRC GOMS[80,81], marked by an enrichment of *Flavonifractor plautii* and increased tryptophan, bile acid and choline metabolism, when compared to their older counterparts. Advancements in the field of microbiome research coupled with the availability of large publicly available cohorts have enabled the discovery of additional biomarkers from oftentimes overshadowed, but equally important, nonbacterial members of gut microbial communities[82]. This includes the discovery of specific virome[76] and mycobiome[83,84] signatures for CRC GOMS, with *in vitro* and *in vivo* experiments showing that the fungi *Aspergillus rambellii* can promote CRC cell growth[83].

GOMS are predictors of clinical outcome to ICI (Table S5-7, Figure 3 and Figure 4)

Immune checkpoint inhibitors (ICI), mostly consisting in monoclonal antibodies (Abs) directed against lymphocyte inhibitory receptors (PD-1, CTLA-4) or their ligands (PD-L1, PD-L2) **(GLOSSARY)**, have revolutionized cancer therapy enabling novel therapeutic indications, as standalone or combined strategies across multiple tumor types[85,86]. However, only a minority of patients exhibits prolonged clinical benefit to ICI. In addition, due to their unique mode of action blocking the inhibitory receptor pathways, ICI generate immune-related adverse events (irAEs) that can be life threatening, limiting

their broad use at early stages in the absence of robust biomarkers **(GLOSSARY)**. Validation of such biomarkers has become a priority to ameliorate the therapeutic index and facilitate clinical management of patients, specifically in the ICI adjuvant or neoadjuvant settings. Currently, only three biomarkers (programmed death-ligand 1 (PD-L1), markers related to the tumor microenvironment (TME) and microsatellite instability) have the US Food and Drug Administration (FDA)-approbation with some limitations **(Table 2)**. Over the last decade, since the epidemiological demonstration of the negative impact of antibiotics on the efficacy of ICI[13,39,87], specific microbial taxa have been associated with response or resistance to ICI across distinct cancer types[23,35–37,39,88–97]. However, despite some unifying bacterial taxa within a specific cancer histotype, the overlap between beneficial or harmful bacteria across studies was modest and could not be simply explained by technical considerations[36,37,94]. Beyond confounding factors that can impact the robustness of the ICI-GOMS for each histotype, the clinical RECIST1.1 criterium used to evaluate each stool MG-based study varied, whether considering objective response rates (ORR) or best outcome or 12 month-survival or overall survival (OS). We will first summarize findings mostly obtained in sizeable cohorts of non-small lung cancer (NSCLC) and melanoma, describing robust GOMS associated with clinical outcome to ICI. Secondly, we will provide the first meta-analysis across all cancer patients treated with anti-PD-1/anti-PD-L1 $\pm$ anti-CTLA-4 Abs and geographical sites, unveiling common GOMS associated with response or resistance to ICI, considering only ORR (CR+PR vs SD+PD) **(GLOSSARY)**.

Non-small cell lung cancer (NSCLC)

Akkermansia muciniphila is a Gram-negative homeostatic commensal, that acts on host metabolism to maintain glucose tolerance and intestinal barrier function. This mucin -producing and -degrading commensal was shown to mitigate gut dysbiosis, preventing gut permeability and liver inflammation[98–100]. In homeostatic or immunostimulatory conditions, *A. muciniphila* activates immune responses, local TFH cells[101] or systemic TH1 cells in an IL-12-dependent manner respectively[39]. In a cohort of 493 NSCLC patients subjected to prospective stool shotgun metagenomic sequencing before PD-1/PD-L1 blockade, the prevalence of *A. muciniphila* (the main species-level genome bin SGB9226 among all *Akkermansia* spp.) was associated with an inflamed tumor microenvironment (TME) and a favorable clinical outcome (considering RECIST1.1 objective response rates and overall survival), specifically when the relative abundance did not exceed the 77th percentile (<4.8% of the whole metagenome (which was found in 30% of advanced NSCLC patients))[38]. Within this range, *Akkermansia* spp. was a surrogate marker of a healthy microbiome characterized by the dominance of *Lachnospiraceae* and *Oscillospiraceae* family members[38]. However, a relative overabundance of SGB9226 (or prevalence of

SGB9228, another species of *Akkermansia*) beyond this threshold, observed in about 9% of advanced NSCLC patients, and coinciding with the relative dominance of the immunosuppressive *Enterocloster* genus and *Clostridium* species[20,22] predicted resistance to PD-1 blockade[38]. Hence, this trichotomic distribution of *Akkermansia* spp. (absence, <4.8%, ≥4.8%) allows to accurately predict the clinical benefit of advanced NSCLC treated in 1st or 2nd line with anti-PD-1/PD-L1 antibodies independently of all the other clinical prognostic factors[38,39]. This bacterium also predicted long term survival of patients in 2nd line renal cell carcinoma patients (RCC) treated with nivolumab[23]. The clinical significance of intestinal *Akkermansia* spp. was extended to neoadjuvant settings of ICI in NSCLC patients[90], validating findings obtained in preclinical avatar models using patient stools orally transferred to hepatocarcinoma[100] , sarcoma, kidney, lung and prostate cancer bearing mice[25,38].

Melanoma

Mouse studies have provided compelling evidence that gut microbiome modifications improve ICI response rates via fecal microbiota transplant (FMT)[35,39,88], however, they have also highlighted that factors such as mouse strain or provider, sex and individual experiments can affect the magnitude of anti-tumor responses[102]. Differences have also been observed in the human setting, with single studies investigating the gut microbiome as a potential biomarker of response as well as a therapeutic target in melanoma, identifying species such as *Faecalibacterium prausnitzii*, *Bifidobacterium longum* and *Bacteroides caccae* to be associated with responders[35,41,88], but with limited concordance on which microbiome characteristics are associated with treatment responses across studies[94]. To overcome this, recent studies have used multiple cohorts and meta-analytical approaches[36,37,103,104], identifying a panel of species, including *Bifidobacterium pseudocatenulatum*, *Roseburia* spp. and *A. muciniphila*, associated with responders (R), while *Veillonella parvula*, *Bacteroides* spp., *Clostridium* spp., *Parasutterella excrementihominis*, *Scardovia wiggsiae*, *Oribacterium sinus*, and *Megasphaera micronuciformis* were associated with non-responders (NR). However, no single species was reproducibly shown as a fully consistent biomarker of response across studies. To solve this problem, McCulloch et al. incremented a new cohort into four published datasets[37]. The authors confirmed that baseline microbiota composition was associated with 1 year-progression- free survival. Meta-analysis of the combined data confirmed that bacteria associated with favorable response belonged to *Lachnospiraceae/Bifidobacteriaceae* families (including many *Ruminococcus/Mediterraneibacter* spp., and *Blautia* spp.) and proposed two opposite gut microbiome signatures enriched for *Lachnospiraceae* spp. and *Streptococcaceae* spp. (for favorable and unfavorable prognosis respectively) to best predict

outcome during immunotherapy[37]. In addition, they identified associations between Gram-negative bacteria, an inflammatory host intestinal gene signature, a rise in the blood neutrophil-to-lymphocyte ratio, and unfavorable outcome. Despite between-cohort heterogeneity, optimized all-minus-one supervised learning algorithms trained on batch-corrected microbiome data consistently predicted outcomes to PD-1 blockade in all melanoma cohorts[37].

Cohort effects, which can encompass many factors, including methodological choices in sample processing and analysis, could potentially reconcile differences in the "responder (R)" versus "non responder (NR)" GOMS found across cohorts. Geographical differences can play a major role in human gut microbiota variation[105] and have been shown to have an effect also in melanoma R/NR GOMS[37,106]. Indeed, cross-validation identified unfavorable bacteria of the *Bacteroidetes* phylum as predictive for most cohorts, while favorable bacteria of the *Clostridium* phylum were predictive only for subsets of cohorts[37]. Dietary driven gut microbiome variation is another driver of cohort effects, as higher dietary fiber has been linked with response to ICIs in melanoma patients[50] and gut microbiome assembly patterns[106].

Pan-cancer R versus NR GOMS

To decipher whether R and NR GOMS were significantly different across cohorts and geographical sites in a meta-and mega-analysis **(GLOSSARY)**, we performed fecal taxonomic profiling with MetaPhlAn 4[34] on 808 patients classified as responders (R, n=263) and non-responders (NR, n=545), based on RECIST1.1, criteria for objective response rates (R and NR assembled PR + CR, and SD +PD respectively) comprising 12 cohorts from 8 published studies[23,35–41] **(Table S5)**. Using the mega-analysis approach at the single SGB level **(refer to supplemental material for detailed methodology and Figure 3)**, NR-GOMS comprised microbes already described as immunosuppressive, such as the *Enterocloster* and the *Anaerotruncus* genera, *Eisenbergiella tayi*, *Hungatella hathewayi* or *C. symbiosum*, or pro-inflammatory *Veillonellaceae, Eggerthellaceae Enterobacteriaceae, Erysipelotrichaceae* family members and oral genera (*Streptococcus* and *Actinomyces*) shared across various pathological disorders[9,20,38,94] **(Figure 3)**. In fact, many taxa from the NR-GOMS were already within those contrasting cancer bearers versus healthy individuals[22] **(Figure 2, Table S1)**. In contrast, R-GOMS encompasses genera belonging to the healthy status and SCFA **(GLOSSARY)** producers such as *Lachnospiraceae* (*Roseburia, Coprococcus, Blautia, Eubacterium, Dorea* spp.), *Ruminococcaceae* family members and the propionate producing *A. muciniphila* (SGB9226). Hence, a number of organisms involved in the fermentation of dietary fibers, and representing a major fraction of the butyrate production (including *Faecalibacterium prausnitzii, Eubacterium rectale, Roseburia* spp.,

Fusicatenibacter saccharivorans and *Anaerobutyricum hallii*) are within this fingerprint **(Figure 3, Table S6)**. The meta-analysis approach **(refer to supplemental material for detailed methodology, Table S1, Figure 4 and Table S7)** unveiled additional taxa associated with ORR, including immunogenic commensals such as *Alistipes shahii*[107], *Bifidobacterium bifidum* and *B. adolescentis*, and *Prevotella copri* SGB1626 (also part of the health-related blueprint)[20,37]. Distinct species from the R-GOMS were already in the list of those taxa associated with the healthy status[22] **(Figure 2)** i.e. *Faecalibacterium* SGB15346*, Clostridia bacterium* SGB15383*, and Roseburia hominis* SGB4936*.*

A Random Forest model applied in a leave-one-dataset-out (LODO) setting on a total of 761 cancer patients amenable to ICI (for whom gender and age were available) built to differentiate patients with objective responses (CR+PR) from NR (SD+PD) had a moderate and rather inconsistent predictive power across left-out datasets and a still modest predictive power when merging all dataset for a single cross-validation evaluation (AUC = 0.71, **Table S5**). These results are consistent with individual reports showing that these groups were compositionally distinguishable but with limited overlap of biomarkers across studies. Of note, NSCLC and RCC displayed better AUC predictive values compared with melanoma cohorts.

Hence, GOMS could become valuable predictors of response to ICI as patients incrementality increase, with some degree of overlap between healthy individuals with ICI responders, and any pathological failure with ICI non responders. Overall, increasing the sample size of single cohorts, standardization of protocols across cohorts, and more systematic integrative analysis together with data sharing, are particularly needed for finding biomarkers of response to immunotherapy.

Monitoring GOMS functions

Immunogenicity of GOMS

T cell responses against commensals are commonly found in healthy individuals, suggesting that they participate in intestinal homeostasis by producing barrier protective cytokines and a large pool of pathobiont-reactive T cells[108]. In a large survey of HV, enteric bacteria-reactive $CD4^+$ T cells were present at precursor frequencies of 40-500 cells per 10^6 circulating $CD4^+$ T cells for almost all enteric bacteria analyzed[108]. Bacteria-reactive T cells were 3- to 8-fold more frequent in gut tissue as compared with those in circulation. Microbiota-reactive T cells produced IL-2 and TNFα, and co-expressed CCR7, CCR4, CD161, and CCR6 in various combinations, some of which also expressed integrin β7 and CCR9. When comparing gut microbiota (*E. coli, B. animalis, F. prausnitzii, R. hominis, R. obeum*, …) -reactive

$CD4^+$ T cells with those reactive to non-enteric organisms (including *S. aureus, M. tuberculosis,* and *C. albicans*), enteric bacteria-reactive T cells were partially enriched only in CCR4 expression. Gut-resident bacteria-reactive T cells produced high amounts of IFNγ, IL-17A and IL-2, while production of IL-22, GM-CSF, and IL-4 was low[108]. Interestingly, lamina propria T cells showed increased IL-17A expression and reduced IFNγ production relative to cells with similar specificity in blood. Microbiota-reactive memory T cells harbored frequent co-expression of IL17A, IL-22, and IFNγ. However, a subset of $CD4^+$ T cells reactive to *F. prausnitzii, L. acidophilus,* or *B. animalis* produced the immunoregulatory cytokine IL-10 in addition to IFNγ and IL-17A. This cytokine release may have biological significance, as suggested by the inhibitory effects of triple blockade of IFNγ, IL17A, and TNFα on the capacity of the bacteria-reactive T cells to activate non hematopoietic intestinal stromal and epithelial cells *in vitro*. In pathological circumstances of mucosal barrier dysfunction such as the one observed in patients suffering from inflammatory bowel diseases (IBD), circulating and gut-resident microbiota-reactive $CD4^+$ T cells expressed increased frequencies of IL-17A[108]. IBD results in excessive translocation of luminal antigens, eliciting both mucosal and systemic immune responses. The humoral immune response against gut microbiota has clinical significance in IBD as it may exacerbate intestinal inflammation[109,110]. The repertoire of IgA- and IgG -tagged commensals has been widely studied in IBD and compared to healthy subjects. A variety of humoral immune responses are directed against the majority of the main fecal genera in HV and IBD patients, with a great overlap between both groups. Anti-IgG-based flow cytometry of fecal samples revealed that between 13-77% (mean: 38%) of bacteria showed IgG-coating after incubation with autologous serum[110]. In particular, serum IgG were directed against representatives of the small intestinal microbiota (such as *Streptococcus, Coprococcus, Dorea, Ruminococcus gnavus*-like bacteria, *Lactobacillus, Dialister, Veillonella*, and *Turicibacter*) as opposed to colonic anaerobic bacterial genera (such as *Faecalibacterium, Roseburia, and Blautia*). IgG-coated bacterial genera are consistently among those reported to be increased in abundance in stools from patients with IBD. The observed enrichment after IgG-coating of several types of Lachnospiraceae and species from the Enterocloster genus (e.g., *Enterocloster bolteae and Enterocloster clostridioformis*) or *Ruminococcus gnavus* could be explained by bacterial flagella or flagellins, reported to be highly immunogenic proteins and dominant antigens in the context of IBD[111,112]. The highly immunogenic properties of flagellin may be related to the seminal function of bacterial flagella which enhance contact with a disrupted epithelial barrier and facilitate bacterial transport across the epithelial mucus layer.

A few lines of evidence indicate the potential clinical relevance of IgG responses against microbial antigens in cancer patients **(Table 2)**. As outlined above, a compromised ileal mucosa is eventually

characterizing some malignancies leading to increased serum levels of sCD14, and ST2, both proxies of intestinal barrier leakage[22]. As demonstrated in mouse models of colon cancers, immune responses directed against gut microbiota participate in cancer immunosurveillance[113]. B cell proliferative responses to several commensals were increased in colorectal cancer patients (compared with HV), mostly directed towards *B. ovatus*, *Hafnia* spp., *Veillonella atypica* and the fungi *Candida albicans*[114]. Recently, Meylan *et al.* unveiled a new pilar of renal cell cancer (RCC) immunosurveillance[115]. RCC favoring the formation of tertiary lymphoid structures (TLS) and in situ B cell maturation promoted IgG secreting plasma cell differentiation culminating in tumor cell labeling with IgG and RCC apoptosis. Patients with IgG-labeled RCC cells had high response rate to ICI and prolonged PFS[115]. Intriguingly, Goubet *et al.* brought up evidence that intra-tumoral bacteria infecting the uroepithelial layer of bladder cancers may represent a prominent target for follicular T helper cells (TFH) and B cells within TLS, linking innate and cognate $CD8^+$ T cell memory responses[116]. Indeed, memory bladder TFH responses against uropathogenic *E.coli* (UPEC) had clinical significance in locally advanced and metastatic muscle invasive bladder cancer (MIBC) patients treated with anti-PD-1 Abs[116]. Circulating central memory TFH accumulated in tumors, where they differentiated into CXCL13-producing effector memory TFH. CXCL13 plasma levels increased in pembrolizumab-treated R but not NR. Memory CXCL13-producing TFH recognized urinary *E. coli* residing in tumor and myeloid cells of the TME. Baseline memory *E. coli*-restricted $CXCL13^+$ TFH immune responses were mostly detectable in MIBC patients prone to respond to neoadjuvant pembrolizumab[116] (**Table 2**). Importantly, serum IgG directed against urothelium invasive *Escherichia coli* (but not the other urinary commensals) were associated with favorable clinical responses in three independent cohorts of stage III or IV MIBC treated with ICI[116]. Finally, the MHC class II-dependent reactivation of bacteria-reactive TFH and antibody secreting cells within MIBC exposed to *E. coli* led to the release of CCL19 and CCL21, two prototypic chemokines involved in TLS formation[116]. Given that urinary commensals and pathobionts could originate from bowels[117,118], the diagnosis of gut dysbiosis might have important consequences at remote sites including the TME. Further validation of the clinical relevance of UPEC in MIBC patients treated with ICI in prospective studies is warranted and may be generalized to any neoplasia developing at portals of entry, where local or intestinal microbiota may be harnessed for ICI optimal efficacy.

Beyond the immunogenicity of intra-tumoral bacteria that will be processed and presented by tumor exposed-MHC molecules, other molecular cues involving molecular mimicry between commensals and cancer antigens or the intrinsic adjuvanticity of intestinal microbes could account for T cell reactivation in the TME. Bacteria-reactive T cells might play the role of by -stander T helper cells or T cells endowed

with cross-reactive T cell receptors, recognizing epitopes shared between the intestinal ecosystem and cancer antigens[119,120]. Several independent studies in cancer patients reported that cellular immune responses against selected intestinal commensals are associated with clinical outcome to cancer therapies across various countries and continents[39,121–124]. Hence, TH1 immune responses directed against *B. fragilis* and *A. muciniphila* were selectively associated with responses to ipilimumab (anti-CTLA-4 Ab) in melanoma patients[121] and to anti-PD-1 Abs in RCC and NSCLC cancers respectively[39] **(Table 2)**. *Enterococcus hirae*-specific memory TH1 cells correlated with clinical benefit to chemotherapy in advanced lung cancer[122] and favorable prognosis in hepatitis C virus-induced hepatocarcinoma in China[123] **(Table 2)**. The presence of an antigenic enterophage which lysogenized *E. hirae* and belonged to the *Siphoviridae* family within stools of RCC and NSCLC patients at baseline was associated with prolonged overall survival[120]. Finally, IgG responses directed against the allogeneic microflora post -fecal microbial transplantation correlated with efficient colonization of the exogenous ecosystem and clinical benefit to the re-introduction of therapy after primary resistance to ICI[124].

Approaching GOMS-related functions

Monitoring of gut microbiota functions has been assessed using several methodologies. Using the metagenomic data, organism-specific gene hits are annotated according to the Kyoto Encyclopedia of Genes and Genomes Orthology **(Table 2)**. Based on these annotations, reads from each sample were reconstructed into metabolic pathways using the MetaCyc hierarchy of pathway classifications. Using the Linear discriminant analysis Effect Size (LEfSe) **(GLOSSARY)**, contrasting hits separating R from NR patients have been reported in many studies, leading to different results[35,37,95,125]. Serial metabolomics of fecal material and/or plasma have been performed in distinct cohorts that will be summarized below. Noninvasive transcriptomics of the exfoliome, the shed intestinal luminal cells contained within fecal samples, allows to identify inflammatory paths expressed by dendritic cells, monocytes, macrophages and neutrophils as well as enterocytes and goblet cells[126].

SCFA

Short-chain fatty acids are major end product metabolites produced by the gut microbiota that act at various levels of host physiology[127]. SCFAs such as acetate, propionate, and butyrate are water-soluble and diffusible gut-microbiota-derived metabolites, reaching their peak concentrations in the caecum and decreasing from the proximal to the distal colon[128]. SCFA exhibit context-dependent functions.

They were shown to promote the expansion of Tregs, but they also could improve effector T cell functions[129–132]. Butyrate was associated with protection from acute inflammatory processes such as autoimmune diseases and graft-versus-host disease[133,134]. Moreover, butyrate also promotes the memory potential and antiviral cytotoxic effector functions of $CD8^+$ T cells[135,136]. Similarly, the SCFA pentanoate (called "valerate") is also a bacterial metabolite generated by low-abundant commensals such as *Megasphaera massiliensis*[137,138]. A recent report showed that *ex vivo* culture of cytotoxic T lymphocytes (CTLs), either derived from the endogenous repertoire or through genetic engineering with a T cell receptor (TCR) or chimeric antigen receptor (CAR), with pentanoate or butyrate could bolster their TH1 cytokine release through mTOR-mediated HDAC inhibition as well as their anti-tumor reactivity[139].

Very few translational research studies analyzed the predictive role of SCFA during immune checkpoint blockade in cancer patients **(Table 2)**. A Japanese study reported in 52 cancer patients amenable to PD-1 blockade that stool SCFA are associated with favorable clinical outcomes in patients with solid cancers treated with PD-1 inhibitors. High concentrations of fecal acetate, propionate, butyrate, and valerate as well as plasma isovalerate were associated with prolonged progression-free survival (PFS)[140]. In contrast, Coutsac *et al.* reported that high blood levels of butyrate and propionate were associated with resistance to CTLA-4 blockade and higher proportion of Treg cells in melanoma patients[141]. Given that preclinical tumor models also unveiled negative effects of SCFA in the efficacy of CTLA-4 blockade or radiotherapy[141,142], further studies need to validate the predictive impact of SCFA in larger cohorts at different geographical sites before leveraging each or all of them, in blood or feces, to the status of biomarkers of immunotherapy (IO) efficacy.

Kynurenine (Kyn)/ Tryptophan (Try) ratio

Indoleamine 2,3-dioxygenase (IDO) is a key enzyme catalyzing the first and rate-limiting step along the kynurenine (Kyn) pathway of tryptophan (Try) metabolism outside the liver, which converts the essential amino acid L-tryptophan to the main metabolite kynurenine[143]. IDO is viewed as an immune checkpoint involved in peripheral immune tolerance since, in the absence of Try, T cell proliferation is inhibited and apoptosis of T cells paves the way to immunosuppression[144]. In NSCLC, Try catabolism is rising, resulting in higher Kyn serum concentration, which has been associated with advanced staging at diagnosis, poorer prognosis and higher resistance to chemotherapy[144,145]. Recently, preclinical evidence suggests that IDO activity can be involved in resistance to immune checkpoint blockade[146]. Two ancillary studies investigated the clinical significance of the Try/Kyn ratio during therapy with ICI in advanced cancer patients **(Table 2)**. First, Botticelli *et al.* assessed baseline serum levels of Try and

Kyn in twenty-six stage IV NSCLC patients treated with second- line nivolumab, enrolled according to the eligibility criteria from registration clinical trials of nivolumab in pretreated NSCLC (CheckMate 017 and CheckMate 057). Analyzing R (7 SD (27%), 5 PR (19%)) and NR (14 PD (54%)) according to RECIST1.1 criteria, they found that patients showing an early progression (within 3 months) to anti-PD-1 Abs harbored significantly higher Kyn/Try ratios than R in univariate and multivariate analysis[147]. Secondly, Li H *et al.* profiled >100 metabolites in pre- and multiple on-treatment patient serum samples from three independent immunotherapy trials (namely in two Phase I trials (CA209-038, NCT01621490; CA209-009, NCT01358721) using liquid chromatography-mass spectrometry, which included 78 patients with advanced melanoma and 91 patients with metastatic RCC treated with nivolumab. They also extended their results to a large randomized Phase III trial (CheckMate 025, NCT01668784) with 743 RCC patients, among which 394 received nivolumab and 349 received everolimus[148]. They identified increased Try to Kyn conversion in response to PD-1 blockade in a subset of melanoma and RCC patients. Kyn/Try temporal raise (by >50%) robustly correlated with reduced overall survival of patients receiving nivolumab. Given the relevance of metabolic adaptations in cancer immunotherapy but the lack of efficacy of the combination of with PD-1 and selective IDO1 co-inhibition among unselected patient populations in the phase 3 ECHO-301/KEYNOTE-252 trial[149], these findings question not only the need for patient stratification based on monitoring serum Kyn/Try evolution in future trials but also the analysis of the dynamic modulation of the gut microbiota during ICI therapy. Indeed, beyond Try catabolism by tumor and myeloid cells, distinct taxa from the gut microbiota deviate Try catabolism into indole and indole derivatives, including indole acetic acid and indole propionic acid capable of engaging AhR[150]. In distinct circumstances such as obesity and/or high fat diet, the increase of IDO activity can shift Try metabolism from the generation of indole derivatives towards Kyn production[151]. These findings are reminiscent of the clinical relevance of the Try/anthranilate pathway in cancer patients during COVID19, an infectious disease exacerbating lymphopenia and reducing patient survival during the first phase of the pandemic[152,153].

L-arginine

Not only Try but also intracellular L-arginine concentrations directly impact both the metabolic fitness and survival of T cells and hence their capacity to mediate effective anti-tumor immune responses in mouse models[154]. Elevating L-arginine (Arg) levels induced global metabolic changes including a shift from glycolysis to oxidative phosphorylation in activated T cells and promoted the generation of central memory-like cells[155]. The correlation between Arg levels and clinical ICI activity was recently

reported by Peyraud *et al.* assessing plasma Arg concentrations before ICI onset in two independent cohorts of patients with advanced cancer (NCT02534649, *n* = 77; NCT03984318, *n* = 296) and in a phase 1 first-in-human study of budigalimab (NCT03000257)[154] **(Table 2)**. In both discovery and validation cohorts, low Arg <42 µM was significantly and independently associated with a reduced clinical benefit rate, progression-free survival, and overall survival. In addition, low Arg levels were associated with increased PD-L1 expression by myeloid cells. Hence, plasma Arg monitoring could represent a suitable biomarker to follow ICI efficacy. In addition, synthetic biological approaches with the use of engineered microbial therapies to deliver high local concentrations of L-Arg represent a unique means of local metabolic modulation of the TME. While dietary L-arginine supplements must be administered daily in high doses, L-Arg bacteria colonize and persist in tumours, continuously releasing L-arginine. The synergy between L-Arg bacterial therapy and PD-L1 blockade leading to potent T cell dependent, long-term anti-tumour immunity was reported[156].

Exfoliome

Investigating advanced melanoma patients treated with PD-1 blockade as a standalone therapy or combined with type I IFN, Mc Culloch *et al.* identified host genes differentially expressed between progressors and responders. Genes encoding pro-inflammatory cytokines (IL-1β and CXCL8), transcription factors (NFKBIZ, NFKBIA, TNFAIP3) and superoxide dismutase were increased in progressors, coinciding with the overrepresentation of Gram negative bacteria in feces, suggesting that LPS could be a major contributor of a pro-inflammatory gene signature in these patients[37] **(Table 2)**. These findings were reminiscent of the first clinical trial assessing fecal transplantation to revert primary resistance to ICI in melanoma, unveiling that plasma CXCL8 stood out as a marker of inefficacy of PD-1 blockade despite microbiota compositional changes[124].

Circulating and intratumoral bacteria

The cancer microbiome has been recently characterized in many different cancer histotypes using a 5R multiplexed bacterial 16S rDNA PCR sequencing technique, FISH and culturomics to gain species-level resolution[66]. This allowed to appreciate the relevant bacterial functional traits for each kind of TME and bacteria intracellular localization in both cancer and immune cells. Whether the tumor microbiome plays a causal role in tumorigenesis or in the metastatic program or whether intratumor bacteria reflect local immunosuppression and superinfections of established neoplasia remain an open conundrum. To determine the clinical relevance of intratumor microbial signatures during ICI-based

therapy, this study examined the bacterial atlas in 29 responders (R) and 48 non responders (NR) in a cohort of metastatic melanoma patients[66]. While the bacterial load was similar in R and NR, multiple bacterial taxa were significantly different between the two groups, notably *Veillonellaceae* and gamma-proteobacteria associated with resistance, as already identified in GOMS.

Moreover, another study investigating biomarkers of response to neoadjuvant pembrolizumab (anti-PD-1 Abs) concluded on the immunological and clinical relevance of uropathogenic *Escherichia coli* in locally advanced urothelial cancers[116]. Pre-existing blood humoral and cellular TFH-based memory $CD4^+$ T cells directed against *E. coli* predicted long term responses to PD-1 blockade that were associated with the presence of tertiary lymphoid structures (TLS) in cystectomy samples[116].

Finally, the cancer mycobiome[157] as well as circulating microbial DNA[158], playing a role in prognosis or early diagnosis of cancer respectively, could also influence the response to ICI and will be another area of prospective research.

Other metabolic pathways handled by the gut microbiota and involved in seminal biological functions relevant in cancer biology or immunosurveillance (such as biliary salts in lipid metabolism and Treg homeostasis[124,159], vitamins[160,161], polyamines[162,163], inosine[164], urolithins[159] , hypoxanthine and histidine[165] or iron bioavailability[37] may turn out to be of potential relevance for therapeutic responses to immunotherapy but prospective studies are awaited to validate these hypotheses.

Altogether, it is likely that the predictive power of GOMS will be improved by other markers (such as PD-L1, DNA mismatch repair, TMB, IL-8, metabolites…) that independently modulates ICI efficacy. Multivariate analyses incorporating these predictors will be performed in meta-cohorts and prospective studies.

GOMS to optimize clinical management

Based on the impact of the gut taxonomic composition on the clinical outcome, at least in response to ICI and potentially CAR-T cell therapy[125], there is a need to prospectively validate the robustness of GOMS patterns in various cancer histological types, cancer staging and lines of therapy and to evaluate GOMS independence from classical and FDA/EMA approved -biomarkers in careful multivariate analyses. Recent findings point out that GOMS may predict efficacy of PD-1 blockade in advanced lung cancers even in PD-L1 negative malignancies[38]. Confounding factors (such as age, gender, comorbidity, comedications, ECOG performance status) should be carefully taken into consideration. It is of

biological relevance to further validate that cancer patients prone to respond to immunotherapy harbor a gut microbiota sharing features of the prototypic health-associated GMS. The next step consists in computing a score encompassing the necessary and sufficient taxa discriminating responders from progressors and in designing user-friendly and actionable tools to monitor their prevalence and/or relative abundance in PCR. Efforts should also be devoted to developing surrogate markers of a healthy or disturbed microbiome, such as metabolic or microbiota-specific humoral and cellular immune response classifiers. These diagnostic tools should allow to prospectively stratify patients exhibiting resistance to ICI, and to follow the dynamics of the fecal taxonomic composition upon cancer treatments and comedications **(Figure 5-6, Table S8)**. Such a strategy may identify patients requiring microbiota-centered interventions (MCI) to improve cancer immunosurveillance and hence guide future clinical trials combining ICI and MCI.

Tables

Table 1. Cancer-associated confounding factors (aging, co-morbidities and co-medications) associated with or causatively link to gut dysbiosis.
October 2022 dating PubMed -related search of stool shotgun metagenomics-defined taxonomic composition in various confounding factors of cancer, listed above. Red boxes: increased relative abundance of the MGS; Blue boxes: decreased relative abundance of the MGS; Purple boxes: increased or decreased relative abundance of the MGS.
The influence of ICI on the intestinal taxonomic composition is currently underway and therefore unavailable for Table 1 and Table S1 completion[166,167].

Table 2. Tumor and host -associated biomarkers of clinical potential to predict ICI efficacy.

Table S1. Gut OncoMicrobiome Signatures (GOMS) pan-disease or pan-cancer versus healthy metagenomes and alignment with the proposed meta-analysis.
This table aims at aligning bacteria composing the core gut microbiome (according to Dutch Microbiome Project; Gacesa et al.)[20], the health-related microbiome (according to Gacesa et al., Yonekura et al.)[20,22] and fecal bacterial taxa with relative overrepresentation across various diseases or in cancer patients regardless of histotypes (according to Gacesa et al., Yonekura et al.)[20,22]. The right columns aligned bacteria significantly retained in the meta-analysis comparing healthy volunteers versus cancer patients presented in **Figure 2.**

Table S2 Cohort description for the meta-analysis comparing GOMS in cancer versus healthy individuals.
Refer to **Figure 2**.

Table S3. Detailed results of Pan-cancer GOMS presented in Figure 2.
We implemented a Bayesian multinomial logistic-normal linear regression model called Pibble from the R package fido, linking covariates that included cancer status, age and gender to compositional

overdispersed count data. We transformed taxonomic relative abundances into count values for Pibble via logistic-normal distribution modeling[168]. Log-ratios with 95% credible intervals were calculated for each SGB (**GLOSSARY**) and each pairwise cancer/control comparison and were supplied to a random effects model via the rem_mv function in the MetaVolcanoR R package (v.1.4.0) using the restricted maximum-likelihood estimator model. We considered only SGBs with 95% credible intervals greater than or less than zero in > 50% of pairwise comparisons and with a rank in at least 6/8 cancers (**Supplementary material**).

Table S4. Gut OncoMicrobiome signatures (GOMS) profile across various cancer histotypes.
For three distinct cancer types for which data are available and reported so far, the bacteria orders, families and genus/species segregating cancer patients from healthy volunteers are detailed. Only bacterial taxa relatively overrepresented (but not underrepresented) in cancer patient fecal samples (compared with health volunteers) are annotated. Cancer histotype-specific bacteria are not in bold.

Table S5. Cohort description and machine learning analysis for R versus NR cancer patients treated with immune checkpoint inhibitors.
We applied a Leave-one-dataset-out (LODO) approach to SGB relative abundances; data from one cohort was set aside as an external validation set, whereas data from the remaining cohorts were pooled together as a single training set, iterating along all the cohorts. Cohorts with more than 20 samples were used in the LODO approach and model performance was assessed using the area under the receiver operator (AUC-ROC) values. RF global CV: random forest global cross validation (**Supplementary material**). A Random Forest model applied in a leave-one-dataset-out (LODO) setting on a total of 761 cancer patients amenable to ICI (for whom gender and age were available) built to differentiate patients with objective responses (CR+PR) from NR (SD+PD) had a moderate and rather inconsistent predictive power across left-out datasets and a still modest predictive power when merging all dataset for a single cross-validation evaluation (AUC = 0.71). These results are consistent with individual reports showing that these groups were compositionally distinguishable but with limited overlap of biomarkers across studies. Of note, NSCLC and RCC displayed better AUC predictive values compared with melanoma cohorts.

Table S6. Baseline GOMS associated with response rates in the mega-analysis presented in Figure 3.
This table reports results from the mega-analysis using Pibble models on clr transformed SGB-level relative abundances presented in **Figure 3** (**Supplementary material**). LogRatio, 95% credible interval and taxonomy by family, genus, species and taxon are detailed. This table includes a summary of the results presented in **Figure 3** by family, genus and species levels.

Table S7. Baseline GOMS associated with response rates in the meta-analysis presented in Figure 4.
This tables reports results from the meta-analysis using different differential abundance methods adjusting for age and gender to identify SGBs associated with ORR, presented in **Figure 4** (**Supplementary material**). This table includes a summary of the results presented in **Figure 4** by family, genus and species levels.

Table S8. Relationships between cancer-associated bacteria relevant for clinical outcome and confounding factors.
The bacteria retained as significant in the meta-and mega-analysis presented in **Table S2-3, S6-7** and **Figure 2-3-4** were highlighted according to their reported association with confounding factors in cancer. October 2022 dating PubMed -related search of stool shotgun metagenomics-defined

taxonomic composition in various confounding factors of cancer, listed above. Red boxes: increased relative abundance of the MGS; Blue boxes: decreased relative abundance of the MGS; Purple boxes: increased or decreased relative abundance of the MGS.

Figure Legends

Figure 1. Microscopic and cellular description of the cancer-induced stress ileopathy.
A-G. Proposed scenario of stress ileopathy induced during a tumorigenic process. Experimental demonstration in cancer bearing mice that tumor inoculation may trigger crypt apoptosis, activation of secretory cells, ectopic proliferation of tyrosine hydroxylase positive and enteroendocrine cells (TH^+ EEC) resulting in a disbalance between cholinergic and adrenergic signaling promoting a transient ileal mucosa atrophy but a protracted gut dysbiosis dominated by vancomycin-sensitive species belonging to the *Enterocloster* genus. Micrograph pictures of HE stained ileal tissues showing patchy abrasion of ileal villosities 7-10 days after tumor implantation in C57BL/6 mice. Bar scale: 100 µm. *CM, circular muscle; ChAT, Choline acetyltransferase; EEC, Enteroendocrine cell; ER, Endoplasmic reticulum; ir-nerves, Immunoreactive nerves; LM, longitudinal muscle; MP, myenteric plexus; REG3γ, Regenerating islet-derived protein 3 gamma; sCD14, Soluble CD14; SMP, submucosal plexus; ST2, Suppression of Tumorigenicity 2 protein; TA, transit amplifying cells; TH, Tyrosine hydroxylase; VAChT, Vesicular acetylcholine transporter*.

Figure 2. Pan-cancer GOMS compared with healthy metagenomics profiles.
Top 30 ranked SGBs in cancer or control cohorts. Ranks were determined by ordering *p-values* calculated using a random effects meta-analysis of all possible cancer and control cohort pairs. Only SGBs with 95% credible intervals greater than or less than zero in > 50% of pairwise comparisons were considered for the ranking.

Figure 3. GOMS-related to R versus NR status before ICI (mega-analysis, ORR).
Results of a mega-analysis using Pibble models on clr transformed SGB-level relative abundances. Pibble models also included age, gender and cohort as covariates. SGBs whose 95% credible interval is greater than or smaller than 0.2 are reported in the figure. Also refer to Table S6 for SGBs with a prevalence higher than 5% and their corresponding 95% credible intervals.

Figure 4. GOMS-related to R versus NR status before ICI (meta-analysis, ORR).
SGBs associated with ORR identified by a meta-analysis using different differential abundance methods adjusting for age and gender. SGBs shown have random-effects model *p-values* < 0.05 in at least three methods. Values inside the cells refer to unadjusted *p-values* < 0.05 obtained by two-tailed Wilcoxon tests on differences in the relative abundance of responders and non-responders. The color of the cell was determined by comparing the mean relative abundance in responders to non-responders; if the mean was higher in responders, then the cells were colored red; if it was higher in non-responders, then it was colored blue. Also refer to Table S7.

Figure 5. Challenges of microbiota-related biomarkers in oncology.
Shotgun metagenomics –based sequencing is currently the state-of the art method to analyze the taxonomic composition of the stools or ileal content and to perform machine learning in cohorts of cancer patients. The challenges of this field are to increment many more patients to stabilize the Gut OncoMicrobiome fingerprint, to design a friendly user diagnosis tool that should be validated prospectively across cancer types, cancer staging, geography, life style, treatments and co-morbidities. This tool will be instrumental to stratify patients according to their gut dysbiosis, for future microbiota centered-intervention or interceptive measures.

Figure 6. Practical prospects toward defining GOMS-related clinical guidelines.
A. Summary of the proposed clinical management of cancer patients amenable to an FDA or EMA-approval of ICI, taking into account gut microbiota composition. Patients with a history of antibiotics (any kind except vancomycin) taken between 60 days prior to, up to 42 after the first administration of anti-PD-1 Abs (alone or combined with anti-CTLA-4 Abs) or comedications known to alter microbiota composition (Proton Pomp Inhibitors (PPI) or laxatives) should be investigated by performing shotgun MG sequencing of stools or targeted PCR at diagnosis to monitor taxonomic composition. **B.** Depending on the relative abundances of *Akkermansia* spp. as well as other family members or genera or species (listed as harmful or beneficial in GOMS) (refer to Figure 3-4), different putative scenarios are described with their respective clinical management as for a potential microbiota-centered intervention to compensate gut dysbiosis. The over-abundance of *Akkermansia* spp. (SGB9226 (*A.muciniphila*) or 9228 or others) is defined by a relative abundance above 4.8% of all species using MetaphLAN or MetaO -MineR algorithms (*A.muc*^{high}). **C.** The pharmacodynamics and kinetics of the MCI should be assessed to monitor their effects on the body metabolic, immunologic or hematologic functions or inflammatory tonus and the gut microbiota composition or deviation from baseline. *Ab, antibody; ATB, antibiotics; Akk, Akkermansia muciniphila; BMI, Body mass index; ECOG PS, Eastern Cooperative Oncology Group performance status; FMT, Fecal microbiota transplant; PPI, Proton pump inhibitor; TILs, Tumor infiltrating lymphocytes; IHC, Immunohistochemistry; sCD14, Soluble CD14; ST2, Suppression of Tumorigenicity 2 protein.*

GLOSSARY

16S ribosomal RNA sequencing (16S rRNA seq): This is a targeted, high-throughput method that consists of amplifying and sequencing the small-subunit ribosomal 16S RNA (rRNA) gene present in a sample (*i.e* a microbial community). Sequences are generally the result of a targeted amplification of one or more variable regions within the 16S rRNA gene, and can be used to profile the taxonomic composition of archaeal and eubacterial members of the microbial community. This method provides lower taxonomic resolution but is generally less computationally intensive, however, there are a variety of processing steps that can introduce bias and limit the ability to combine data from different studies.

Biomarker: A defined characteristic that is measured as an indicator of normal or pathogenic processes or responses to an exposure or therapeutic intervention.

Co-medications: Other treatments received by patients alongside anticancer drugs to treat comorbidities.

Co-morbidities: Presence of other concomitant diseases along with cancer.

Dysbiosis: Characterization of a microbiota imbalance with changes in composition and functions.

***Enterocloster* genus:** This genus of the bacteria taxonomy has previously been placed in the genus of *Clostridium group XIV.*

Exposome: The exposome corresponds to a large number of individual expositions from various origins, such as chemical, physical, biological or psychological stimuli. The exposome also takes into account the time dimension of the exposition (short or long, early or late, punctual or repeated

exposition). The exposome has an impact on individual biological functions and to a larger extent, overall health.

ICI: Immune checkpoint inhibitors joined the effective cancer immunotherapies approved by FDA or EMA in 2011 and 2014 and consist of monoclonal antibodies that prevent immune checkpoint receptor binding to their ligands and their intracellular signaling.

LEfSe: Linear discriminant analysis Effect Size determines the features (organisms, clades, operational taxonomic units, genes, or functions) most likely to explain differences between classes by coupling standard tests for statistical significance with additional tests encoding biological consistency and effect relevance.

Meta-analysis: The analysis encompasses various statistical methods to synthesize empirical research.

Mega-analysis: The analysis gathers raw data across multiple studies.

ORR (CR+PR vs SD+PD): complete and partial responses (objective responses) according to RECIST 1.1 criteria as opposed to non-objective responses which are stable diseases or progression.

SCFA: Short-chain fatty acids are metabolic by-products derived from the fermentation of carbohydrate by anaerobic bacteria in the gut.

SGB: Large-scale metagenomics has uncovered a myriad of bacteria never before described. The species-level genome bins (SGBs) nomenclature helps annotate sequenced bacteria to the species level.

Shotgun metagenomic sequencing (MGS): This is a non-targeted, high-throughput method that consists of sequencing all DNA present in a sample (*i.e* a microbial community). These DNA sequences are computationally analyzed and can be used to profile the taxonomic composition of members of the microbial community, including bacteria, fungi and viruses.

Stress ileopathy: Ileal mucosa atrophy associated with dominance of sympathetic over cholinergic signaling provoked by intra and extraintestinal malignancies.

Abbreviations:
16S rRNA, 16S ribosomal RNA; Abs, Antibodies; Adrb2, Adrenoceptor Beta 2; AMP, Antimicrobial peptide; Arg, Arginine; ATB, Antibiotics; AUC, Area under the ROC Curve; BC, Breast cancer; CAR, Chimeric antigen receptor; ChAT, Choline acetyltransferase; CRC, Colorectal cancer; CTLs, Cytotoxic T lymphocytes; DMP, Dutch Microbiome Project; ECOG PS, Eastern Cooperative Oncology Group performance status; EEC, Enteroendocrine cell; EMA, European Medicines Agency; EO, Early-onset; FDA, US Food and Drug Administration ; FISH , Fluorescent in situ hybridization; FMT, Fecal microbiota transplant; GM-CSF, Granulocyte-monocyte colony-stimulating factor; GMHI, Gut Microbiome Health Index; GMS, Gut Microbiome Signature; GOMS, Gut OncoMicrobiome Signature; HDAC, Histone deacetylase; HV, Healthy volunteer; IBD, Inflammatory bowel diseases; ICI, Immune checkpoint inhibitors; IDO, Indoleamine 2,3-dioxygenase; IFNγ, Interferon gamma; Ig, Immunoglobulin; IL, Interleukin; IO, Immunotherapy; irAEs, Immune-related adverse events; ir-nerves, Immunoreactive nerves; Kyn, Kynurenine; LEfSe, Linear discriminant analysis Effect Size; LODO, Leave-one-dataset-out; LP, Lamina propria; LPS, Lipopolysaccharide; MCI, Microbiota-centered interventions; MHC, Major

histocompatibility complex; MIBC, Muscle invasive bladder cancer; mTOR, Mechanistic Target Of Rapamycin Kinase; NR, Non-responder; NSCLC, Non-small lung cancer; ORR, Objective response rate; OS, Overall survival; PCR, Polymerase chain reaction; PDAC, Pancreatic ductal carcinoma; PFS, Progression-free survival; PPI, Proton pump inhibitor; R, Responder; RCC, Renal cell carcinoma; RECIST 1.1, Response Evaluation Criteria In Solid Tumors v1.1 (revised); REG3γ, Regenerating islet-derived protein 3 gamma; ROC curve, Receiver operating characteristic curve; sCD14, Soluble CD14; SGB, Species-level genome bin; sp, Specie; spp, Several species; ST2, Suppression of Tumorigenicity 2 protein; TCR, T cell receptor; TFH, T follicular helper; TH, Tyrosine hydroxylase; TILs, Tumor infiltrating lymphocytes; TLS, Tertiary lymphoid structures; TME, Tumor microenvironment; TNFα, Tumor necrosis factor alpha; Tregs, T regulatory cells; Try, Tryptophan; UPEC, Uropathogenic Escherichia coli; VAChT, Vesicular acetylcholine transporter

Supplementary Methods (separate online file)

Authors' contribution: LZ wrote the main text except the description of the CRC and melanoma microbiome subparts performed by AMT and NS. AMT and NS performed the meta-and mega-analyses. GK and JAW edited the English. MF and BR performed the Tables and Figures.

CONFLICTS OF INTEREST

L.Z is the scientific cofounder and the President of the scientific advisory board of EverImmune, a company devoted to the use of commensal microbes Oncobax for the treatment of cancers. LZ receives research grants from 9 meters, everImmune, Pileje, Daichi Sankyo to deconvolute the therapeutic mode of action of new drugs, prebiotics, or Oncobax on the gut ecosystem and immune responses. L.Z was a former member of the board of directors of Transgene and a former consulting expert for BMS, GSK, Tusk, Lytix biotherapeutics. A.M.T., M.F., N.S. have no conflict of interest. B.R. reports grants from AstraZeneca, Merck, Bristol Myers Squibb, Davoltera, Kaleido, and Vedanta outside the submitted work, as well as a patent for G17004-00006-AD (use of castalagin or analogs thereof for anticancer efficacy and to increase the response to immune-checkpoint inhibitors) pending. G.K. has been holding research contracts with Daiichi Sankyo, Elior, Kaleido, Lytix Pharma, PharmaMar, Samsara, Sanofi, Tollys, Vascage and Vasculox/Tioma. G.K. is on the Board of Directors of the Bristol Myers Squibb Foundation France. G.K. is a scientific co-founder of everImmune, Osasona Therapeutics, Samsara Therapeutics and Therafast Bio. G.K. is the inventor of patents covering therapeutic targeting of aging, cancer, cystic fibrosis and metabolic disorders. J.A.W. is an inventor on a US patent application (PCT/US17/53.717) submitted by the University of Texas MD Anderson Cancer Center which covers methods to enhance immune checkpoint blockade responses by modulating the microbiome, reports compensation for speaker's bureau and honoraria from Imedex, Dava Oncology, Omniprex, Illumina, Gilead, PeerView, Physician Education Resource, MedImmune, Exelixis and Bristol Myers Squibb, and

has served as a consultant/advisory board member for Roche/Genentech, Novartis, AstraZeneca, GlaxoSmithKline, Bristol Myers Squibb, Micronoma, OSE therapeutics, Merck, and Everimmune. Dr. Wargo receives stock options from Micronoma and OSE therapeutics.

Acknowledgements

L. Zitvogel was supported by RHU5 "ANR-21-RHUS-0017" IMMUNOLIFE, SIRIC Stratified Oncology Cell DNA Repair and Tumor Immune Elimination (SOCRATE), SIGN'IT ARC foundation, European Union's Horizon 2020 research and innovation programme under grant agreement number 825410 [project acronym: ONCOBIOME, project title: Gut OncoMicrobiome Signatures (GOMS) associated with cancer incidence,prognosis, and prediction of treatment response], European Union's Horizon Europe research and innovation programme under grant agreement number 101095604 - GAP-101095604 -[project acronym: PREVALUNG-EU, project title: Personalized lung cancer risk assessment leading to stratified Interception], ANR grant–French-German Ileobiome 19-CE15-0029-01. L.Zitvogel and G. Kroemer received a donation from the Seerave Foundation. L. Zitvogel and G. Kroemer were supported by the Ligue contre le Cancer (Equipe labelisée); ANR projets blancs;Cancéopole Ile-de-France; Fondation pour la Recherche Médicale (FRM); a donation by Elior; Institut National du Cancer (INCa); Inserm (HTE); Institut Universitaire de France; the LabEx Immuno-Oncology; and FHU CARE, Dassault, and Badinter Philantropia. M. Fidelle was funded by SEERAVE Foundation. N. Segata was supported by the European Research Council (ERC-STG project MetaPG-716575 and ERC-CoG microTOUCH-101045015), by the European H2020 program (ONCOBIOME-825410 project, MASTER-818368 project, and IHMCSA-964590), by the National Cancer Institute of the National Institutes of Health (1U01CA230551), and by the Premio Internazionale Lombardia e Ricerca 2019. Andrew Maltez Thomas is a new employee of Microbiotica. B. Routy was supported by the Fonds de la Recherche Québec-Santé (FRQS), Canadian Institute for Health Research (CIHR), Weston and Seerave foundations, and Terry Fox Marathon of Hope Program. J.A.W. is supported by NIH (1 R01 CA219896-01A1), Melanoma Research Alliance (4022024), American Association for Cancer Research Stand Up To Cancer (SU2C-AACR-IRG-19-17), and MD Anderson Cancer Center's Melanoma Moon Shots Program.

References:

1. Hanahan, D. Hallmarks of Cancer: New Dimensions. *Cancer Discovery* **12**, 31–46 (2022).
2. Cassidy, L. D. *et al.* Temporal inhibition of autophagy reveals segmental reversal of ageing with increased cancer risk. *Nat Commun* **11**, 307 (2020).
3. Demaria, M. *et al.* Cellular Senescence Promotes Adverse Effects of Chemotherapy and Cancer Relapse. *Cancer Discovery* **7**, 165–176 (2017).
4. López-Otín, C. & Kroemer, G. Hallmarks of Health. *Cell* **184**, 33–63 (2021).
5. Derosa, L. *et al.* The immuno-oncological challenge of COVID-19. *Nat Cancer* **1**, 946–964 (2020).
6. Rutkowski, M. R. *et al.* Microbially Driven TLR5-Dependent Signaling Governs Distal Malignant Progression through Tumor-Promoting Inflammation. *Cancer Cell* **27**, 27–40 (2015).
7. McKee, A. M. *et al.* Antibiotic-induced disturbances of the gut microbiota result in accelerated breast tumor growth. *iScience* **24**, (2021).
8. Buchta Rosean, C. *et al.* Preexisting Commensal Dysbiosis Is a Host-Intrinsic Regulator of Tissue Inflammation and Tumor Cell Dissemination in Hormone Receptor–Positive Breast Cancer. *Cancer Research* **79**, 3662–3675 (2019).
9. Ghosh, T. S., Das, M., Jeffery, I. B. & O'Toole, P. W. Adjusting for age improves identification of gut microbiome alterations in multiple diseases. *eLife* **9**, e50240 (2020).
10. Wilmanski, T. *et al.* Gut microbiome pattern reflects healthy ageing and predicts survival in humans. *Nat Metab* **3**, 274–286 (2021).
11. Bindels, L. B. *et al.* Increased gut permeability in cancer cachexia: mechanisms and clinical relevance. *Oncotarget* **9**, 18224–18238 (2018).

12. Ubachs, J. *et al.* Gut microbiota and short-chain fatty acid alterations in cachectic cancer patients. *Journal of Cachexia, Sarcopenia and Muscle* **12**, 2007–2021 (2021).
13. Zitvogel, L., Ma, Y., Raoult, D., Kroemer, G. & Gajewski, T. F. The microbiome in cancer immunotherapy: Diagnostic tools and therapeutic strategies. *Science* **359**, 1366–1370 (2018).
14. Claesson, M. J. *et al.* Composition, variability, and temporal stability of the intestinal microbiota of the elderly. *Proc Natl Acad Sci U S A* **108 Suppl 1**, 4586–4591 (2011).
15. Roager, H. M. & Licht, T. R. Microbial tryptophan catabolites in health and disease. *Nat Commun* **9**, 3294 (2018).
16. Sonowal, R. *et al.* Indoles from commensal bacteria extend healthspan. *Proceedings of the National Academy of Sciences* **114**, E7506–E7515 (2017).
17. Alexeev, E. E. *et al.* Microbiota-Derived Indole Metabolites Promote Human and Murine Intestinal Homeostasis through Regulation of Interleukin-10 Receptor. *The American Journal of Pathology* **188**, 1183–1194 (2018).
18. Bindels, L. B. *et al.* Synbiotic approach restores intestinal homeostasis and prolongs survival in leukaemic mice with cachexia. *ISME J* **10**, 1456–1470 (2016).
19. Sato, Y. *et al.* Novel bile acid biosynthetic pathways are enriched in the microbiome of centenarians. *Nature* **599**, 458–464 (2021).
20. Gacesa, R. *et al.* Environmental factors shaping the gut microbiome in a Dutch population. *Nature* **604**, 732–739 (2022).
21. Jackson, M. A. *et al.* Proton pump inhibitors alter the composition of the gut microbiota. *Gut* **65**, 749–756 (2016).

22. Yonekura, S. *et al.* Cancer Induces a Stress Ileopathy Depending on β-Adrenergic Receptors and Promoting Dysbiosis that Contributes to Carcinogenesis. *Cancer Discovery* **12**, 1128–1151 (2022).
23. Derosa, L. *et al.* Gut Bacteria Composition Drives Primary Resistance to Cancer Immunotherapy in Renal Cell Carcinoma Patients. *Eur Urol* **78**, 195–206 (2020).
24. Terrisse, S. *et al.* Intestinal microbiota influences clinical outcome and side effects of early breast cancer treatment. *Cell Death Differ* **28**, 2778–2796 (2021).
25. Terrisse, S. *et al.* Immune system and intestinal microbiota determine efficacy of androgen deprivation therapy against prostate cancer. *J Immunother Cancer* **10**, e004191 (2022).
26. Pernigoni, N. *et al.* Commensal bacteria promote endocrine resistance in prostate cancer through androgen biosynthesis. *Science* **374**, 216–224 (2021).
27. Geller, L. T. *et al.* Potential role of intratumor bacteria in mediating tumor resistance to the chemotherapeutic drug gemcitabine. *Science* **357**, 1156–1160 (2017).
28. Collins, J. R. Small Intestinal Mucosal Damage with Villous Atrophy: A Review of the Literature. *American Journal of Clinical Pathology* **44**, 36–44 (1965).
29. Gilat, T., Fischel, B., Danon, J. & Loewenthal, M. Morphology of Small Bowel Mucosa in Malignancy. *DIG* **7**, 147–155 (1972).
30. Stanley, D. *et al.* Translocation and dissemination of commensal bacteria in post-stroke infection. *Nat Med* **22**, 1277–1284 (2016).
31. Singh, V. *et al.* Microbiota Dysbiosis Controls the Neuroinflammatory Response after Stroke. *J. Neurosci.* **36**, 7428–7440 (2016).
32. Lynch, S. V. & Pedersen, O. The Human Intestinal Microbiome in Health and Disease. *N Engl J Med* **375**, 2369–2379 (2016).

33. Gupta, V. K. *et al.* A predictive index for health status using species-level gut microbiome profiling. *Nat Commun* **11**, 4635 (2020).

34. Blanco-Miguez, A. *et al.* Extending and improving metagenomic taxonomic profiling with uncharacterized species with MetaPhlAn 4. 2022.08.22.504593 Preprint at https://doi.org/10.1101/2022.08.22.504593 (2022).

35. Gopalakrishnan, V. *et al.* Gut microbiome modulates response to anti-PD-1 immunotherapy in melanoma patients. *Science* **359**, 97–103 (2018).

36. Lee, K. A. *et al.* Cross-cohort gut microbiome associations with immune checkpoint inhibitor response in advanced melanoma. *Nat Med* **28**, 535–544 (2022).

37. McCulloch, J. A. *et al.* Intestinal microbiota signatures of clinical response and immune-related adverse events in melanoma patients treated with anti-PD-1. *Nat Med* **28**, 545–556 (2022).

38. Derosa, L. *et al.* Intestinal Akkermansia muciniphila predicts clinical response to PD-1 blockade in patients with advanced non-small-cell lung cancer. *Nat Med* **28**, 315–324 (2022).

39. Routy, B. *et al.* Gut microbiome influences efficacy of PD-1-based immunotherapy against epithelial tumors. *Science* **359**, 91–97 (2018).

40. Wind, T. T. *et al.* Gut microbial species and metabolic pathways associated with response to treatment with immune checkpoint inhibitors in metastatic melanoma. *Melanoma Res* **30**, 235–246 (2020).

41. Frankel, A. E. *et al.* Metagenomic Shotgun Sequencing and Unbiased Metabolomic Profiling Identify Specific Human Gut Microbiota and Metabolites Associated with Immune Checkpoint Therapy Efficacy in Melanoma Patients. *Neoplasia* **19**, 848–855 (2017).

42. Nagata, N. *et al.* Metagenomic Identification of Microbial Signatures Predicting Pancreatic Cancer From a Multinational Study. *Gastroenterology* **163**, 222–238 (2022).
43. Yu, J. *et al.* Metagenomic analysis of faecal microbiome as a tool towards targeted non-invasive biomarkers for colorectal cancer. *Gut* **66**, 70–78 (2017).
44. Feng, Q. *et al.* Gut microbiome development along the colorectal adenoma-carcinoma sequence. *Nat Commun* **6**, 6528 (2015).
45. Yachida, S. *et al.* Metagenomic and metabolomic analyses reveal distinct stage-specific phenotypes of the gut microbiota in colorectal cancer. *Nat Med* **25**, 968–976 (2019).
46. Wirbel, J. *et al.* Meta-analysis of fecal metagenomes reveals global microbial signatures that are specific for colorectal cancer. *Nat Med* **25**, 679–689 (2019).
47. Thomas, A. M. *et al.* Metagenomic analysis of colorectal cancer datasets identifies cross-cohort microbial diagnostic signatures and a link with choline degradation. *Nat Med* **25**, 667–678 (2019).
48. Vogtmann, E. *et al.* Colorectal Cancer and the Human Gut Microbiome: Reproducibility with Whole-Genome Shotgun Sequencing. *PLoS One* **11**, e0155362 (2016).
49. Zeller, G. *et al.* Potential of fecal microbiota for early-stage detection of colorectal cancer. *Mol Syst Biol* **10**, 766 (2014).
50. Spencer, C. N. *et al.* Dietary fiber and probiotics influence the gut microbiome and melanoma immunotherapy response. *Science* **374**, 1632–1640 (2021).
51. Kartal, E. *et al.* A faecal microbiota signature with high specificity for pancreatic cancer. *Gut* **71**, 1359–1372 (2022).
52. Peters, B. A. *et al.* Relating the gut metagenome and metatranscriptome to immunotherapy responses in melanoma patients. *Genome Med* **11**, 61 (2019).

53. Asnicar, F. *et al.* Microbiome connections with host metabolism and habitual diet from 1,098 deeply phenotyped individuals. *Nat Med* **27**, 321–332 (2021).

54. De Filippis, F. *et al.* Distinct Genetic and Functional Traits of Human Intestinal Prevotella copri Strains Are Associated with Different Habitual Diets. *Cell Host Microbe* **25**, 444-453.e3 (2019).

55. Dhakan, D. B. *et al.* The unique composition of Indian gut microbiome, gene catalogue, and associated fecal metabolome deciphered using multi-omics approaches. *Gigascience* **8**, giz004 (2019).

56. Human Microbiome Project Consortium. Structure, function and diversity of the healthy human microbiome. *Nature* **486**, 207–214 (2012).

57. Keohane, D. M. *et al.* Microbiome and health implications for ethnic minorities after enforced lifestyle changes. *Nat Med* **26**, 1089–1095 (2020).

58. Zhernakova, A. *et al.* Population-based metagenomics analysis reveals markers for gut microbiome composition and diversity. *Science* **352**, 565–569 (2016).

59. Vieira-Silva, S. *et al.* Statin therapy is associated with lower prevalence of gut microbiota dysbiosis. *Nature* **581**, 310–315 (2020).

60. Nielsen, H. B. *et al.* Identification and assembly of genomes and genetic elements in complex metagenomic samples without using reference genomes. *Nat Biotechnol* **32**, 822–828 (2014).

61. Qin, J. *et al.* A metagenome-wide association study of gut microbiota in type 2 diabetes. *Nature* **490**, 55–60 (2012).

62. Qin, N. *et al.* Alterations of the human gut microbiome in liver cirrhosis. *Nature* **513**, 59–64 (2014).

63. Schirmer, M. *et al.* Linking the Human Gut Microbiome to Inflammatory Cytokine Production Capacity. *Cell* **167**, 1897 (2016).
64. Xie, H. *et al.* Shotgun Metagenomics of 250 Adult Twins Reveals Genetic and Environmental Impacts on the Gut Microbiome. *Cell Syst* **3**, 572-584.e3 (2016).
65. Zeevi, D. *et al.* Personalized Nutrition by Prediction of Glycemic Responses. *Cell* **163**, 1079–1094 (2015).
66. Nejman, D. *et al.* The human tumor microbiome is composed of tumor type–specific intracellular bacteria. *Science* **368**, 973–980 (2020).
67. Bogert, B. van den, Meijerink, M., Zoetendal, E. G., Wells, J. M. & Kleerebezem, M. Immunomodulatory Properties of Streptococcus and Veillonella Isolates from the Human Small Intestine Microbiota. *PLOS ONE* **9**, e114277 (2014).
68. Hong, H.-E., Kim, A.-S., Kim, M.-R., Ko, H.-J. & Jung, M. K. Does the Use of Proton Pump Inhibitors Increase the Risk of Pancreatic Cancer? A Systematic Review and Meta-Analysis of Epidemiologic Studies. *Cancers* **12**, 2220 (2020).
69. Zackular, J. P., Rogers, M. A. M., Ruffin, M. T. & Schloss, P. D. The human gut microbiome as a screening tool for colorectal cancer. *Cancer Prev Res (Phila)* **7**, 1112–1121 (2014).
70. Beghini, F. *et al.* Integrating taxonomic, functional, and strain-level profiling of diverse microbial communities with bioBakery 3. *Elife* **10**, e65088 (2021).
71. Rubinstein, M. R. *et al.* Fusobacterium nucleatum promotes colorectal carcinogenesis by modulating E-cadherin/β-catenin signaling via its FadA adhesin. *Cell Host Microbe* **14**, 195–206 (2013).
72. Long, X. *et al.* Peptostreptococcus anaerobius promotes colorectal carcinogenesis and modulates tumour immunity. *Nat Microbiol* **4**, 2319–2330 (2019).

73. Drewes, J. L. *et al.* High-resolution bacterial 16S rRNA gene profile meta-analysis and biofilm status reveal common colorectal cancer consortia. *NPJ Biofilms Microbiomes* **3**, 34 (2017).

74. Flemer, B. *et al.* The oral microbiota in colorectal cancer is distinctive and predictive. *Gut* **67**, 1454–1463 (2018).

75. Schmidt, T. S. *et al.* Extensive transmission of microbes along the gastrointestinal tract. *Elife* **8**, e42693 (2019).

76. Nakatsu, G. *et al.* Alterations in Enteric Virome Are Associated With Colorectal Cancer and Survival Outcomes. *Gastroenterology* **155**, 529-541.e5 (2018).

77. Tomkovich, S. *et al.* Human colon mucosal biofilms from healthy or colon cancer hosts are carcinogenic. *J Clin Invest* **129**, 1699–1712 (2019).

78. Dejea, C. M. *et al.* Microbiota organization is a distinct feature of proximal colorectal cancers. *Proc Natl Acad Sci U S A* **111**, 18321–18326 (2014).

79. Lui, R. N. *et al.* Global Increasing Incidence of Young-Onset Colorectal Cancer Across 5 Continents: A Joinpoint Regression Analysis of 1,922,167 Cases. *Cancer Epidemiol Biomarkers Prev* **28**, 1275–1282 (2019).

80. Yang, Y. *et al.* Dysbiosis of human gut microbiome in young-onset colorectal cancer. *Nat Commun* **12**, 6757 (2021).

81. Kong, C. *et al.* Integrated metagenomic and metabolomic analysis reveals distinct gut-microbiome-derived phenotypes in early-onset colorectal cancer. *Gut* gutjnl-2022-327156 (2022) doi:10.1136/gutjnl-2022-327156.

82. Thomas, A. M. & Segata, N. Multiple levels of the unknown in microbiome research. *BMC Biol* **17**, 48 (2019).

83. Lin, Y. *et al.* Altered Mycobiota Signatures and Enriched Pathogenic Aspergillus rambellii Are Associated With Colorectal Cancer Based on Multicohort Fecal Metagenomic Analyses. *Gastroenterology* **163**, 908–921 (2022).

84. Liu, N.-N. *et al.* Multi-kingdom microbiota analyses identify bacterial-fungal interactions and biomarkers of colorectal cancer across cohorts. *Nat Microbiol* **7**, 238–250 (2022).

85. Topalian, S. L., Taube, J. M. & Pardoll, D. M. Neoadjuvant checkpoint blockade for cancer immunotherapy. *Science* **367**, eaax0182 (2020).

86. Matson, V., Chervin, C. S. & Gajewski, T. F. Cancer and the Microbiome-Influence of the Commensal Microbiota on Cancer, Immune Responses, and Immunotherapy. *Gastroenterology* **160**, 600–613 (2021).

87. Derosa, L. *et al.* Microbiota-Centered Interventions: The Next Breakthrough in Immuno-Oncology? *Cancer Discovery* **11**, 2396–2412 (2021).

88. Matson, V. *et al.* The commensal microbiome is associated with anti-PD-1 efficacy in metastatic melanoma patients. *Science* **359**, 104–108 (2018).

89. Hakozaki, T. *et al.* The Gut Microbiome Associates with Immune Checkpoint Inhibition Outcomes in Patients with Advanced Non-Small Cell Lung Cancer. *Cancer Immunol Res* **8**, 1243–1250 (2020).

90. Cascone, T. *et al.* Neoadjuvant nivolumab or nivolumab plus ipilimumab in operable non-small cell lung cancer: the phase 2 randomized NEOSTAR trial. *Nat Med* **27**, 504–514 (2021).

91. Salgia, N. J. *et al.* Stool Microbiome Profiling of Patients with Metastatic Renal Cell Carcinoma Receiving Anti-PD-1 Immune Checkpoint Inhibitors. *Eur Urol* **78**, 498–502 (2020).

92. Jin, Y. *et al.* The Diversity of Gut Microbiome is Associated With Favorable Responses to Anti-Programmed Death 1 Immunotherapy in Chinese Patients With NSCLC. *J Thorac Oncol* **14**, 1378–1389 (2019).
93. Newsome, R. C. *et al.* Interaction of bacterial genera associated with therapeutic response to immune checkpoint PD-1 blockade in a United States cohort. *Genome Med* **14**, 35 (2022).
94. Park, E. M. *et al.* Targeting the gut and tumor microbiota in cancer. *Nat Med* **28**, 690–703 (2022).
95. Mao, J. *et al.* Gut microbiome is associated with the clinical response to anti-PD-1 based immunotherapy in hepatobiliary cancers. *J Immunother Cancer* **9**, e003334 (2021).
96. Peng, Z. *et al.* The Gut Microbiome Is Associated with Clinical Response to Anti-PD-1/PD-L1 Immunotherapy in Gastrointestinal Cancer. *Cancer Immunol Res* **8**, 1251–1261 (2020).
97. Zheng, Y. *et al.* Gut microbiome affects the response to anti-PD-1 immunotherapy in patients with hepatocellular carcinoma. *J Immunother Cancer* **7**, 193 (2019).
98. Depommier, C. *et al.* Supplementation with Akkermansia muciniphila in overweight and obese human volunteers: a proof-of-concept exploratory study. *Nat Med* **25**, 1096–1103 (2019).
99. de Vos, W. M., Tilg, H., Van Hul, M. & Cani, P. D. Gut microbiome and health: mechanistic insights. *Gut* **71**, 1020–1032 (2022).
100. Schneider, K. M. *et al.* Imbalanced gut microbiota fuels hepatocellular carcinoma development by shaping the hepatic inflammatory microenvironment. *Nat Commun* **13**, 3964 (2022).

101. Ansaldo, E. *et al.* Akkermansia muciniphila induces intestinal adaptive immune responses during homeostasis. *Science* **364**, 1179–1184 (2019).

102. Shaikh, F. Y. *et al.* Murine fecal microbiota transfer models selectively colonize human microbes and reveal transcriptional programs associated with response to neoadjuvant checkpoint inhibitors. *Cancer Immunol Immunother* **71**, 2405–2420 (2022).

103. Shaikh, F. Y. *et al.* A Uniform Computational Approach Improved on Existing Pipelines to Reveal Microbiome Biomarkers of Nonresponse to Immune Checkpoint Inhibitors. *Clin Cancer Res* **27**, 2571–2583 (2021).

104. Limeta, A., Ji, B., Levin, M., Gatto, F. & Nielsen, J. Meta-analysis of the gut microbiota in predicting response to cancer immunotherapy in metastatic melanoma. *JCI Insight* **5**, 140940 (2020).

105. He, Y. *et al.* Regional variation limits applications of healthy gut microbiome reference ranges and disease models. *Nat Med* **24**, 1532–1535 (2018).

106. Simpson, R. C. *et al.* Diet-driven microbial ecology underpins associations between cancer immunotherapy outcomes and the gut microbiome. *Nat Med* (2022) doi:10.1038/s41591-022-01965-2.

107. Iida, N. *et al.* Commensal bacteria control cancer response to therapy by modulating the tumor microenvironment. *Science* **342**, 967–970 (2013).

108. Hegazy, A. N. *et al.* Circulating and Tissue-Resident CD4+ T Cells With Reactivity to Intestinal Microbiota Are Abundant in Healthy Individuals and Function Is Altered During Inflammation. *Gastroenterology* **153**, 1320-1337.e16 (2017).

109. Rengarajan, S. *et al.* Dynamic immunoglobulin responses to gut bacteria during inflammatory bowel disease. *Gut Microbes* **11**, 405–420 (2020).

110. Bourgonje, A. R. *et al.* Patients With Inflammatory Bowel Disease Show IgG Immune Responses Towards Specific Intestinal Bacterial Genera. *Front Immunol* **13**, 842911 (2022).

111. Lodes, M. J. *et al.* Bacterial flagellin is a dominant antigen in Crohn disease. *J Clin Invest* **113**, 1296–1306 (2004).

112. Lloyd-Price, J. *et al.* Multi-omics of the gut microbial ecosystem in inflammatory bowel diseases. *Nature* **569**, 655–662 (2019).

113. Overacre-Delgoffe, A. E. *et al.* Microbiota-specific T follicular helper cells drive tertiary lymphoid structures and anti-tumor immunity against colorectal cancer. *Immunity* **54**, 2812-2824.e4 (2021).

114. Noble, A. *et al.* Altered immunity to microbiota, B cell activation and depleted γδ/resident memory T cells in colorectal cancer. *Cancer Immunol Immunother* (2022) doi:10.1007/s00262-021-03135-8.

115. Meylan, M. *et al.* Tertiary lymphoid structures generate and propagate anti-tumor antibody-producing plasma cells in renal cell cancer. *Immunity* **55**, 527-541.e5 (2022).

116. Goubet, A.-G. *et al.* Escherichia coli-specific CXCL13-producing TFH are associated with clinical efficacy of neoadjuvant PD-1 blockade against muscle-invasive bladder cancer. *Cancer Discov* CD-22-0201 (2022) doi:10.1158/2159-8290.CD-22-0201.

117. Wu, J. *et al.* A highly polarized TH2 bladder response to infection promotes epithelial repair at the expense of preventing new infections. *Nat Immunol* **21**, 671–683 (2020).

118. Yacouba, A., Tidjani Alou, M., Lagier, J.-C., Dubourg, G. & Raoult, D. Urinary microbiota and bladder cancer: A systematic review and a focus on uropathogens. *Semin Cancer Biol* S1044-579X(21)00303–5 (2022) doi:10.1016/j.semcancer.2021.12.010.

119. Zitvogel, L. & Kroemer, G. Cross-reactivity between microbial and tumor antigens. *Curr Opin Immunol* **75**, 102171 (2022).

120. Fluckiger, A. *et al.* Cross-reactivity between tumor MHC class I-restricted antigens and an enterococcal bacteriophage. *Science* **369**, 936–942 (2020).

121. Vétizou, M. *et al.* Anticancer immunotherapy by CTLA-4 blockade relies on the gut microbiota. *Science* **350**, 1079–1084 (2015).

122. Daillère, R. *et al.* Enterococcus hirae and Barnesiella intestinihominis Facilitate Cyclophosphamide-Induced Therapeutic Immunomodulatory Effects. *Immunity* **45**, 931–943 (2016).

123. Rong, Y. *et al.* Reactivity toward Bifidobacterium longum and Enterococcus hirae demonstrate robust CD8+ T cell response and better prognosis in HBV-related hepatocellular carcinoma. *Exp Cell Res* **358**, 352–359 (2017).

124. Davar, D. *et al.* Fecal microbiota transplant overcomes resistance to anti-PD-1 therapy in melanoma patients. *Science* **371**, 595–602 (2021).

125. Smith, M. *et al.* Gut microbiome correlates of response and toxicity following anti-CD19 CAR T cell therapy. *Nat Med* **28**, 713–723 (2022).

126. Whitfield-Cargile, C. M. *et al.* The non-invasive exfoliated transcriptome (exfoliome) reflects the tissue-level transcriptome in a mouse model of NSAID enteropathy. *Sci Rep* **7**, 14687 (2017).

127. Koh, A., De Vadder, F., Kovatcheva-Datchary, P. & Bäckhed, F. From Dietary Fiber to Host Physiology: Short-Chain Fatty Acids as Key Bacterial Metabolites. *Cell* **165**, 1332–1345 (2016).

128. Haenen, D. *et al.* A diet high in resistant starch modulates microbiota composition, SCFA concentrations, and gene expression in pig intestine. *J Nutr* **143**, 274–283 (2013).

129. Arpaia, N. *et al.* Metabolites produced by commensal bacteria promote peripheral regulatory T-cell generation. *Nature* **504**, 451–455 (2013).

130. Smith, P. M. *et al.* The microbial metabolites, short-chain fatty acids, regulate colonic Treg cell homeostasis. *Science* **341**, 569–573 (2013).

131. Park, J., Goergen, C. J., HogenEsch, H. & Kim, C. H. Chronically Elevated Levels of Short-Chain Fatty Acids Induce T Cell-Mediated Ureteritis and Hydronephrosis. *J Immunol* **196**, 2388–2400 (2016).

132. Kespohl, M. *et al.* The Microbial Metabolite Butyrate Induces Expression of Th1-Associated Factors in CD4+ T Cells. *Front Immunol* **8**, 1036 (2017).

133. Mariño, E. *et al.* Gut microbial metabolites limit the frequency of autoimmune T cells and protect against type 1 diabetes. *Nat Immunol* **18**, 552–562 (2017).

134. Mathewson, N. D. *et al.* Gut microbiome-derived metabolites modulate intestinal epithelial cell damage and mitigate graft-versus-host disease. *Nat Immunol* **17**, 505–513 (2016).

135. Trompette, A. *et al.* Dietary Fiber Confers Protection against Flu by Shaping Ly6c-Patrolling Monocyte Hematopoiesis and CD8+ T Cell Metabolism. *Immunity* **48**, 992-1005.e8 (2018).

136. Bachem, A. *et al.* Microbiota-Derived Short-Chain Fatty Acids Promote the Memory Potential of Antigen-Activated CD8+ T Cells. *Immunity* **51**, 285-297.e5 (2019).

137. Luu, M. *et al.* The short-chain fatty acid pentanoate suppresses autoimmunity by modulating the metabolic-epigenetic crosstalk in lymphocytes. *Nat Commun* **10**, 760 (2019).

138. Yuille, S., Reichardt, N., Panda, S., Dunbar, H. & Mulder, I. E. Human gut bacteria as potent class I histone deacetylase inhibitors in vitro through production of butyric acid and valeric acid. *PLoS One* **13**, e0201073 (2018).

139. Luu, M. *et al.* Microbial short-chain fatty acids modulate CD8+ T cell responses and improve adoptive immunotherapy for cancer. *Nat Commun* **12**, 4077 (2021).

140. Nomura, M. *et al.* Association of Short-Chain Fatty Acids in the Gut Microbiome With Clinical Response to Treatment With Nivolumab or Pembrolizumab in Patients With Solid Cancer Tumors. *JAMA Netw Open* **3**, e202895 (2020).

141. Coutzac, C. *et al.* Systemic short chain fatty acids limit antitumor effect of CTLA-4 blockade in hosts with cancer. *Nat Commun* **11**, 2168 (2020).

142. Uribe-Herranz, M. *et al.* Gut microbiota modulate dendritic cell antigen presentation and radiotherapy-induced antitumor immune response. *J Clin Invest* **130**, 466–479 (2020).

143. Munn, D. H. *et al.* Inhibition of T cell proliferation by macrophage tryptophan catabolism. *J Exp Med* **189**, 1363–1372 (1999).

144. Uyttenhove, C. *et al.* Evidence for a tumoral immune resistance mechanism based on tryptophan degradation by indoleamine 2,3-dioxygenase. *Nat Med* **9**, 1269–1274 (2003).

145. Wang, Y., Hu, G.-F. & Wang, Z.-H. The status of immunosuppression in patients with stage IIIB or IV non-small-cell lung cancer correlates with the clinical characteristics and response to chemotherapy. *Onco Targets Ther* **10**, 3557–3566 (2017).

146. Holmgaard, R. B., Zamarin, D., Munn, D. H., Wolchok, J. D. & Allison, J. P. Indoleamine 2,3-dioxygenase is a critical resistance mechanism in antitumor T cell immunotherapy targeting CTLA-4. *J Exp Med* **210**, 1389–1402 (2013).

147. Botticelli, A. *et al.* Can IDO activity predict primary resistance to anti-PD-1 treatment in NSCLC? *J Transl Med* **16**, 219 (2018).

148. Li, H. *et al.* Metabolomic adaptations and correlates of survival to immune checkpoint blockade. *Nat Commun* **10**, 4346 (2019).

149. Long, G. V. *et al.* Epacadostat plus pembrolizumab versus placebo plus pembrolizumab in patients with unresectable or metastatic melanoma (ECHO-301/KEYNOTE-252): a phase 3, randomised, double-blind study. *Lancet Oncol* **20**, 1083–1097 (2019).

150. Kaur, H., Bose, C. & Mande, S. S. Tryptophan Metabolism by Gut Microbiome and Gut-Brain-Axis: An in silico Analysis. *Front Neurosci* **13**, 1365 (2019).

151. Laurans, L. *et al.* Genetic deficiency of indoleamine 2,3-dioxygenase promotes gut microbiota-mediated metabolic health. *Nat Med* **24**, 1113–1120 (2018).

152. Goubet, A.-G. *et al.* Prolonged SARS-CoV-2 RNA virus shedding and lymphopenia are hallmarks of COVID-19 in cancer patients with poor prognosis. *Cell Death Differ* **28**, 3297–3315 (2021).

153. Danlos, F.-X. *et al.* Metabolomic analyses of COVID-19 patients unravel stage-dependent and prognostic biomarkers. *Cell Death Dis* **12**, 258 (2021).

154. Peyraud, F. *et al.* Circulating L-arginine predicts the survival of cancer patients treated with immune checkpoint inhibitors. *Annals of Oncology* **33**, 1041–1051 (2022).

155. Geiger, R. *et al.* L-Arginine Modulates T Cell Metabolism and Enhances Survival and Anti-tumor Activity. *Cell* **167**, 829-842.e13 (2016).

156. Canale, F. P. *et al.* Metabolic modulation of tumours with engineered bacteria for immunotherapy. *Nature* **598**, 662–666 (2021).

157. Narunsky-Haziza, L. *et al.* Pan-cancer analyses reveal cancer-type-specific fungal ecologies and bacteriome interactions. *Cell* **185**, 3789-3806.e17 (2022).

158. Poore, G. D. *et al.* Microbiome analyses of blood and tissues suggest cancer diagnostic approach. *Nature* **579**, 567–574 (2020).

159. Messaoudene, M. *et al.* A Natural Polyphenol Exerts Antitumor Activity and Circumvents Anti-PD-1 Resistance through Effects on the Gut Microbiota. *Cancer Discov* **12**, 1070–1087 (2022).

160. Grajeda-Iglesias, C. *et al.* Oral administration of Akkermansia muciniphila elevates systemic antiaging and anticancer metabolites. *Aging (Albany NY)* **13**, 6375–6405 (2021).

161. Montégut, L., de Cabo, R., Zitvogel, L. & Kroemer, G. Science-Driven Nutritional Interventions for the Prevention and Treatment of Cancer. *Cancer Discov* OF1–OF22 (2022) doi:10.1158/2159-8290.CD-22-0504.

162. Pietrocola, F. *et al.* Caloric Restriction Mimetics Enhance Anticancer Immunosurveillance. *Cancer Cell* **30**, 147–160 (2016).

163. Bourgin, M. *et al.* Circulating acetylated polyamines correlate with Covid-19 severity in cancer patients. *Aging (Albany NY)* **13**, 20860–20885 (2021).

164. Mager, L. F. *et al.* Microbiome-derived inosine modulates response to checkpoint inhibitor immunotherapy. *Science* **369**, 1481–1489 (2020).

165. Nie, X. *et al.* Serum Metabolite Biomarkers Predictive of Response to PD-1 Blockade Therapy in Non-Small Cell Lung Cancer. *Front Mol Biosci* **8**, 678753 (2021).

166. Thompson, N. A. *et al.* The MITRE trial protocol: a study to evaluate the microbiome as a biomarker of efficacy and toxicity in cancer patients receiving immune checkpoint inhibitor therapy. *BMC Cancer* **22**, 99 (2022).

167. Shoji, F. *et al.* Chronological analysis of the gut microbiome for efficacy of atezolizumab-based immunotherapy in non-small cell lung cancer: Protocol for a multicenter prospective observational study. *Thoracic Cancer* **13**, 2829–2833 (2022).

168. Aitchison, J. & Shen, S. M. Logistic-Normal Distributions: Some Properties and Uses. *Biometrika* **67**, 261–272 (1980).

Table 1. Cancer-associated confounding factors (aging, co-morbidities and co-medi

Associated with cancer status	*Alistipes putredinis*	■
	Anaerotruncus colihominis	■
	Bacteroides cellulosilyticus	
	Bacteroides fragilis	
	Bacteroides thetaiotaomicron	■
	Bifidobacterium dentium	■
	Bilophila wadsworthia	■
	Clostridium leptum	
	Clostridium symbiosum	■
	Eggerthella lenta	■
	Eisenbergiella massiliensis	■
	Enterocloster asparagiformis	■
	Enterocloster bolteae	■
	Enterocloster citroniae	■
	Enterocloster clostridioformis	■
	Escherichia coli	■
	Eubacterium siraeum	
	Flavonifractor plautii	■
	Holdemanella biformis	
	Hungatella hathewayi	■
	Lachnospiraceae bacterium 3_1_57FAA_CT1	
	Lactobacillus gasseri	
	Ligilactobacillus salivarius	
	Limosilactobacillus fermentum	
	Limosilactobacillus mucosae	
	Odoribacter splanchnicus	■
	Parabacteroides distasonis	■
	Phocaeicola plebeius	
	Phocaeicola vulgatus	
	Pseudoflavonifractor capillosus	■
	Ruminococcus gnavus	
	Shigella flexneri	
	Streptococcus anginosus	
	Streptococcus parasanguinis	
	Streptococcus pseudopneumoniae	

	Streptococcus salivarius	
	Streptococcus vestibularis	
	Veillonella atypica	
	Veillonella dispar	
	Veillonella parvula	
Associated with cancer-free status	*Alistipes senegalensis*	
	Alistipes shahii	
	Anaerobutyricum hallii	
	Anaerostipes hadrus	
	Barnesiella intestinihominis	
	Bifidobacterium adolescentis	
	Bifidobacterium pseudocatenulatum	
	Collinsella aerofaciens	
	Coprobacter fastidiosus	
	Coprococcus comes	
	Desulfovibrio piger	
	Dorea longicatena	
	Eubacterium ramulus	
	Eubacterium rectale	
	Eubacterium ventriosum	
	Faecalibacterium prausnitzii	
	Lachnospira eligens	
	Ligilactobacillus ruminis	
	Methanobrevibacter smithii	
	Phocaeicola dorei	
	Prevotella copri	
	Prevotella stercorea	
	Roseburia faecis	
	Ruminococcus bromii	
	Ruminococcus lactaris	
	Ref.	[1-3]

Yonekura et al., 2020; Gacesa et al., 2022; Park et al., 2022

Increased in relative abundance

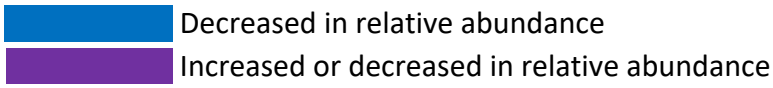
Decreased in relative abundance
Increased or decreased in relative abundance

ications) associated with or causatively link to gut dysbiosis.

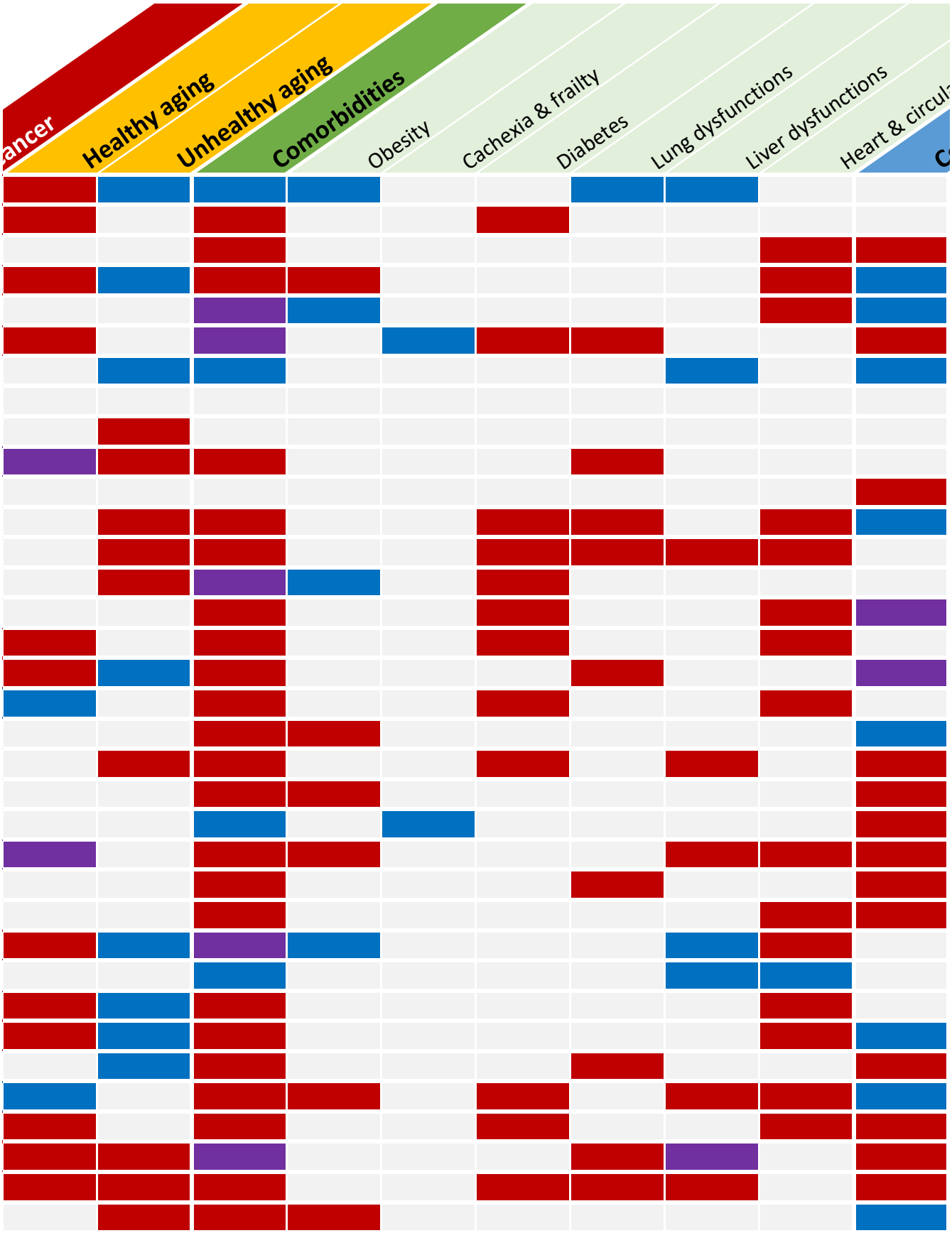

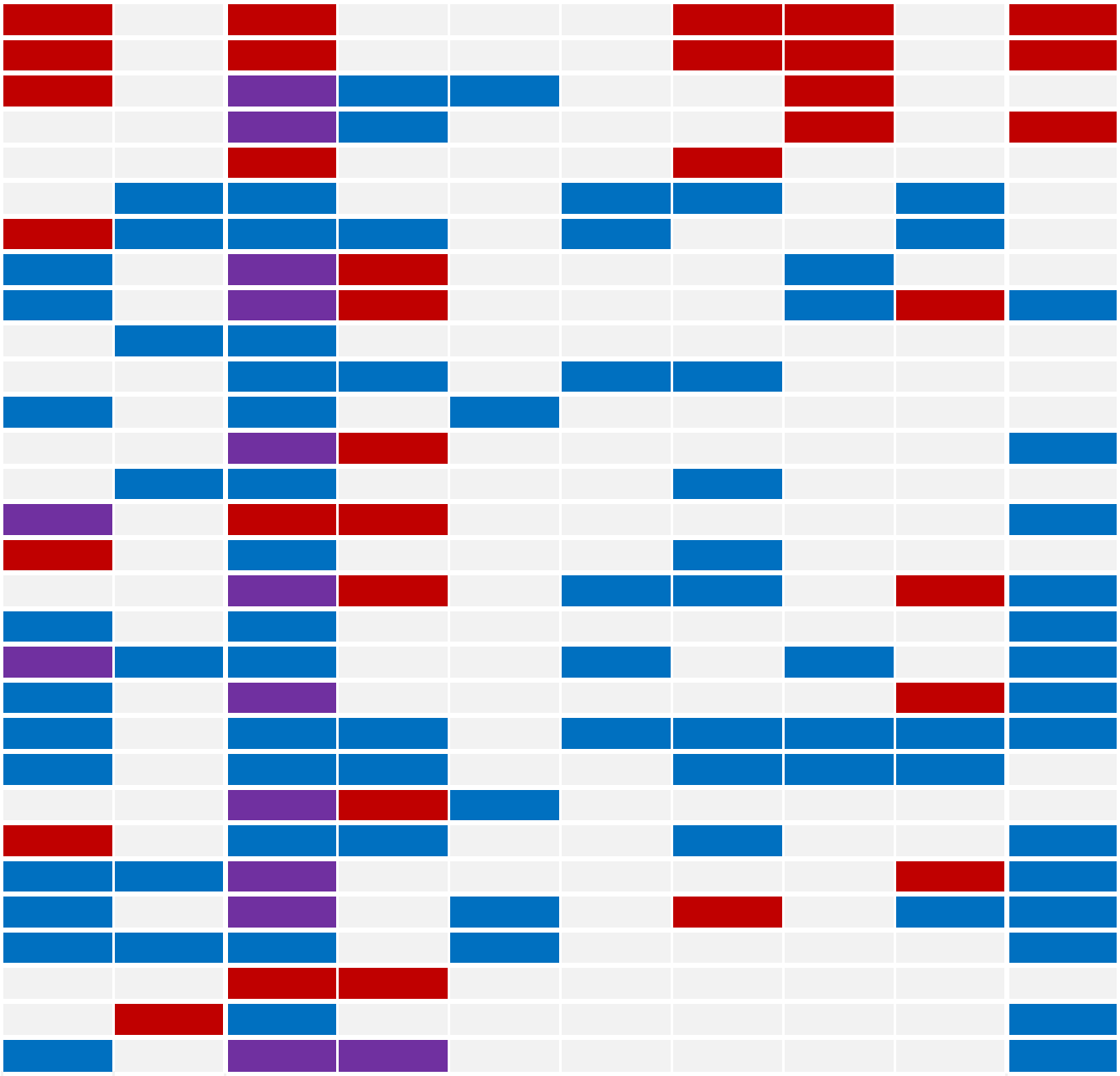

[4-7]	[8-10]	[2,11-23]
Li et al., 2022; Rampelli et al., 2020; Wang et al., 2022; Sato et al., 2021	Luan et al., 2020; Ghosh et al., 2020; Zhang et al., 2021	Qin et al., 2014; Liu et al., 2017; Wang et al., 2018; Cui et al., 2018; Crovesy et al., 2020; Bowerman et al., 2020; Calderón-Pérez et al., 2020; Ni et al., 2021; Jiao et al., 2021; Behary et al., 2021;

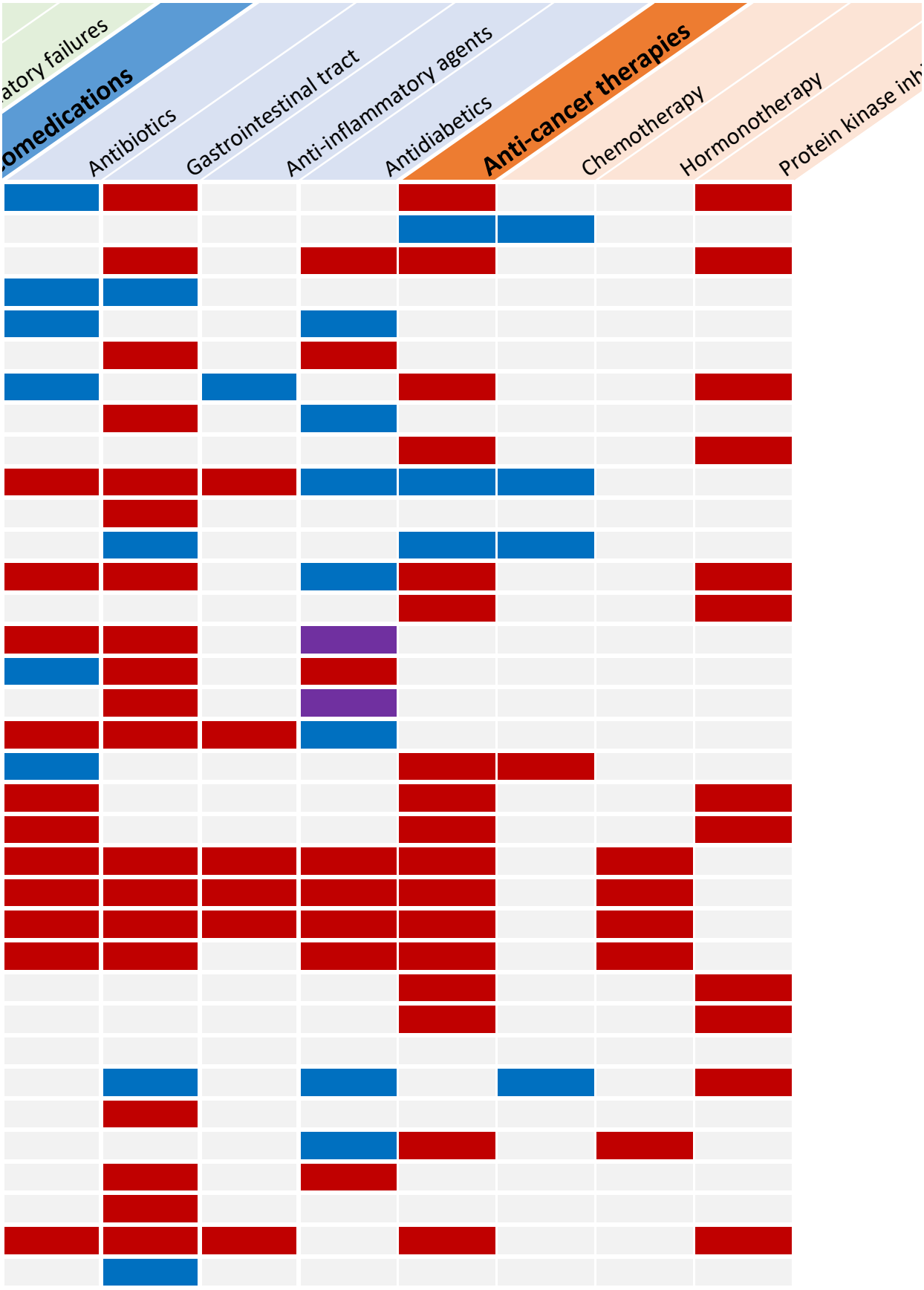
atory failures
omedications
Antibiotics
Gastrointestinal tract
Anti-inflammatory agents
Antidiabetics
Anti-cancer therapies
Chemotherapy
Hormonotherapy
Protein kinase inh

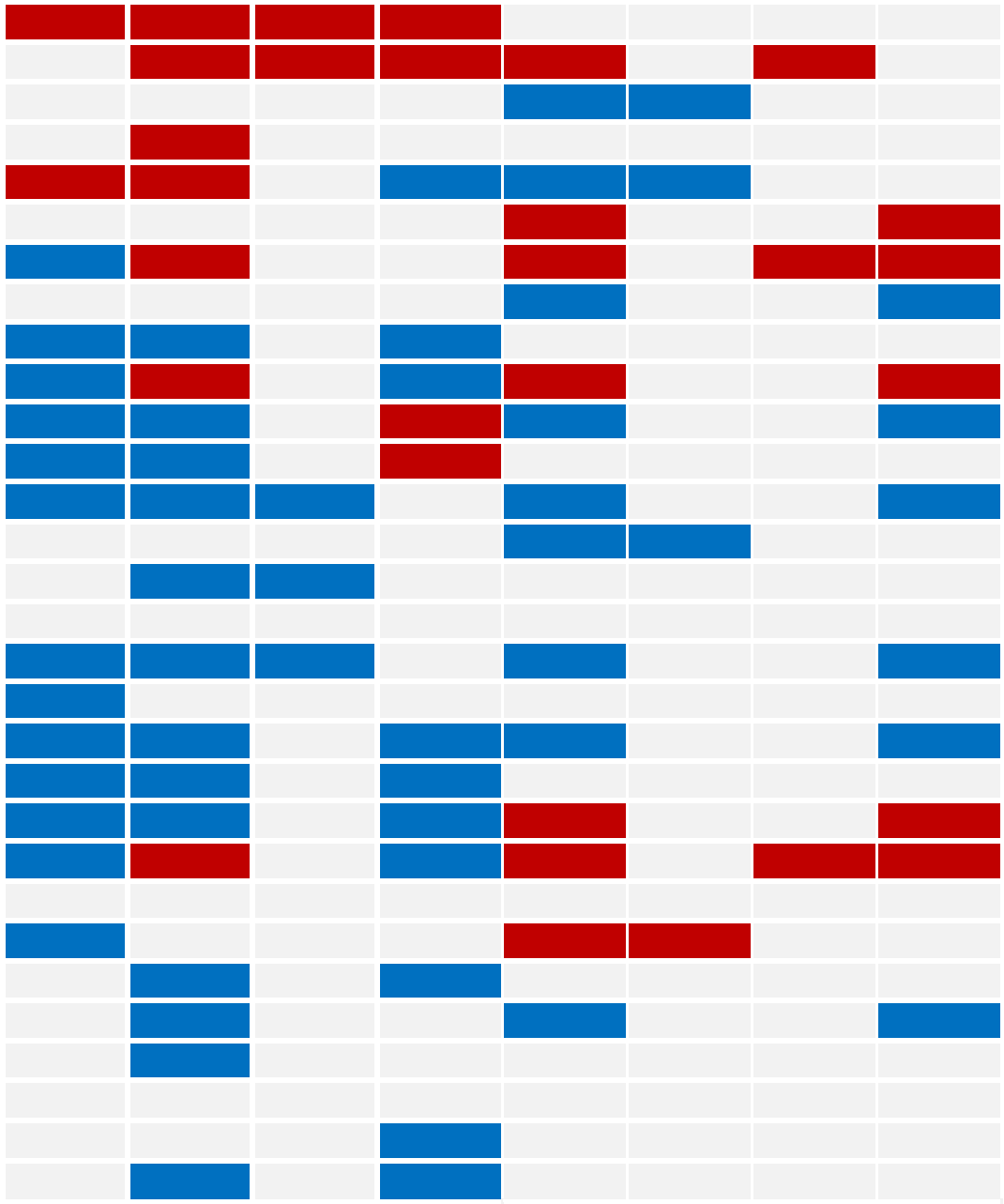

[23-32]

Aasmets et al., 2022
Clooney et al., 2016
Derosa et al., 2020
Imhann et al., 2016
Lin et al., 2021
Nagata et al., 2022
Palleja et al. 2018
Parker et al., 2017
Singh et al., 2022
Vich Vila et al. 2020

[25,28,33-34]

Derosa et al., 2020
Li et al., 2021
Nagata et al., 2022
Terrisse et al., 2021


ibitors

Table 2. Biomarkers of clinical relevance during cancer therapy with immune checkpoint inhibitors.

Classical biomarkers				
	Biomarker	**Detection**	**Correlation with clinical outcome**	**Role in routine clinical oncology**
Tumor microenvironment: cancer cells	PD-L1	IHC	Expression of PD-L1 on tumor cells (TPS) positively correlates with ICI efficacy in several tumors. Linear correlation with ICI efficacy in NSCLC.[1]	Validated in Phase III randomized trials. TPS governs management of NSCLC patients for ICI therapies.
	DNA mismatch repair (MMR)	Sequencing	Positive in MMR deficiencies Associated with TMB and CD8 TILs	Used to access ICI (including neo-adjuvant for certain tumors) in colon, anal cancers and any MMR deficient advanced tumors[2]
	TMB	Sequencing	Positive correlation with log (TMB) in various cancers, different cut-off values in different cancers[3,4]	Available in various tumors, for example with FoundationOne[5]
	Neo-antigen	Sequencing	Presence of neo-antigens binding to MHC molecules promotes strong T cell immune response[6]	Challenge with computational prediction of neoantigens and standardization of the pipeline
	Gene pathways	Sequencing	(IFN)-γ pathway genes[7], B2M mutation JAK2 negative[8], STK11[9], β-catenin pathway associated with resistance	Not routinely used, currently being evaluated in clinical trials
	Driver mutation	Sequencing	Presence of EGFR mutations, ALK rearrangements,... associated with poor outcome, targeted therapy preferred[10]	Routinely performed in patients with advanced NSCLC
Tumor microenvironment : Immune cells	PD-L1	IHC	CPS combines tumor and immune cells (lymphocytes and macrophages). PD-L1 expression[11] and patients with high CPS respond better	CPS was validated in Phase III trials and used to determine ICI indication in various tumors
	Immune infiltration	TILs	Tumors enriched with TILs CD8, high immunoscore, TLS correlate with better prognostic and response to ICI in various tumours[12]	Not routinely performed (except for the immunoscore in colon) in absence of standardization and cut-off
	Inflamed vs not inflamed tumors	IHC, Sequencing	Absence of intratumor CD8 or CD4 correspond to immune-excluded (vascular or extracellular matrix) tumors or immune-deserts[13] refractory to ICI	Not performed in the absence of standardization cut-off value. Alternative treatment available
Baseline blood cells and molecules	Neutrophil to lymphocyte ratio (NLR)	Peripheral blood	NLR<3 prior ICI associated with positive outcomes[14]	Can be routinely measured. However, does not change clinical management
	Lung Immune Prognostic Score (LIPI)	Peripheral blood	Measurement of the association between NLR and the LDH. Initially stratified NSCLC patients but used in other cancers (melanoma, head and neck)[15]	Prognostic value similar to NLR
	LDH	Peripheral blood	High LDH was associated with a lower objective response rate in melanoma[16]	Included in baseline blood test pre-ICI in melanoma patients
	CRP, SAA	Peripheral blood	Elevated CRP [17] and high serum amyloid A[18] correlated with shorter survival	Not routinely measured
	IL-8	Peripheral blood	Elevated CXCL8 serum levels>23pg/ml correlated with shorter survival in melanoma, kidney and squamous or non squamous NSCLC[19,20].	Not routinely measured

	Eosinophils	Peripheral blood	Low eosinophil count associated with response in melanoma[21]	Included in baseline blood tests pre-ICI in melanoma patients
Microbiota-related biomarkers				
	Biomarker	**Detection**	**Correlation with clinical outcome**	**Potential application in routine clinical oncology**
Gut OncoMicrobiome Signatures	Microbial composition	Feces	Some bacterial taxa are associated with beneficial (Akkermansiaceae , Lachnospiraceae, Oscillospiraceae, Ruminococcaceae, Prevotellaceae) or poor (Eggerthellaceae, *Enterocloster* genus, Streptococcaceae, Veillonellaceae)[22–33] clinical outcome post- ICI.	Gut microbiota composition assessed by 16S rRNA, shotgun metagenomics sequencing or targeted-PCR on specific taxa (refer to Figures 5-6)
	Taxonomic diversities	Feces	Low alpha diversity or richness is associated with poor clinical outcome[29,34].	
	Microbiota-derived compounds			
	Short-chain fatty acids (SCFA)	Blood and feces	High levels of specific SCFA may be associated with better outcomes in patients treated with ICI[35].	Plasma and fecal SFCA levels may support recommendation in favor of high fiber intake to increase response to ICI[36].
	Kynurenine (Kyn)/ Tryptophan (Try) ratio	Blood	In NSCLC, RCC and melanoma, higher plasmatic Kyn/Trp ratio is associated with early progression and reduced overall survival to ICI[37,38]. Gut microbiota can convert Tryptophan into indole derivatives instead of Kynurenine[39].	Plasmatic levels of Kynurenine and Tryptophan can be measured by liquid chromatography-mass spectrometry. The conversion of Try to Kyn can be blocked by IDO inhibitors or by MCI to boost ICI efficacy.
	Inosine	Blood	Commensals such as *B. pseudolongum* and *L. johnsonii* can produce inosine which bind to the T cell adenosine A_{2A} receptor. In proinflammatory conditions, inosine stimulates antitumor immunity and response to ICI[40] in mouse models.	Awaits validation in prospective human studies. Of note, in the absence of inflammation, inosine suppresses T cell immune response.
	L-arginine	Blood	Low ARG levels at baseline (<42 μM) were significantly and independently associated with a worse clinical benefit rate, progression-free survival, and overall survival in 2 cohorts of patients treated with ICI [43,44].	Plasma L-arginine is a potential surrogate marker of T cell immune tonus and polyamine-producing microbiota. To be validated in prospective cohorts to determine a cut-off value, but test readily available.
	Commensal-specific memory T and B cell responses			
	T cells	PBMC	Memory bacteria-reactive T cells can be found in the intestine but also in circulation. Those cells can be characterized by gut mucosal markers (integrin α4β7, CCR9, CCR6 and CD161), IL-2 and TNF-α secretion[41].	Circulating memory T cell immune responses directed against specific commensals, such as *A. muciniphila,* could be used to predict response to ICI and follow MCI[24].
	B cells (IgA and IgG titers)	Blood and feces	Quantification of IgA and IgG bound to bacteria by flow cytometry monitor memory humoral immune response against commensals[42,43].	Flow cytometric determination of Ig response in the plasma to assess prevalence of bacteria and immunogenicity of specific taxa.

Intestinal microenvironment	**Intestinal barrier integrity**			
	sCD14, ST2 and LBP	Blood	Serum levels of sCD14 and ST2 are surrogate markers of leaky gut syndrome and could be associated to gut microbiota dysbiosis which dampened response to ICI[24,26,44].	Assessing biomarkers associated with leaky gut syndrome in the plasma could document the intestinal barrier integrity and guide MCI.
	Exfoliome (mamalian DNA, IL-1β, CXCL8)	Blood and feces	Genes encoding pro-inflammatory cytokines (IL-1β and CXCL8) are increased in ICI or FMT non-responder patients and linked to LPS-producing Gram-negative bacteria[27]. Mammalian DNA contamination of stool microbes could be a surrogate marker of epithelial or immune apoptosis.	Plasmatic CXCL8, IL-1β levels and noninvasive exfoliated transcriptome assessed on fecal samples during ICI could document alteration of the intestinal barrier associated with resistance.
	Intestinal immune system and response to ICI			
	Peptidoglycans, phospholipids and muropeptides	Feces	In mice, Enterococcus spp. produce the enzyme SagA which contributes to peptidoglycan and NOD2 engagement, improving ICI efficacy and adaptive immune response[45,46]. *B. bifidum* produce peptidoglycans which stimulate cancer immune responses through TLR2[47,48]. Immunogenicity of diacyl phosphatidylethanolamine in *Akkermansia* (via TLR1-2 heterodimer)[49]	Assessing distinct patterns of peptidoglycans, phospholipids, lectins, in feces after probiotic uptake (refer to Figure 6) by metabolomics.
	Apolipoproteins and mucins	Plasma	The presence of apolipoproteins and transmembrane mucins are associated with healthy intestinal mucosa and positive response to ICI[50].	Plasmatic levels of apolipoproteins could be used as biomarkers for ICI response.
Tumor-associated microbiota and immune system	TLS and TFH	Tumor biopsy and blood	Intratumoral formation and maturation of TLS, maturation of B cells, IgG secretion and CXCL13-producing effector memory TFH have been associated with response to ICI and prolonged PFS[51,52].	Geolocalization of TLS, B cells, TFH and IgG-labeled cells in tumors can be assessed by IHC or with high spatial resolution imaging technologies. TFH response can be assessed by CXCL13 and IL-21 plasmatic dosage[53].
	Antigen mimicry	Tumor biopsy	Intratumoral or phage-associated bacteria can express HLA class I and II-restricted epitopes. Molecular mimicry with oncogenes and cross-reactivities of T cells lead to tumor regression[54,55].	This finding could help developing bacteria-derived peptide vaccines to favor long lasting memory antitumor response[56–59]. Clinical trials are ongoing (NCT04116658, NCT04187404).
	Tumor or T cell cytokine modulation	Tumor biopsy	Commensals such as *A. muciniphila*, Bifidobacterium spp. , L-arginine[60] producing commensals, and *L. rhamnosus*[61–63]. promote antitumoral immune responses by triggering type 1 IFN secreting myeloid cells[61–63], TNFα producing T cells and decreasing T cell exhaustion[60].	The analysis relies on transcript assessment (PCR or RNA sequencing) in the TME. FMT-based MCI modulated Type I IFN production and responses to ICI[61,64].
	Intratumoral metabolites	Tumor biopsy	Taurine conjugated bile acids were accumulating in the tumor and serum of mice following oral supplementation with castalagin prebiotic while decreasing in feces[65].	Need to be validated in patients with cancer. Challenges for pre-analytical phase and need for standardization.

16S rRNA; 16S ribosomal RNA, A(A2)R; Adenosine A2 receptor, BMI; Body mass-index, CPS; Combine positive score, CRP; C reactive protein, FMT; Fecal microbiota transplant, ICI; Immune Checkpoint Inhibitors, IHC; Immunohistochemistry, LDH; Lactate dehydrogenase, MCI; Microbiota-centered interventions, MHC; Major histocompatibility complex, NOD2; Nucleotide-binding oligomerization domain-containing protein 2, NSCLC; Non-small cell lung cancer, PBMC; Peripheral blood mononuclear cells, SAA; Serum amyloid A, SagA; Secreted antigen A, STING; Stimulator of interferon genes, TFH; T follicular helper, TILs; Tumor infiltrating lymphocytes, TLS; Tertiary lymphoid structure, TMB; Tumor mutational burden, TPS; Tumor prognostic score

1. Mok, T. *et al.* Phase 3 KEYNOTE-042 trial of pembrolizumab (MK-3475) versus platinum doublet chemotherapy in treatment-naive patients (pts) with PD-L1–positive advanced non-small cell lung cancer (NSCLC). *J. Clin. Oncol.* **33**, TPS8105–TPS8105 (2015).
2. Marabelle, A. *et al.* Efficacy of Pembrolizumab in Patients With Noncolorectal High Microsatellite Instability/Mismatch Repair-Deficient Cancer: Results From the Phase II KEYNOTE-158 Study. *J. Clin. Oncol. Off. J. Am. Soc. Clin. Oncol.* **38**, 1–10 (2020).
3. Snyder, A. *et al.* Genetic basis for clinical response to CTLA-4 blockade in melanoma. *N. Engl. J. Med.* **371**, 2189–2199 (2014).
4. Rizvi, H. *et al.* Molecular Determinants of Response to Anti-Programmed Cell Death (PD)-1 and Anti-Programmed Death-Ligand 1 (PD-L1) Blockade in Patients With Non-Small-Cell Lung Cancer Profiled With Targeted Next-Generation Sequencing. *J. Clin. Oncol. Off. J. Am. Soc. Clin. Oncol.* **36**, 633–641 (2018).
5. Hellmann, M. D. *et al.* Nivolumab plus Ipilimumab in Lung Cancer with a High Tumor Mutational Burden. *N. Engl. J. Med.* **378**, 2093–2104 (2018).
6. Fluckiger, A. *et al.* Cross-reactivity between tumor MHC class I-restricted antigens and an enterococcal bacteriophage. *Science* **369**, 936–942 (2020).
7. Herbst, R. S. *et al.* Predictive correlates of response to the anti-PD-L1 antibody MPDL3280A in cancer patients. *Nature* **515**, 563–567 (2014).

8. Zaretsky, J. M. *et al.* Mutations Associated with Acquired Resistance to PD-1 Blockade in Melanoma. *N. Engl. J. Med.* **375**, 819–829 (2016).
9. Skoulidis, F. *et al.* STK11/LKB1 Mutations and PD-1 Inhibitor Resistance in KRAS-Mutant Lung Adenocarcinoma. *Cancer Discov.* **8**, 822–835 (2018).
10. Mazieres, J. *et al.* Immune checkpoint inhibitors for patients with advanced lung cancer and oncogenic driver alterations: results from the IMMUNOTARGET registry. *Ann. Oncol.* **30**, 1321–1328 (2019).
11. Kojima, T. *et al.* Randomized Phase III KEYNOTE-181 Study of Pembrolizumab Versus Chemotherapy in Advanced Esophageal Cancer. *J. Clin. Oncol. Off. J. Am. Soc. Clin. Oncol.* **38**, 4138–4148 (2020).
12. Fumet, J.-D. *et al.* Prognostic and predictive role of CD8 and PD-L1 determination in lung tumor tissue of patients under anti-PD-1 therapy. *Br. J. Cancer* **119**, 950–960 (2018).
13. Chen, D. S. & Mellman, I. Elements of cancer immunity and the cancer-immune set point. *Nature* **541**, 321–330 (2017).
14. Nakaya, A. *et al.* Neutrophil-to-lymphocyte ratio as an early marker of outcomes in patients with advanced non-small-cell lung cancer treated with nivolumab. *Int. J. Clin. Oncol.* **23**, 634–640 (2018).
15. Mezquita, L. *et al.* Association of the Lung Immune Prognostic Index With Immune Checkpoint Inhibitor Outcomes in Patients With Advanced Non-Small Cell Lung Cancer. *JAMA Oncol.* **4**, 351–357 (2018).
16. Ribas, A. *et al.* Association of Pembrolizumab With Tumor Response and Survival Among Patients With Advanced Melanoma. *JAMA* **315**, 1600–1609 (2016).

17. Riedl, J. M. *et al.* C-Reactive Protein (CRP) Levels in Immune Checkpoint Inhibitor Response and Progression in Advanced Non-Small Cell Lung Cancer: A Bi-Center Study. *Cancers* **12**, 2319 (2020).
18. Di Noia, V. *et al.* Blood serum amyloid A as potential biomarker of pembrolizumab efficacy for patients affected by advanced non-small cell lung cancer overexpressing PD-L1: results of the exploratory "FoRECATT" study. *Cancer Immunol. Immunother.* **70**, 1583–1592 (2021).
19. Schalper, K. A. *et al.* Elevated serum interleukin-8 is associated with enhanced intratumor neutrophils and reduced clinical benefit of immune-checkpoint inhibitors. *Nat. Med.* **26**, 688–692 (2020).
20. Yuen, K. C. *et al.* High systemic and tumor-associated IL-8 correlates with reduced clinical benefit of PD-L1 blockade. *Nat. Med.* **26**, 693–698 (2020).
21. Weide, B. *et al.* Baseline Biomarkers for Outcome of Melanoma Patients Treated with Pembrolizumab. *Clin. Cancer Res. Off. J. Am. Assoc. Cancer Res.* **22**, 5487–5496 (2016).
22. Vétizou, M. *et al.* Anticancer immunotherapy by CTLA-4 blockade relies on the gut microbiota. *Science* **350**, 1079–1084 (2015).
23. Daillère, R. *et al.* Enterococcus hirae and Barnesiella intestinihominis Facilitate Cyclophosphamide-Induced Therapeutic Immunomodulatory Effects. *Immunity* **45**, 931–943 (2016).
24. Routy, B. *et al.* Gut microbiome influences efficacy of PD-1-based immunotherapy against epithelial tumors. *Science* **359**, 91–97 (2018).
25. Matson, V. *et al.* The commensal microbiome is associated with anti-PD-1 efficacy in metastatic melanoma patients. *Science* **359**, 104–108 (2018).

26. Derosa, L. *et al.* Gut Bacteria Composition Drives Primary Resistance to Cancer Immunotherapy in Renal Cell Carcinoma Patients. *Eur. Urol.* **78**, 195–206 (2020).
27. McCulloch, J. A. *et al.* Intestinal microbiota signatures of clinical response and immune-related adverse events in melanoma patients treated with anti-PD-1. *Nat. Med.* **28**, 545–556 (2022).
28. Lee, K. A. *et al.* Cross-cohort gut microbiome associations with immune checkpoint inhibitor response in advanced melanoma. *Nat. Med.* **28**, 535–544 (2022).
29. Gopalakrishnan, V. *et al.* Gut microbiome modulates response to anti-PD-1 immunotherapy in melanoma patients. *Science* **359**, 97–103 (2018).
30. Frankel, A. E. *et al.* Metagenomic Shotgun Sequencing and Unbiased Metabolomic Profiling Identify Specific Human Gut Microbiota and Metabolites Associated with Immune Checkpoint Therapy Efficacy in Melanoma Patients. *Neoplasia N. Y. N* **19**, 848–855 (2017).
31. Zheng, Y. *et al.* Gut microbiome affects the response to anti-PD-1 immunotherapy in patients with hepatocellular carcinoma. *J. Immunother. Cancer* **7**, 193 (2019).
32. Newsome, R. C. *et al.* Interaction of bacterial genera associated with therapeutic response to immune checkpoint PD-1 blockade in a United States cohort. *Genome Med.* **14**, 35 (2022).
33. Park, E. M. *et al.* Targeting the gut and tumor microbiota in cancer. *Nat. Med.* **28**, 690–703 (2022).
34. Byrd, A. L. *et al.* Gut microbiome stability and dynamics in healthy donors and patients with non-gastrointestinal cancers. *J. Exp. Med.* **218**, e20200606 (2021).

35. Nomura, M. *et al.* Association of Short-Chain Fatty Acids in the Gut Microbiome With Clinical Response to Treatment With Nivolumab or Pembrolizumab in Patients With Solid Cancer Tumors. *JAMA Netw. Open* **3**, e202895 (2020).
36. Spencer, C. N. *et al.* Dietary fiber and probiotics influence the gut microbiome and melanoma immunotherapy response. *Science* **374**, 1632–1640 (2021).
37. Botticelli, A. *et al.* Can IDO activity predict primary resistance to anti-PD-1 treatment in NSCLC? *J. Transl. Med.* **16**, 219 (2018).
38. Li, H. *et al.* Metabolomic adaptations and correlates of survival to immune checkpoint blockade. *Nat. Commun.* **10**, 4346 (2019).
39. Ghiboub, M. *et al.* Nutritional Therapy to Modulate Tryptophan Metabolism and Aryl Hydrocarbon-Receptor Signaling Activation in Human Diseases. *Nutrients* **12**, 2846 (2020).
40. Mager, L. F. *et al.* Microbiome-derived inosine modulates response to checkpoint inhibitor immunotherapy. *Science* **369**, 1481–1489 (2020).
41. Hegazy, A. N. *et al.* Circulating and Tissue-Resident CD4+ T Cells With Reactivity to Intestinal Microbiota Are Abundant in Healthy Individuals and Function Is Altered During Inflammation. *Gastroenterology* **153**, 1320-1337.e16 (2017).
42. Moor, K. *et al.* Analysis of bacterial-surface-specific antibodies in body fluids using bacterial flow cytometry. *Nat. Protoc.* **11**, 1531–1553 (2016).
43. Bourgonje, A. R. *et al.* Patients With Inflammatory Bowel Disease Show IgG Immune Responses Towards Specific Intestinal Bacterial Genera. *Front. Immunol.* **13**, 842911 (2022).

44. Yonekura, S. *et al.* Cancer Induces a Stress Ileopathy Depending on β-Adrenergic Receptors and Promoting Dysbiosis that Contributes to Carcinogenesis. *Cancer Discov.* **12**, 1128–1151 (2022).
45. Kim, B. *et al.* Enterococcus faecium secreted antigen A generates muropeptides to enhance host immunity and limit bacterial pathogenesis. *eLife* **8**, e45343 (2019).
46. Griffin, M. E. *et al.* Enterococcus peptidoglycan remodeling promotes checkpoint inhibitor cancer immunotherapy. *Science* **373**, 1040–1046 (2021).
47. Al-Sadi, R. *et al.* Bifidobacterium bifidum Enhances the Intestinal Epithelial Tight Junction Barrier and Protects against Intestinal Inflammation by Targeting the Toll-like Receptor-2 Pathway in an NF-κB-Independent Manner. *Int. J. Mol. Sci.* **22**, 8070 (2021).
48. Lee, W. S. *et al.* Intratumoral immunotherapy using a TLR2/3 agonist, L-pampo, induces robust antitumor immune responses and enhances immune checkpoint blockade. *J. Immunother. Cancer* **10**, e004799 (2022).
49. Bae, M. *et al.* Akkermansia muciniphila phospholipid induces homeostatic immune responses. *Nature* **608**, 168–173 (2022).
50. Karlsson, M. J. *et al.* Inflammation and Apolipoproteins Are Potential Biomarkers for Stratification of Cutaneous Melanoma Patients for Immunotherapy and Targeted Therapy. *Cancer Res.* **81**, 2545–2555 (2021).
51. Meylan, M. *et al.* Tertiary lymphoid structures generate and propagate anti-tumor antibody-producing plasma cells in renal cell cancer. *Immunity* **55**, 527-541.e5 (2022).

52. Goubet, A.-G. *et al.* Escherichia coli-specific CXCL13-producing TFH are associated with clinical efficacy of neoadjuvant PD-1 blockade against muscle-invasive bladder cancer. *Cancer Discov.* CD-22-0201 (2022) doi:10.1158/2159-8290.CD-22-0201.
53. Davar, D. *et al.* Fecal microbiota transplant overcomes resistance to anti-PD-1 therapy in melanoma patients. *Science* **371**, 595–602 (2021).
54. Fluckiger, A. *et al.* Cross-reactivity between tumor MHC class I-restricted antigens and an enterococcal bacteriophage. *Science* **369**, 936–942 (2020).
55. Kalaora, S. *et al.* Identification of bacteria-derived HLA-bound peptides in melanoma. *Nature* **592**, 138–143 (2021).
56. Mizukoshi, E. *et al.* Peptide vaccine-treated, long-term surviving cancer patients harbor self-renewing tumor-specific CD8+ T cells. *Nat. Commun.* **13**, 3123 (2022).
57. Liang, J. *et al.* Personalized cancer vaccines from bacteria-derived outer membrane vesicles with antibody-mediated persistent uptake by dendritic cells. *Fundam. Res.* **2**, 23–36 (2022).
58. Cheng, K. *et al.* Bioengineered bacteria-derived outer membrane vesicles as a versatile antigen display platform for tumor vaccination via Plug-and-Display technology. *Nat. Commun.* **12**, 2041 (2021).
59. Zitvogel, L. & Kroemer, G. Cross-reactivity between microbial and tumor antigens. *Curr. Opin. Immunol.* **75**, 102171 (2022).
60. Canale, F. P. *et al.* Metabolic modulation of tumours with engineered bacteria for immunotherapy. *Nature* **598**, 662–666 (2021).
61. Lam, K. C. *et al.* Microbiota triggers STING-type I IFN-dependent monocyte reprogramming of the tumor microenvironment. *Cell* **184**, 5338-5356.e21 (2021).

62. Si, W. *et al.* Lactobacillus rhamnosus GG induces cGAS/STING- dependent type I interferon and improves response to immune checkpoint blockade. *Gut* **71**, 521–533 (2022).
63. Shi, Y. *et al.* Intratumoral accumulation of gut microbiota facilitates CD47-based immunotherapy via STING signaling. *J. Exp. Med.* **217**, e20192282 (2020).
64. Baruch, E. N. *et al.* Fecal microbiota transplant promotes response in immunotherapy-refractory melanoma patients. *Science* **371**, 602–609 (2021).
65. Messaoudene, M. *et al.* A Natural Polyphenol Exerts Antitumor Activity and Circumvents Anti-PD-1 Resistance through Effects on the Gut Microbiota. *Cancer Discov.* **12**, 1070–1087 (2022).

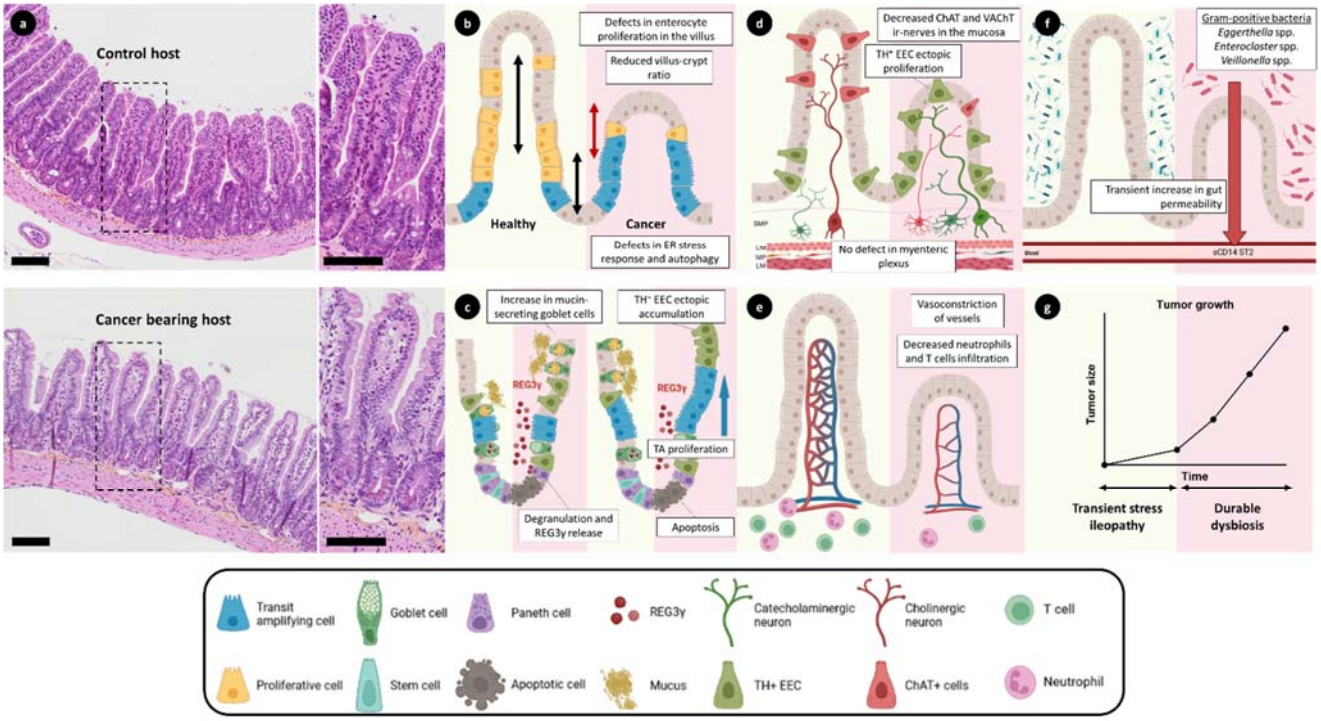

Figure 1. Microscopic and cellular description of the cancer-induced stress ileopathy.

A-G. Proposed scenario of stress ileopathy induced during a tumorigenic process. Experimental demonstration in cancer bearing mice that tumor inoculation may trigger crypt apoptosis, activation of secretory cells, ectopic proliferation of tyrosine hydroxylase positive and enteroendocrine cells (TH^+ EEC) resulting in a disbalance between cholinergic and adrenergic signaling promoting a transient ileal mucosa atrophy but a protracted gut dysbiosis dominated by vancomycin-sensitive species belonging to the *Enterocloster* genus. Micrograph pictures of HE stained ileal tissues showing patchy abrasion of ileal villosities 7-10 days after tumor implantation in C57BL/6 mice. Bar scale: 100 µm. *CM, circular muscle; ChAT, Choline acetyltransferase; EEC, Enteroendocrine cell; ER, Endoplasmic reticulum; ir-nerves, Immunoreactive nerves; LM, longitudinal muscle; MP, myenteric plexus; REG3γ, Regenerating islet-derived protein 3 gamma; sCD14, Soluble CD14; SMP, submucosal plexus; ST2, Suppression of Tumorigenicity 2 protein; TA, transit amplifying cells; TH, Tyrosine hydroxylase; VAChT, Vesicular acetylcholine transporter*.

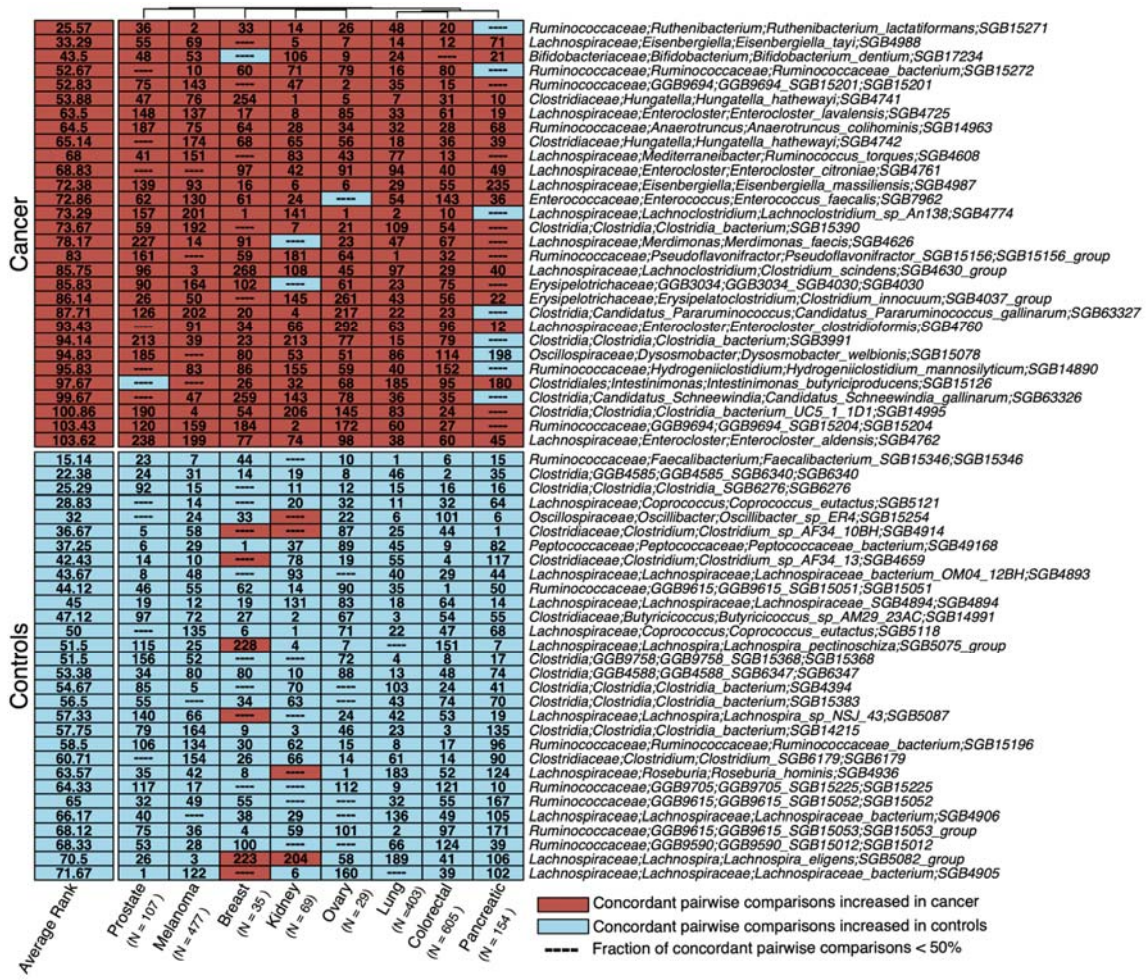

Figure 2. Pan-cancer GOMS compared with healthy metagenomics profiles. Top 30 ranked SGBs in cancer or control cohorts. Ranks were determined by ordering *p-values* calculated using a random effects meta-analysis of all possible cancer and control cohort pairs. Only SGBs with 95% credible intervals greater than or less than zero in > 50% of pairwise comparisons were considered for the ranking.

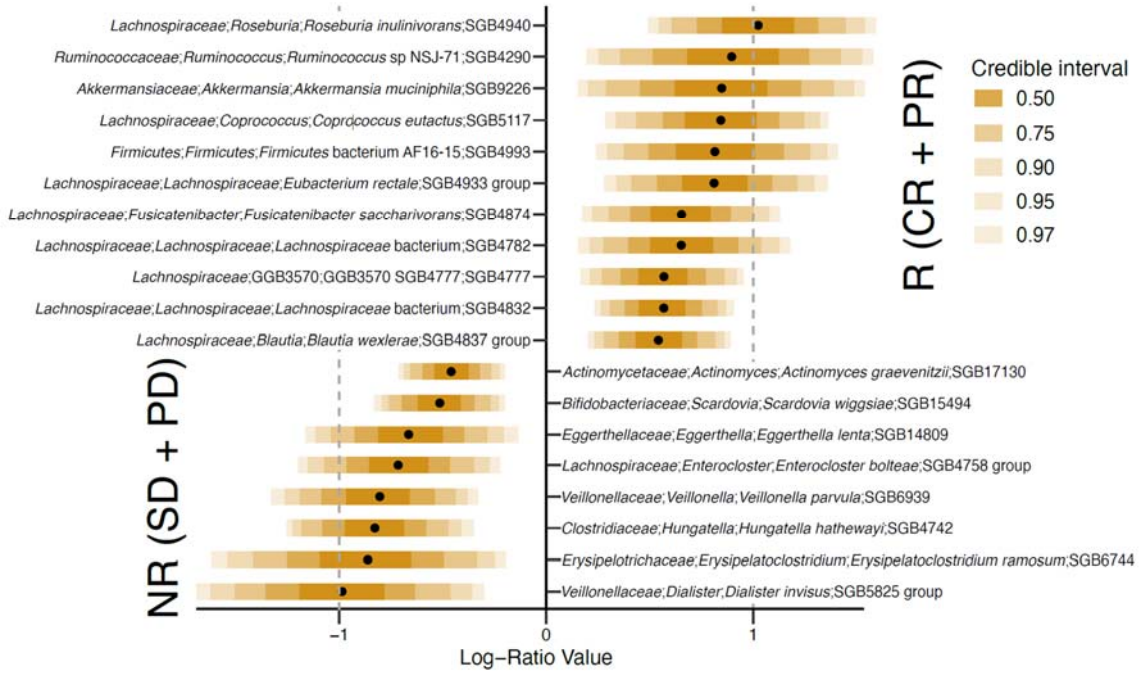

Figure 3. GOMS-related to R versus NR status before ICI (mega-analysis, ORR).

Results of a mega-analysis using Pibble models on clr transformed SGB-level relative abundances. Pibble models also included age, gender and cohort as covariates. SGBs whose 95% credible interval is greater than or smaller than 0.2 are reported in the figure. Also refer to Table S6 for SGBs with a prevalence higher than 5% and their corresponding 95% credible intervals.

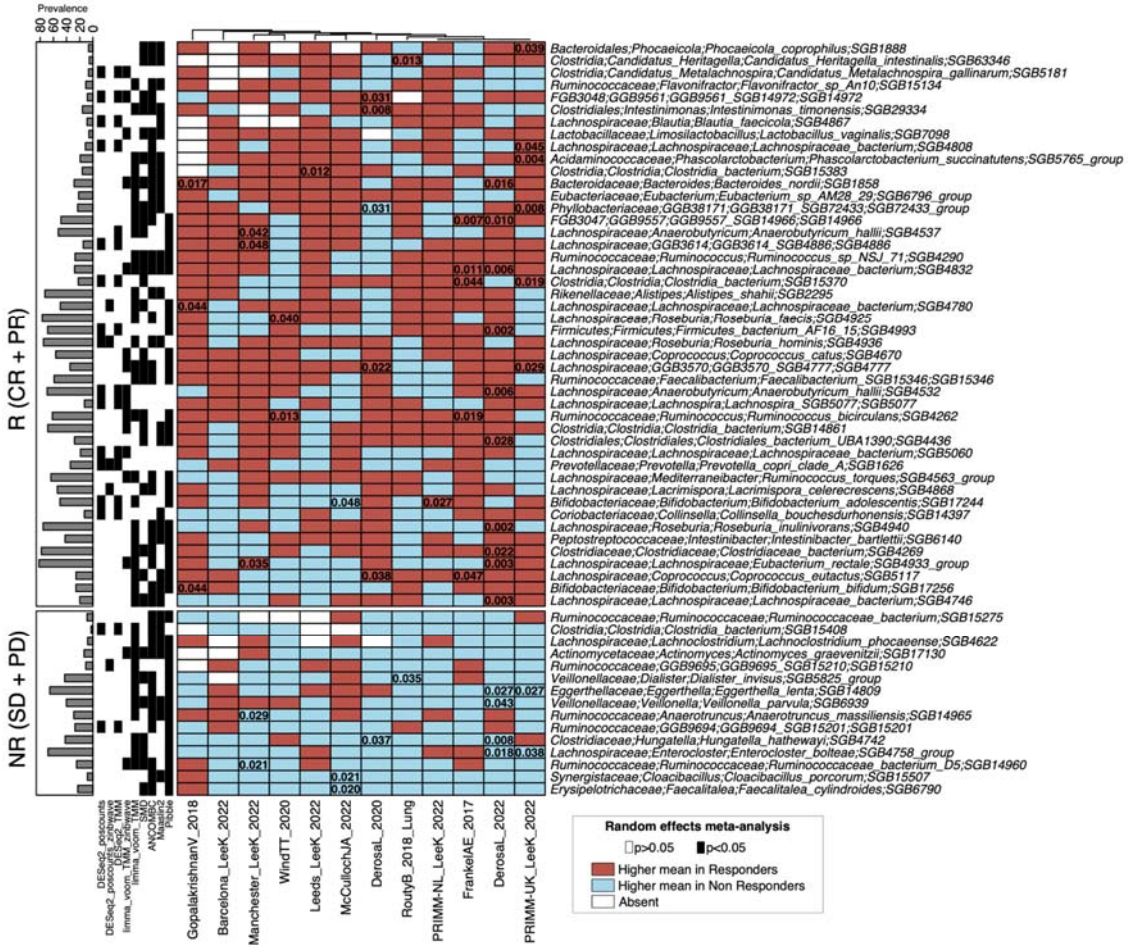

Figure 4. GOMS-related to R versus NR status before ICI (meta-analysis, ORR). SGBs associated with ORR identified by a meta-analysis using different differential abundance methods adjusting for age and gender. SGBs shown have random-effects model *p-values* < 0.05 in at least three methods. Values inside the cells refer to unadjusted *p-values* < 0.05 obtained by two-tailed Wilcoxon tests on differences in the relative abundance of responders and non-responders. The color of the cell was determined by comparing the mean relative abundance in responders to non-responders; if the mean was higher in responders, then the cells were colored red; if it was higher in non-responders, then it was colored blue. Also refer to Table S7.

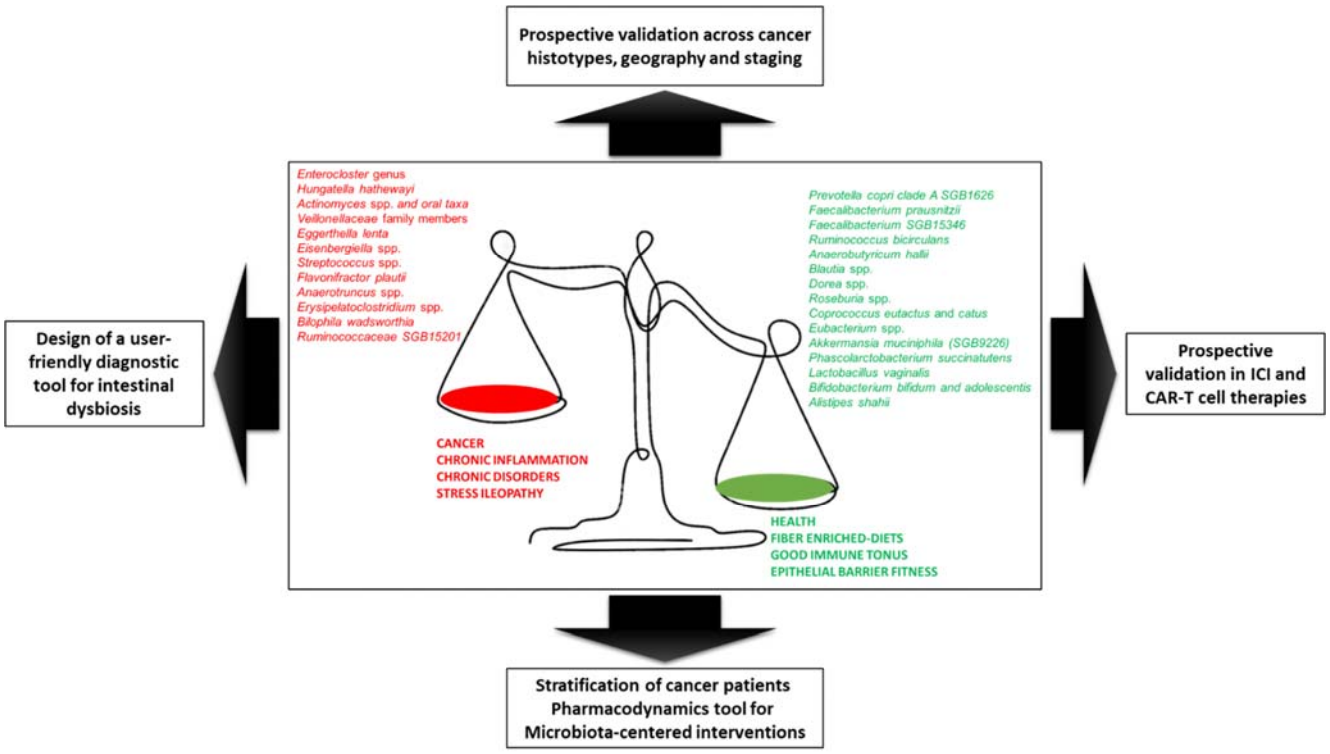

Figure 5. Challenges of microbiota-related biomarkers in oncology.

Shotgun metagenomics –based sequencing is currently the state-of the art method to analyze the taxonomic composition of the stools or ileal content and to perform machine learning in cohorts of cancer patients. The challenges of this field are to increment many more patients to stabilize the Gut OncoMicrobiome fingerprint, to design a friendly user diagnosis tool that should be validated prospectively across cancer types, cancer staging, geography, life style, treatments and co-morbidities. This tool will be instrumental to stratify patients according to their gut dysbiosis, for future microbiota centered-intervention or interceptive measures.

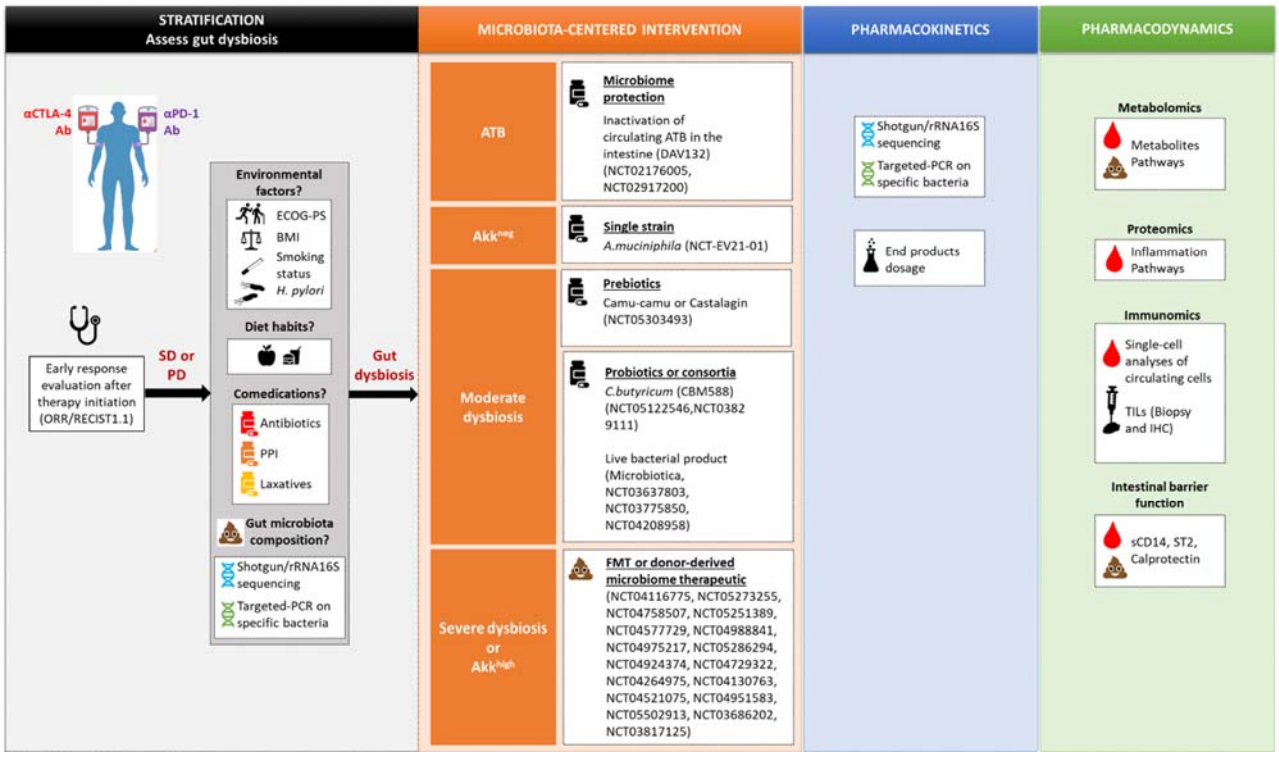

Figure 6. Practical prospects toward defining GOMS-related clinical guidelines.

A. Summary of the proposed clinical management of cancer patients amenable to an FDA or EMA-approval of ICI, taking into account gut microbiota composition. Patients with a history of antibiotics (any kind except vancomycin) taken between 60 days prior to, up to 42 after the first administration of anti-PD-1 Abs (alone or combined with anti-CTLA-4 Abs) or comedications known to alter microbiota composition (Proton Pomp Inhibitors (PPI) or laxatives) should be investigated by performing shotgun MG sequencing of stools or targeted PCR at diagnosis to monitor taxonomic composition. B. Depending on the relative abundances of *Akkermansia* spp. as well as other family members or genera or species (listed as harmful or beneficial in GOMS) (refer to Figure 3-4), different putative scenarios are described with their respective clinical management as for a potential microbiota-centered intervention to compensate gut dysbiosis. The over-abundance of *Akkermansia* spp. (SGB9226 (*A.muciniphila*) or 9228 or others) is defined by a relative abundance above 4.8% of all species using MetaphLAN or MetaO -MineR algorithms (*A.muc*^{high}). C. The pharmacodynamics and kinetics of the MCI should be assessed to monitor their effects on the body metabolic, immunologic or hematologic functions or inflammatory tonus and the gut microbiota composition or deviation from baseline. *Ab, antibody; ATB, antibiotics; Akk, Akkermansia muciniphila; BMI, Body mass index; ECOG PS, Eastern Cooperative Oncology Group performance status; FMT, Fecal microbiota transplant; PPI, Proton pump inhibitor; TILs, Tumor infiltrating lymphocytes; IHC, Immunohistochemistry; sCD14, Soluble CD14; ST2, Suppression of Tumorigenicity 2 protein.*

Table S1. Gut OncoMicrobiome Signatures (GO

Order	Family
Acidaminococcales	*Acidaminococcaceae*
Bifidobacteriales	*Bifidobacteriaceae*
Bacteroidales	*Rikenellaceae*
Bacteroidales	*Rikenellaceae*
Eubacteriales	*Lachnospiraceae*
Eubacteriales	*Lachnospiraceae*
Eubacteriales	*Oscillospiraceae*
Bacteroidales	*Bacteroidaceae*
Bacteroidales	*Bacteroidaceae*
Bacteroidales	*Barnesiellaceae*
Bifidobacteriales	*Bifidobacteriaceae*
Bifidobacteriales	*Bifidobacteriaceae*
Desulfovibrionales	*Desulfovibrionaceae*
Eubacteriales	*Clostridiaceae*
Bacteroidales	*Odoribacteraceae*
Eubacteriales	*Lachnospiraceae*
Campylobacterales	*Campylobacteraceae*
Clostridiales	*Clostridia*
Clostridiales	*Clostridia*
Eubacteriales	*Clostridiaceae*
Eubacteriales	*Clostridiaceae*
Eubacteriales	*Oscillospiraceae*
Coriobacteriales	*Coriobacteriaceae*
Eubacteriales	*Lachnospiraceae*
Eubacteriales	*Lachnospiraceae*
Desulfovibrionales	*Desulfovibrionaceae*
Veillonellales	*Veillonellaceae*
Eubacteriales	*Lachnospiraceae*
Eubacteriales	*Oscillospiraceae*
Eggerthellales	*Eggerthellaceae*
Eubacteriales	*Lachnospiraceae*
Eubacteriales	*Lachnospiraceae*
Lactobacillales	*Enterococcaceae*
Erysipelotrichales	*Erysipelotrichaceae*
Eubacteriales	*Eubacteriaceae*
Eubacteriales	*Oscillospiraceae*
Tissierellales	*Peptoniphilaceae*
Eubacteriales	*Oscillospiraceae*
Eubacteriales	*Lachnospiraceae*
Enterobacterales	*Hafniaceae*

Eubacteriales	*Oscillospiraceae*
Erysipelotrichales	*Erysipelotrichaceae*
Eubacteriales	*Clostridiaceae*
Eubacteriales	*Oscillospiraceae*
Eubacteriales	*Eubacteriales*
Eubacteriales	*Lachnospiraceae*
Eubacteriales	*Lachnospiraceae*
Eubacteriales	*Lachnospiraceae*
Eubacteriales	*Lachnospiraceae*
Lactobacillales	*Lactobacillaceae*
Eubacteriales	*Oscillospiraceae*
Lactobacillales	*Lactobacillaceae*
Eubacteriales	*Lachnospiraceae*
Eubacteriales	*Lachnospiraceae*
Eubacteriales	*Oscillospiraceae*
Bacteroidales	*Prevotellaceae*
Bacteroidales	*Prevotellaceae*
Eubacteriales	*Oscillospiraceae*
Eubacteriales	*Lachnospiraceae*
Eubacteriales	*Lachnospiraceae*
Eubacteriales	*Oscillospiraceae*
Lactobacillales	*Streptococcaceae*
Eubacteriales	*Oscillospiraceae*
Erysipelotrichales	*Turicibacteraceae*
Oscillospiraceae	*Faecalibacterium*
Eubacteriales	*Lachnospiraceae*
Eubacteriales	*Oscillospiraceae*
Eubacteriales	*Oscillospiraceae*
Eubacteriales	*Peptococcaceae*
Veillonellales	*Veillonellaceae*

MS) pan-diseases or pan-cancers versus healthy metagenomes and alignment with proposed met

Genus (Species)
Acidaminococcus (A. fermentans)
Aeriscardovia (A. aeriphila)
Alistipes (A. onderdonkii, A. putredinis, A. shahii)
Alistipes (A. senegalensis, A. shahii, A. communis (Bacteroidales bacterium ph8))
Anaerobutyricum (A. hallii)
Anaerostipes (A. hadrus)
Anaerotruncus (A. colihominis, A. sp.)
Bacteroides (B. galacturonicus)
Bacteroides (B. uniformis, B. vulgatus)
Barnesiella (B. intestinihominis)
Bifidobacterium (B. adolescentis, B. pseudocatenulatum)
Bifidobacterium (B. dentium)
Bilophila (B. wadsworthia)
Butyricicoccus (B. sp. AM29-23AC)
Butyricimonas (B. synergistica, B. virosa)
Butyrivibrio (B. crossotus)
Campylobacter (C. gracilis)
Candidatus Pararuminococcus (CP. gallinarum)
Candidatus Schneewindia (CS. gallinarum)
Clostridium (C. bolteae CAG:59, C. sp. CAG:58, sp. CAG:242)
Clostridium (C. sp. AF34-13, C. sp. AF34-10BH)
Clostridium leptum
Collinsella (C. aerofaciens)
Coprococcus (C. comes)
Coprococcus (C. eutactus)
Desulfovibrio (D. piger)
Dialister (D. sp. CAG:357)
Dorea (D. longicatena)
Dysosmobacter (D. welbionis)
Eggerthella (E. lenta, E. sp.)
Eisenbergiella (E. massiliensis, E. tayi)
Enterocloster (E. asparagiformis, E. bolteae, E. citroniae, E. clostridioformis, E. lavalensis)
Enterococcus (E. faecalis)
Erysipelatoclostridium (Clostridium innocuum)
Eubacterium (E. ventriosum, E. sp. CAG:274)
Faecalibacterium (F. prausnitzii)
Finegoldia (F. magna)
Flavonifractor (F. plautii)
Fusicatenibacter (F. saccharivorans)
Hafnia (H. alvei)

Harryflintia (H. acetispora)
Holdemania (H. filiformis)
Hungatella (H. hathewayi)
Hydrogeniiclostridium (H. mannosilyticum)
Intestinimonas (I. butyriciproducens)
Lachnoclostridium (Clostridium scindens, L. sp. An138)
Lachnoclostridium (Clostridium symbiosum)
Lachnospira (L. eligens, L. pectinoschiza, L. sp. NSJ-43)
Lachnospiraceae (Eubacterium rectale)
Lactobacillus (L. rogosae)
Lawsonibacter (L. asaccharolyticus)
Ligilactobacillus (L. ruminis)
Mediterraneibacter (Ruminococcus gnavus, R. torques)
Merdimonas (Merdimonas faecis)
Oscillibacter (Oscillibacter sp.)
Paraprevotella (P. clara, P. sp.)
Prevotella (P. copri, P. stercorea, P. sp. CAG:520)
Pseudoflavonifractor (P. capillosus, P. sp.)
Roseburia (R. faecis, R. sp. CAG:471)
Roseburia (R. hominis)
Ruthenibacterium (R. lactatiformans)
Streptococcus (S. parasanguinis, S. salivarius)
Subdoligranulum sp.
Turicibacter (T. sanguinis)
unclassified Faecalibacterium (Faecalibacterium sp.)
unclassified Lachnospira (Lachnospiraceae bacterium)
unclassified Oscillospiraceae (Oscillospiraceae bacterium)
unclassified Oscillospiraceae (Ruminococcaceae bacterium D16)
unclassified Peptococcaceae (Peptococcaceae bacterium)
Veillonella (V. parvula)

a-analysis.

Core gut microbiome	ref	Health	ref
		x	Yonekura, S. et al.
x	Gacesa, R. et al.		
		x	Gacesa, R. et al.
		x	Yonekura, S. et al.
		x	Yonekura, S. et al.
		x	Yonekura, S. et al.
x	Gacesa, R. et al.		
		x	Gacesa, R. et al.
		x	Gacesa, R. et al., Yonekura, S. et al.
		x	Gacesa, R. et al.
		x	Yonekura, S. et al.
		x	Yonekura, S. et al.
		x	Gacesa, R. et al.
		x	Yonekura, S. et al.
		x	Gacesa, R. et al., Yonekura, S. et al.
		x	Yonekura, S. et al.
x	Gacesa, R. et al.	x	Gacesa, R. et al.
		x	Yonekura, S. et al.
		x	Yonekura, S. et al.

		x	Yonekura, S. et al.
x	Gacesa, R. et al.	x	Yonekura, S. et al.
		x	Yonekura, S. et al.
		x	Yonekura, S. et al.
		x	Yonekura, S. et al.
x	Gacesa, R. et al.		
		x	Gacesa, R. et al.
		x	Gacesa, R. et al., Yonekura, S. et al.
		x	Yonekura, S. et al.
x	Gacesa, R. et al.	x	Gacesa, R. et al.
		x	Yonekura, S. et al.

Pan-disease	ref	Pan-Cancer	ref	Health (Meta-analysis)	ref
		x	Yonekura, S. et al.		
x	Gacesa, R. et al.	x	Yonekura, S. et al.		
x	Gacesa, R. et al.	x	Yonekura, S. et al.		
		x	Yonekura, S. et al.		
				x	Figure 2
		x	Yonekura, S. et al.		
		x	Yonekura, S. et al.		
		x	Yonekura, S. et al.		
				x	Figure 2
x	Gacesa, R. et al.				
				x	Figure 2
x	Gacesa, R. et al.				
		x	Yonekura, S. et al.		
x	Gacesa, R. et al.	x	Yonekura, S. et al.		
x	Gacesa, R. et al.				
		x	Yonekura, S. et al.		

		x	Yonekura, S. et al.		
x	Gacesa, R. et al.				
x	Gacesa, R. et al.				
		x	Yonekura, S. et al.		
		x	Yonekura, S. et al.		
				x	Figure 2
		x	Yonekura, S. et al.		
x	Gacesa, R. et al.				
x	Gacesa, R. et al.			x	Figure 2
x	Gacesa, R. et al.				
				x	Figure 2
		x	Yonekura, S. et al.		
x	Gacesa, R. et al.				
				x	Figure 2
x	Gacesa, R. et al.			x	Figure 2
				x	Figure 2
x	Gacesa, R. et al.				
				x	Figure 2
x	Gacesa, R. et al.				

Pan-Cancer (Meta-analysis)	ref
x	Figure 2
x	Figure 2
x	Figure 2
x	Figure 2
x	Figure 2
x	Figure 2
x	Figure 2
x	Figure 2
x	Figure 2

x	Figure 2
x	Figure 2
x	Figure 2
x	Figure 2
x	Figure 2
x	Figure 2
x	Figure 2
x	Figure 2
x	Figure 2

Table S2. Cohort description for the meta-analysis comparing GOMS in c

Study Name	Cancer
Terrisse et al., JITC., 2022	Prostate Cancer
Pernigoni et al., Science., 2021	Prostate Cancer
Terrisse et al., Cell Death & Diff., 2021	Breast Cancer
Derosa et al., Nature Med., 2022	Lung Cancer
Routy et al., Science., 2018	Lung Cancer
Yonekura et al., Cancer Discovery., 2022	Ovarian Cancer
Derosa et al., European Urology., 2020	Kidney Cancer
Kartal et al., Gut., 2022	Pancreatic Cancer
Nagata et al., Gastroenterology., 2022	Pancreatic Cancer
Spencer et al., Science., 2021	Melanoma
Lee et al., Nature Med., 2022	Melanoma
McCulloch et al., Nature Med., 2022	Melanoma
Gopalakrishnan et al., Science., 2018	Melanoma
Wind et al., Melanoma Research., 2020	Melanoma
Frankel et al., Neoplasia., 2017	Melanoma
Peters et al., Genome Med., 2019	Melanoma
Thomas et al., Nat Med., 2019	Colorectal Cancer
Wirbel et al., Nat Med., 2019	Colorectal Cancer
Yu et al., Gut., 2017	Colorectal Cancer
Feng et al., Nat Commun., 2015	Colorectal Cancer
Vogtmann et al., PloS One., 2016	Colorectal Cancer
Zeller et al., Mol Syst Biol., 2014	Colorectal Cancer
Yachida et al., Nat Med., 2019	Colorectal Cancer
Total	
Xie et al., Cell Syst., 2016	Healthy Controls
Asnicar et al., Nat Med., 2021	Healthy Controls
Zhernakova et al., Science., 2016	Healthy Controls
Schirmer et al., Cell., 2016	Healthy Controls
HMP Consortium., Nature., 2012	Healthy Controls
Qin et al., Nature., 2014	Healthy Controls
Qin et al., Nature., 2012	Healthy Controls
Vieira-Silva et al., Nature., 2020	Healthy Controls
De Filippis et al., Cell Host Microbe., 2019	Healthy Controls
Keohane et al., Nat Med., 2020	Healthy Controls
Dhakan et al., Gigascience., 2019	Healthy Controls
Yachida et al., Nat Med., 2019	Healthy Controls
Nielsen et al., Nat Biotechnol., 2014	Healthy Controls
Zeevi et al., Cell., 2015	Healthy Controls
Total	

cMD: curatedMetagenomicData

ancer versus healthy individuals.

Number of patients	Cohort name
33	Oncobiotics
74	
35	CANTO
338	Lung Oncobiotics
65	
29	
69	
111	
43	
112	
163	PRIMM
94	
24	
20	
37	
27	
61	
60	
75	
46	
52	
53	
258	
1879	
250	Twins UK
1098	PREDICT 1
1129	LifeLines Deep
465	Human Functional Genomics Project
94	HMP 1
114	
174	
322	MetaCARDIS
97	
117	
110	
246	
247	MetaHIT
878	
5341	

Country	PubMedID	in cMD
France	35296557	no
Switzerland/UK	34618582	no
France	33963313	no
France	35115705	no
France	29097494	no
France	34930787	no
France	32376136	no
Spain/Germany	35260444	no
Japan	35788347	no
USA	34941392	no
UK/Netherlands/Spain	35228751	yes
USA	35228752	no
USA	29097493	yes
Netherlands	31990790	yes
USA	28923537	yes
USA	31597568	yes
Italy	30936548	yes
Germany	30936547	yes
China	26408641	yes
Austria	25758642	yes
USA	27171425	yes
France	25432777	yes
Japan	31171880	yes
UK	27818083	yes
UK/USA	33432175	yes
Netherlands	27126040	yes
Netherlands	27814509	yes
USA	22699609	yes
China	25079328	yes
China	23023125	yes
Germany/France	32433607	yes
Italy	30799264	yes
Ireland	32632193	yes
India	30698687	yes
Japan	31171880	yes
Denmark/Spain	24997787	yes
Israel	26590418	yes

Table S3. Detailed results of Pan-cancer GOMS presented in Figure 2.

Sheet name	Content
Legend	Color legend and detailed parameters
Summary	PanCancer meta-analysis (Healthy vs Cancer individuals) summary
breast	Breast cancer GOMS compared with healthy metagenomics profiles
melanoma	Melanoma GOMS compared with healthy metagenomics profiles
ovary	Ovarian cancer GOMS compared with healthy metagenomics profiles
pancreatic	Pancreatic cancer GOMS compared with healthy metagenomics profiles
prostate	Prostate cancer GOMS compared with healthy metagenomics profiles
crc	Colorectal cancer (CRC)GOMS compared with healthy metagenomics profiles
kidney	Kidney cancer GOMS compared with healthy metagenomics profiles
lung	Lung cancer GOMS compared with healthy metagenomics profiles

Table S4. Gut OncoMicrobiome signatures (GOMS) profile across various cancer histotypes. Only bacterial taxa histotypes

Order	Family	Genus (Species)
Acidaminococcales	*Acidaminococcaceae*	*Acidaminococcus (A. fermentans)*
Actinomycetales	*Actinomycetaceae*	*Actinomyces (A. graevenitzii, A. sp. ICM39)*
Bacteroidales	*Rikenellaceae*	*Alistipes (A. indistinctus, A. putredinis, A. shahii, A. sp. CAG:831, A. communis (Bacteroidales bacterium ph8))*
Bifidobacteriales	*Bifidobacteriaceae*	*Alloscardovia (A. omnicolens)*
Tissierellales	*Peptoniphilaceae*	*Anaerococcus (A. obesiensis, A. vaginalis)*
Eubacteriales	*Oscillospiraceae*	*Anaerotruncus (A. colihominis)*
Bacteroidales	*Bacteroidaceae*	***Bacteroides (B. finegoldii, B. fragilis, B. nordii, B. ovatus, B. sp. 43_108, B. sp. CAG:633, B. sp. CAG:661, B. thetaiotaomicron, B.uniformis))***
Bacteroidales	*Bacteroidaceae*	*Bacteroides (B. fragilis)*
Bacteroidales	*Barnesiellaceae*	*Barnesiella (B. intestinihominis)*
Bifidobacteriales	*Bifidobacteriaceae*	*Bifidobacterium (B. dentium)*
Desulfovibrionales	*Desulfovibrionaceae*	*Bilophila (B. wadsworthia)*
Bacteroidales	*Odoribacteraceae*	*Butyricimonas (B. synergistica, B. virosa)*
Eubacteriales	*Lachnospiraceae*	*Butyrivibrio (B. crossotus)*
Campylobacterales	*Campylobacteraceae*	*Campylobacter (C. gracilis)*
Eggerthellales	*Eggerthellaceae*	*Eggerthella (E. lenta)*
Eubacteriales	*Lachnospiraceae*	*Eisenbergiella (E. massiliensis, E. tayi)*
Eubacteriales	*Lachnospiraceae*	***Enterocloster (E. aldenensis , E. asparagiformis , E. bolteae, E. citroniae, E. clostridioformis, E. lavalensis)***
Lactobacillales	*Enterococcaceae*	*Enterococcus (E. faecalis, E. durans)*
Enterobacterales	*Enterobacteriaceae*	*Escherichia (E. coli)*
Eubacteriales	*Eubacteriaceae*	*Eubacterium (E. sp. CAG:180)*
Eubacteriales	*Oscillospiraceae*	*Faecalibacterium (F. prausnitzii)*
Eubacteriales	*Oscillospiraceae*	*Flavonifractor (F. plautii, F. sp. An100)*
Fusobacteriales	*Fusobacteriaceae*	*Fusobacterium (F. nucleatum subsp. animalis, nucleatum, vincentii, F. sp. oral taxon 370)*
Bacillales	*Bacillales Family XI.*	*Gemella (G. morbillorum)*
Enterobacterales	*Hafniaceae*	*Hafnia (H. alvei, H. paralvei)*
Eubacteriales	*Oscillospiraceae*	*Harryflintia (H. acetispora)*
Eubacteriales	*Clostridiaceae*	***Hungatella (H. hathewayi)***
Eubacteriales	*Eubacteriaceae*	*Intestinimonas (I. butyriciproducens)*
Enterobacterales	*Enterobacteriaceae*	*Klebsiella (K. pneumoniae)*
Eubacteriales	*Lachnospiraceae*	*Lachnoclostridium (Clostridium symbiosum)*
Eubacteriales	*Lachnospiraceae*	*Lachnospira (L. eligens)*
Eubacteriales	*Oscillospiraceae*	*Lawsonibacter (L. asaccharolyticus)*
Eubacteriales	*Lachnospiraceae*	*Mediterraneibacter (Ruminococcus torques)*
Methanobacteriales	*Methanobacteriaceae*	*Methanobrevibacter (M. smithii)*
Enterobacterales	*Morganellaceae*	*Morganella (M. morganii)*
Bacteroidales	*Odoribacteraceae*	*Odoribacter (O. splanchnicus)*
Coriobacteriales	*Atopobiaceae*	*Olsenella (O. uli)*

Eubacteriales	*Oscillospiraceae*	*Oscillospiraceae incertae sedis (Clostridium leptum)*
Bacteroidales	*Tannerellaceae*	*Parabacteroides (P. distasonis, P. merdae)*
Tissierellales	*Peptoniphilaceae*	*Parvimonas (P. micra , P. sp.)*
Eubacteriales	*Peptostreptococcaceae*	*Peptostreptococcus (P. anaerobius, P. stomatis)*
Acidaminococcales	*Acidaminococcaceae*	*Phascolarctobacterium (P. sp. CAG:266)*
Bacteroidales	*Bacteroidaceae*	*Phocaeicola (P. barnesiae)*
Bacteroidales	*Porphyromonadaceae*	*Porphyromonas (P. asaccharolytica, P. somerae, P. uenonis)*
Bacteroidales	*Prevotellaceae*	***Prevotella (P. copri, P. intermedia, P. nigrescens, P. sp. CAG:617, P. sp.)***
Enterobacterales	*Morganellaceae*	*Proteus (P. mirabilis)*
Eubacteriales	*Lachnospiraceae*	*Roseburia (R. intestinalis)*
Eubacteriales	*Oscillospiraceae*	*Ruthenibacterium (R. lactatiformans)*
Bacteroidales	*Porphyromonadaceae*	*Sanguibacteroides (S. justesenii)*
Erysipelotrichales	*Erysipelotrichaceae*	*Solobacterium (S. moorei)*
Lactobacillales	*Streptococcaceae*	*Streptococcus (S. anginosus, S. oralis, S. vestibularis)*
Lactobacillales	*Streptococcaceae*	*Streptococcus (S. parasanguinis)*
Eubacteriales	*Oscillospiraceae*	*Subdoligranulum (S. sp. 4_3_54A2FAA)*
Burkholderiales	*Sutterellaceae*	*Sutterella (S. wadsworthensis)*
Desulfovibrionales	*Desulfovibrionaceae*	*unclassified Desulfovibrionaceae (D. bacterium)*
Eubacteriales	*Lachnospiraceae*	*unclassified Lachnospiraceae (L. bacterium 3_1_57FAA_CT1)*
Eubacteriales	*Oscillospiraceae*	*unclassified Oscillospiraceae (Ruminococcaceae bacterium D16, D5)*
Veillonellales	*Veillonellaceae*	*Veillonella (V. atypica, V. dispar, V. parvula)*

relatively over-represented (but not under-represented) in cancer patient fecal sample

Breast cancer	ref	Pancreatic ductal carcinoma
x	Yonekura, S. et al.	
		x
x	Terrisse, S. et al., Yonekura, S. et al.	
		x
x	Yonekura, S. et al.	
x	Terrisse, S. et al., Yonekura, S. et al.	x
x	Terrisse, S. et al.	
x	Terrisse, S. et al.	
x	Yonekura, S. et al.	
x	Terrisse, S. et al., Yonekura, S. et al.	
x	Yonekura, S. et al.	
		x
x	Yonekura, S. et al.	
x	Yonekura, S. et al.	
x	Yonekura, S. et al.	
x	Terrisse, S. et al., Yonekura, S. et al.	x
x	Yonekura, S. et al.	
x	Yonekura, S. et al.	
x	Yonekura, S. et al.	
x	Terrisse, S. et al.	
x	Yonekura, S. et al.	
x	Yonekura, S. et al.	
x	Yonekura, S. et al.	
x	Yonekura, S. et al.	x
x	Yonekura, S. et al.	
x	Terrisse, S. et al.	
		x
x	Terrisse, S. et al.	
x	Yonekura, S. et al.	
		x
x	Yonekura, S. et al.	
x	Terrisse, S. et al., Yonekura, S. et al.	
x	Yonekura, S. et al.	

x	Terrisse, S. et al., Yonekura, S. et al.	
x	Yonekura, S. et al.	
x	Terrisse, S. et al.	
x	Terrisse, S. et al., Yonekura, S. et al.	x
x	Yonekura, S. et al.	
x	Terrisse, S. et al.	
x	Yonekura, S. et al.	
x	Yonekura, S. et al.	
		x
		x
x	Yonekura, S. et al.	
x	Terrisse, S. et al., Yonekura, S. et al.	
		x

s (compared with health subjects) are annotated. Cance

ref	Colorectal cancer
	x
Nagata, N. et al.	x
	x
Kartal, E. et al.	
	x
	x
Kartal, E. et al.	x
	x
	x
	x
Kartal, E. et al.	
	x
	x
	x
Nagata, N. et al.	x
	x
	x
	x
	x
	x
	x
	x
	x
Nagata, N. et al.	x
	x
Nagata, N. et al.	x
	x
	x
Kartal, E. et al.	
	x
	x

	x
	x
	x
	x
	x
	x
Kartal, E. et al.	x
	x
	x
	x
	x
Nagata, N. et al.	
	x
	x
Nagata, N. et al.	
	x
	x
	x
Kartal, E. et al., Nagata, N. et al.	

r histotype-specific species are not in bold.

ref
Yonekura, S. et al.
Thomas, A. M. et al.
Yonekura, S. et al.
Wirbel, J. et al.
Thomas, A. M. et al., Yonekura, S. et al.
Yonekura, S. et al.
Yonekura, S. et al.
Yonekura, S. et al.
Yonekura, S. et al.
Yonekura, S. et al.
Yonekura, S. et al.
Yonekura, S. et al.
Wirbel, J. et al., Yonekura, S. et al.
Yonekura, S. et al.
Thomas, A. M. et al., Yonekura, S. et al.
Yonekura, S. et al.
Yonekura, S. et al.
Thomas, A. M. et al., Wirbel, J. et al.
Thomas, A. M. et al., Wirbel, J. et al.
Yonekura, S. et al.
Yonekura, S. et al.
Wirbel, J. et al., Yonekura, S. et al.
Yonekura, S. et al.
Thomas, A. M. et al., Wirbel, J. et al., Yonekura, S. et al.
Yonekura, S. et al.
Wirbel, J. et al.
Yonekura, S. et al.
Yonekura, S. et al.

Thomas, A. M. et al.
Yonekura, S. et al.
Thomas, A. M. et al., Wirbel, J. et al.
Thomas, A. M. et al., Wirbel, J. et al.
Yonekura, S. et al.
Thomas, A. M. et al., Wirbel, J. et al.
Thomas, A. M. et al., Wirbel, J. et al., Yonekura, S. et al.
Yonekura, S. et al.
Yonekura, S. et al.
Yonekura, S. et al.
Wirbel, J. et al.
Thomas, A. M. et al.
Wirbel, J. et al.
Yonekura, S. et al.
Thomas, A. M. et al.
Yonekura, S. et al.

Table S5. Cohort description and machine learning analysis for R versus NR cancer patients treated with

Cohort	Cancer	ICI	NR	R	Total	RF	LASSO
						LODO AUC	LODO AUC
FrankelAE_2017	Melanoma	CTLA-4 + PD-1	20	17	**37**	0.66	0.55
GopalakrishnanaV_2018	Melanoma	PD-1	13	10	**23**	0.58	0.62
Manchester_LeeK_2022	Melanoma	CTLA-4 + PD-1	15	10	**25**	0.73	0.52
McCullochJA_2022	Melanoma	PD-1	35	59	**94**	0.53	0.52
PRIMM-NL_LeeK_2022	Melanoma	CTLA-4 + PD-1	33	22	**55**	0.62	0.57
PRIMM-UK_LeeK_2022	Melanoma	CTLA-4 + PD-1	32	23	**55**	0.49	0.42
DerosaL_2022	NSCLC	PD-1	263	75	**338**	0.70	0.55
RoutyB_2018_Lung	NSCLC	PD-1	53	12	**65**	0.78	0.70
DerosaL_2020	RCC	PD-1	49	20	**69**	0.65	0.66
		Total	**513**	**248**	**761**	**RF Global CV AUC**	
		Total for Global AUC			**761**	**0.71**	

ICI: Immune checkpoint inhibitors
NR: Non-responder (SD+PD)
R: Responder (CR+PR)
RF: Random Forrest
LASSO: Least Absolute Shrinkage and Selection Operator
AUC: area under the curve
cMD: curatedMetagenomicData

immune checkpoint inhibitors.

Reference	Country	PubMedID	in cMD
Frankel et al., Neoplasia., 2017	USA	28923537	yes
Gopalakrishnan et al., Science., 2018	USA	29097493	yes
Lee et al., Nature Med., 2022	UK	35228751	yes
McCulloch et al., Nature Med., 2022	USA	35228752	no
Lee et al., Nature Med., 2022	Netherlands	35228751	yes
Lee et al., Nature Med., 2022	UK	35228751	yes
Derosa et al., Nature Med., 2022	France	35115705	no
Routy et al., Science., 2018	France	29097494	no
Derosa et al., European Urology., 2020	France	32376136	no

Table S6. Baseline GOMS associated with response rates in the mega-analysis presented in Fig

Sheet name	Content
Legend	Color legend and detailed parameters
Summary	GOMS-related to R versus NR status before ICI (mega-analysis, ORR) summary.
Table S6	GOMS-related to R versus NR status before ICI (mega-analysis, ORR) results.

gure 3.

Table S7. Baseline GOMS associ

Sheet name
Legend
Summary
limma_voom_TMM_zinbwave
limma_voom_TMM
DESeq2_poscounts
DESeq2_poscounts_zinbwave
DESeq2_TMM
ANCOMBC
maaslin2
SMD
Pibble

ated with response rates in the meta-analysis presented in Figure 4.

Content
Color legend and detailed parameters
GOMS-related to R versus NR status before ICI (meta-analysis, ORR) summary
Differential abundance methods and normalizations (8 in total) were used to estimate fold changes (or log ratios) with their respective confidence intervals between responders and non-responders (Supplementary material).
Bayesian multinomial logistic-normal linear regression model

Table S8. Relationships between cancer-associated bacteria relevant for clinical

Cat.	Bacteria issued from the Meta and Mega-Analysis	Cancer	H
Cancer and NR	*Anaerotruncus colihominis*		
	Bacteroides clarus		
	Bacteroides fragilis		
	Bifidobacterium dentium		
	Bilophila wadsworthia		
	Clostridium innocuum		
	Clostridium scindens		
	Clostridium symbiosum		
	Dialister invisus		
	Eggerthella lenta		
	Eisenbergiella massiliensis		
	Eisenbergiella tayi		
	Enterocloster aldenensis		
	Enterocloster bolteae		
	Enterocloster citroniae		
	Enterocloster clostridioformis		
	Enterocloster lavalensis		
	Erysipelatoclostridium ramosum		
	Escherichia coli		
	Faecalicatena fissicatena		
	Faecalitalea cylindroides		
	Hungatella hathewayi		
	Intestinimonas butyriciproducens		
	Lancefieldella parvula		
	Ruminococcaceae bacterium D5		
	Ruminococcus torques		
	Ruthenibacterium lactatiformans		
	Scardovia wiggsiae		
	Streptococcus cristatus		
	Streptococcus mutans		
	Streptococcus sanguinis		
	Veillonella parvula		
	Akkermansia muciniphila		
	Alistipes shahii		
	Anaerobutyricum hallii		
	Anaerostipes hadrus		

Control and R	*Bacteroides caccae*		
	Bacteroides nordii		
	Bifidobacterium adolescentis	■	
	Bifidobacterium bifidum		
	Blautia wexlerae		■
	Coprococcus catus		
	Coprococcus eutactus		
	Dorea formicigenerans		
	Eubacterium rectale	■	■
	Eubacterium ventriosum	■	■
	Faecalibacterium prausnitzii		■
	Fusicatenibacter saccharivorans	■	
	Intestinibacter bartlettii		
	Lachnospira eligens		■
	Lachnospira pectinoschiza	■	
	Limosilactobacillus vaginalis		
	Phascolarctobacterium succinatutens		
	Phocaeicola coprophilus		
	Prevotella copri	■	■
	Roseburia faecis	■	
	Roseburia hominis		
	Roseburia intestinalis		
	Roseburia inulinivorans		
	Ruminococcus bicirculans		
	Ruminococcus torques	■	
	Sutterella wadsworthensis		
	Ref.	**[1-3]**	**[4-7]**
		Gacesa et al., 2022; Park et al., 2022	Li et al., 2022; Rampelli et al., 2020; Wang et al., 2022; Sato et al., 2021

■ Increased in relative abundance
■ Decreased in relative abundance
■ Increased or decreased in relative abundance

outcome and confounding factors.

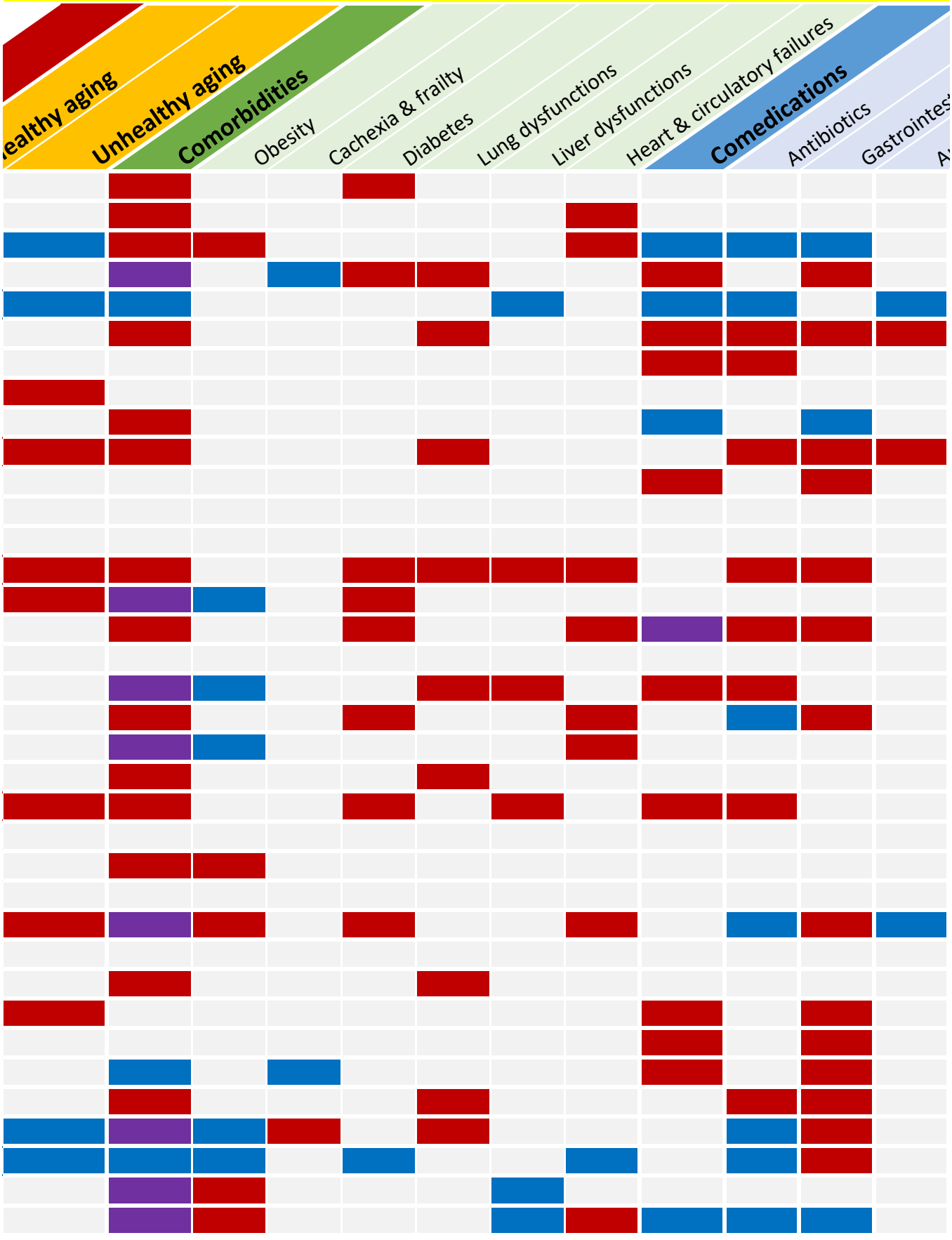

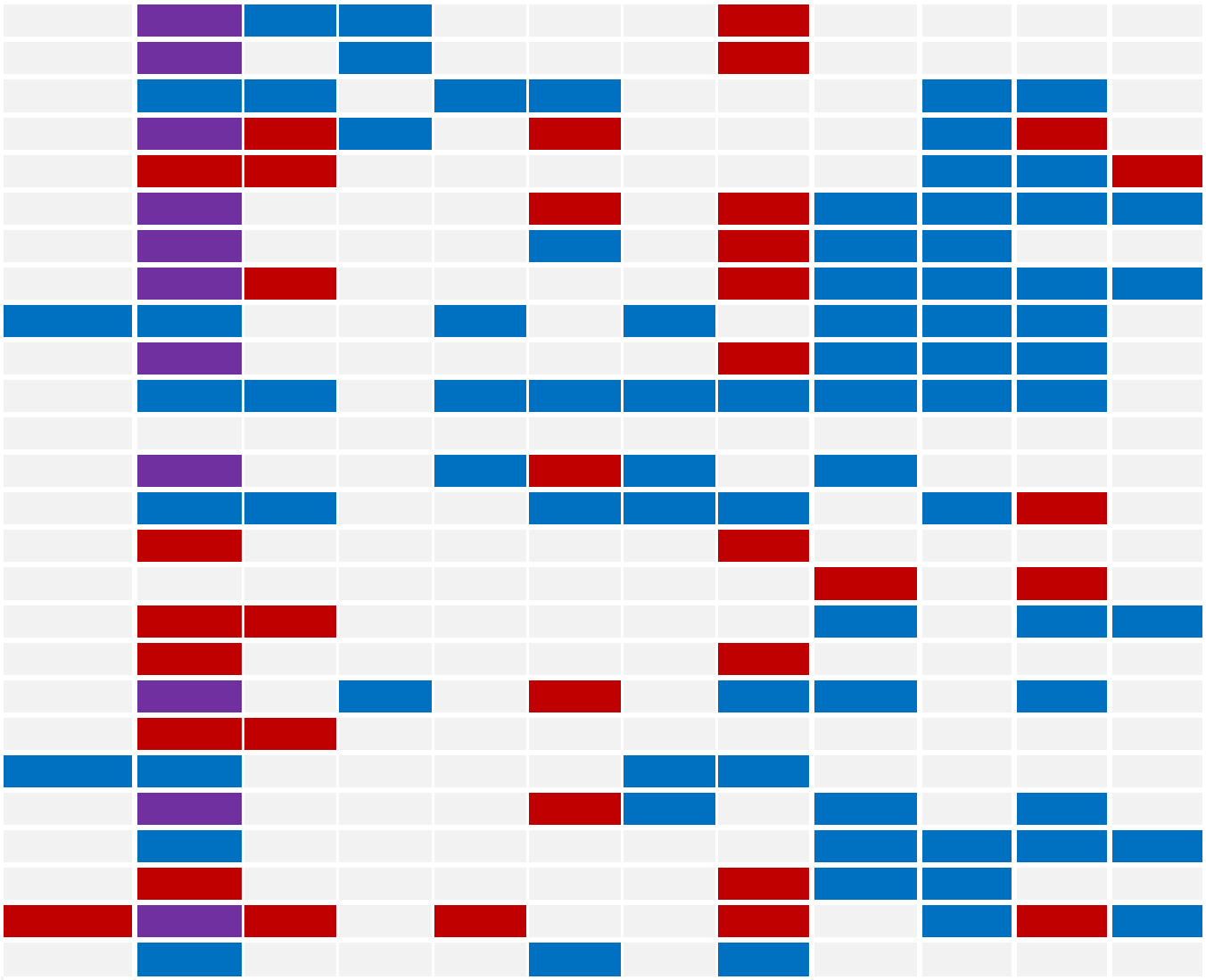

[8-10]	[2,11-23]	[23-32]
Luan et al., 2020; Ghosh et al., 2020; Zhang et al., 2021	Qin et al., 2014; Liu et al., 2017; Wang et al., 2018; Cui et al., 2018; Crovesy et al., 2020; Bowerman et al., 2020; Calderón-Pérez et al., 2020; Ni et al., 2021; Jiao et al., 2021; Behary et al., 2021;	Aasmets et al., 2022 Clooney et al., 2016 Derosa et al., 2020 Imhann et al., 2016 Lin et al., 2021 Nagata et al., 2022 Nagata et al., 2022 Palleja et al. 2018 Parker et al., 2017 Singh et al., 2022


tinal tract
nti-inflammatory agents
Antidiabetics
Anti-cancer therapies
Chemotherapy
Hormonotherapy
Protein kinase inhibitors

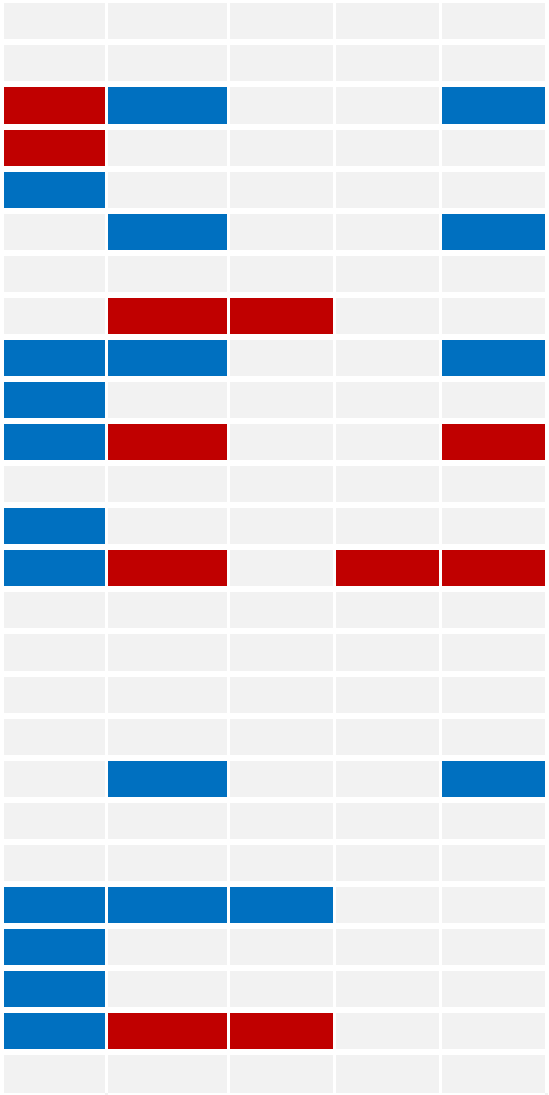

[25,28,33-34]

Derosa et al., 2020
Li et al., 2021
Nagata et al., 2022
Terrisse et al., 2021